This is to certify that the
dissertation entitled

ULTRATHIN, SELECTIVE POLYIMIDE MEMBRANES
PREPARED FROM LAYERED POLYELECTROLYTES

presented by

DANIEL M. SULLIVAN

has been accepted towards fulfillment
of the requirements for the

Doctoral degree in Chemistry

Major Professor's Signature

May 11, 2004

Date

Ultrathin, Selective Polyimide Membranes Prepared from Layered Polyelectrolytes

By

Daniel M. Sullivan

A Dissertation

Submitted to
Michigan State University
in partial fulfillment of the requirements
for the degree of

DOCTOR OF PHILOSOPHY

Department of Chemistry

2004

ABSTRACT

ULTRATHIN, SELECTIVE POLYIMIDE MEMBRANES PREPARED FROM LAYERED POLYELECTROLYTES

By

Daniel M. Sullivan

The work presented in this dissertation applies layer-by-layer techniques and subsequent heat-induced imidization to form ultrathin polyimide films. Two layer-by-layer methods are discussed, one that employs polymers that covalently bond to each other, and another that uses electrostatic interactions for film buildup. The polyimide films presented here were tailored for two areas of application; anti-corrosion coatings and high flux, selective membranes.

Ultrathin, passivating films are attractive for protecting metal surfaces without completely masking substrate properties. Layer-by-layer covalent deposition of Gantrez™/poly(allylamine) films yields ultrathin amic acid-linked layers that can be imidized by heating. Impedances of Al electrodes coated with Gantrez™/poly(allylamine) films depend on the number of deposited bilayers, and the imidized films increase aluminum oxide resistance by up to two orders of magnitude. These results suggest that increases in film resistance play a role in oxide passivation in this system.

Low fluxes often restrict practical applications of membrane-based separations. A reduction in the thickness of the membrane increases flux, but currently, thicknesses below 50 nm are difficult to achieve. Alternating polyelectrolyte deposition (APD) offers a simple and convenient method to

fabricate ultrathin membrane skins, but the selectivity of polyelectrolyte films is generally low.

To develop discriminating, ultrathin polyelectrolyte films, we first adsorb poly(amic acid) salts and poly(allylamine hydrochloride) (PAH) on porous alumina. Subsequent heating yields highly selective polyimide membranes. Remarkably, after imidization at temperatures ranging between 150 and 180 °C, membranes composed of poly(p-phenylenepyromellitamic acid) and PAH have Cl^-/SO_4^{2-} selectivities as high as 1000 and K^+/Mg^{2+} selectivities of 100-300. The minimal thickness (4 to 9 nm) of these membranes allows fluxes that are 50% of those through the bare porous alumina support.

For gas separations, we utilized fluorinated polyimides because these materials offer both high selectivity and high permeability. Selectivities (O_2/N_2 up to 6.9 and CO_2/CH_4 up to 68) and permeabilities of three different, fully imidized, poly(amic acid)/PAH membranes are comparable to literature values for the corresponding bulk polyimides, even when films are 35 to 40 nm thick.

We also investigated pervaporation separations of water from alcohol solutions using cross-linked polyimide membranes. The poly(amic acids) employed in these studies contain diaminobenzoic acid groups that can form amide cross-links with the polycation when heated. Water-selective pervaporation separations using cross-linked polyimide membranes are highly selective (water/alcohol selectivities are 1100 and 6100 for solutions containing 10% and 90% isopropanol, respectively) and the fluxes are also high, ranging from 2 to 11 $kg \cdot m^{-2} \cdot h^{-1}$.

To my wife, Sarah

ACKNOWLEDGEMENTS

I would like to first thank my advisor Dr. Merlin Bruening for giving me the opportunity to work in his group. Over the years, he taught me how to be thorough in both research and writing. He is not only a good advisor, but a good friend (and yes, a better golfer).

I also need to pay gratitude to my fellow group members, both past and present. They were helpful and supporting at each stage of my graduate career. I also enjoyed the many stimulating conversations and the cultural experiences they were able to provide. Along with my group members, I also would like to thank the many friends that I made in the Chemistry Department. The most notable people include Jeremy, who taught me the art of sensitivity (sarcasm at the fullest) and both Jason and Carl, with who I spent many hours watching bad movies (intentionally) and brewing good beer (well, most were good).

My family was also very helpful during my many, many years in college. I would especially like to thank my wife, Sarah, for being very supportive of the long hours and the stressful times. I don't think I could have done this without her.

Lastly, thanks for reading this, you are probably the only one who ever has or will.

TABLE OF CONTENTS

LIST OF TABLES

LIST OF FIGURES

Chapter 1

Introduction and Background

1.1 Thin polymer films

Thin polymer films play an increasingly important role in a range of technological areas, including protective coatings,[1-3] adhesives,[4] lithography,[5,6] organic light-emitting diodes,[7,8] sensors,[9-11] membranes,[12-14] and optical coatings.[15,16] Properties such as permeability, refractive index, wetting, and film functionality are easy to control by selecting the coating material, and polymer films are, in general, inexpensive to produce. In several ways, thin film technologies have become an indispensable part of everyday life. As an example, thin coatings of photoresist polymers are essential in fabrication of microelectronic devices. Polymer films are spin-coated onto silicon substrates, and after treatment with UV light and chemical etching, these films give rise to the three-dimensional structures that make up microchips.[17]

The most common techniques for forming thin polymer films include spraying and dip-, flow-, or spin-coating. These methods allow for good control over film thickness down to 100 nm, but some applications would benefit from much thinner polymer films. Deposition of "ultrathin" films (thicknesses <100 nm) requires different coating strategies that allow regulation of film thickness at the macromolecular level. Control over both thickness and the properties of polymer films is an ongoing challenge; therefore, new methods for depositing polymer films are constantly being sought.

Various methods have been developed to better control polymer film thickness. The Langmuir-Blodgett (LB) technique was the first method used to deposit single layers of organic molecules on solid surfaces.[18] Although this technique was originally employed for deposition of small molecules, it has been further applied to amphiphilic, polymeric materials.[19,20] Film deposition occurs by dipping a substrate perpendicularly though a film suspended at a liquid/air interface. Multiple layers can be applied through repeated dipping cycles, and this coating method affords good control over the film thickness since monolayers are deposited during each dipping step. Unfortunately, the LB method has many limitations that prevent it from becoming a practical film deposition technique. The biggest problem is the need for complicated deposition instrumentation. By its nature, the deposition procedure restricts substrate dimensions to those of the Langmuir trough. Additionally, polymers used to form LB films must be amphiphilic, and this requirement greatly reduces the variety of films that can be produced. Finally, since van der Waals forces hold LB films together, coatings are not very stable.

More recently, other layer-by-layer methods have been developed for controlled deposition of ultrathin films, and some of these techniques are essentially free of the complications that arise in LB deposition.[21-24] Such layer-by-layer techniques typically involve cycles of dipping a substrate into a polymer solution, rinsing with an appropriate solvent, and then dipping once again into another polymer solution. Each layer is typically bound to the previous layer by either covalent or ionic interactions, making these films much more stable than

those prepared by LB. Additionally, many types of polymers can be utilized in layer-by-layer techniques, so the chemistry of films can be easily adjusted to suit specific applications.

The work presented in this dissertation applies layer-by-layer techniques and subsequent heat-induced imidization to form ultrathin polyimide films. The ultrathin polyimide films used as the anti-corrosion coatings described in Chapter 2 were fabricated using polymers that form covalent bonds between layers. Films as thin as 30 nm increase the resistance of aluminum oxide by 2 orders of magnitude. Chapters 3 – 5 discuss a different method for polyimide film fabrication, alternating polyelectrolyte deposition. In this work, ultrathin, polyimide membranes were prepared for the selective separation of ions, gases, and liquids. The highly selective ion-separation membranes (Cl^-/SO_4^{2-} selectivity of 1000) described in Chapter 3 contained selective polyimide skins (4-9 nm thick) deposited on a highly permeable gutter layer. Chapter 4 presents the fabrication of ultrathin gas-separation membranes composed of fluorinated polyimides. Even though these polyimide films are as thin as 35 nm, they provide selectivities and permeabilities that are identical to the bulk, cast materials. Using cross-linkable materials, the pervaporation membranes described in Chapter 5 provide selectivities and fluxes as high as 6100 and 2 $kg \cdot m^{-2} \cdot h^{-1}$, respectively, for the removal of water from 90% isopropanol solutions. A common thread through all of these chapters is the exploitation of the layer-by-layer process to achieve high-performance, ultrathin polyimide coatings. In all of these areas, the thickness and chemistry of the films are easily controlled. The

remainder of this introduction provides important background concerning polyimides, corrosion, multilayer polyelectrolyte films, ion separations, gas separations, and pervaporation.

1.2 Polyimides

Polyimides are an attractive family of polymers because of their high thermal stability, resistance to chemical degradation, mechanical strength, and low dielectric constant.[25] Due to these properties, these materials have industrial applications in electronics (insulators and photoresists),[26,27] optical waveguides,[28,29] composites for aerospace applications,[30,31] high temperature adhesives,[32,33] and membrane-based separations.[34]

The majority of polyimides are infusible and insoluble. Thus, the synthesis of these polymers takes place in a two step process, where the first step involves the formation of a soluble poly(amic acid), and the second step is imide formation (Figure 1.1).[25] Poly(amic acids) are usually formed by a simple condensation polymerization of dianhydrides and diamines, which are often aromatic. The reaction is performed in a dipolar, aprotic solvent and proceeds by a nucleophilic attack of the amino group on the carbonyl carbon of the anhydride.

Cyclization to the imide occurs by the reaction of the carboxylic acid and the amide with the release of water as a by product (Figure 1.1). This reaction is induced by either thermal or chemical means, but the thermal method is more common. In the thermal reaction, heating poly(amic acids) at 250 to 350 °C will effect full imidization. This method is usually employed with "solid state"

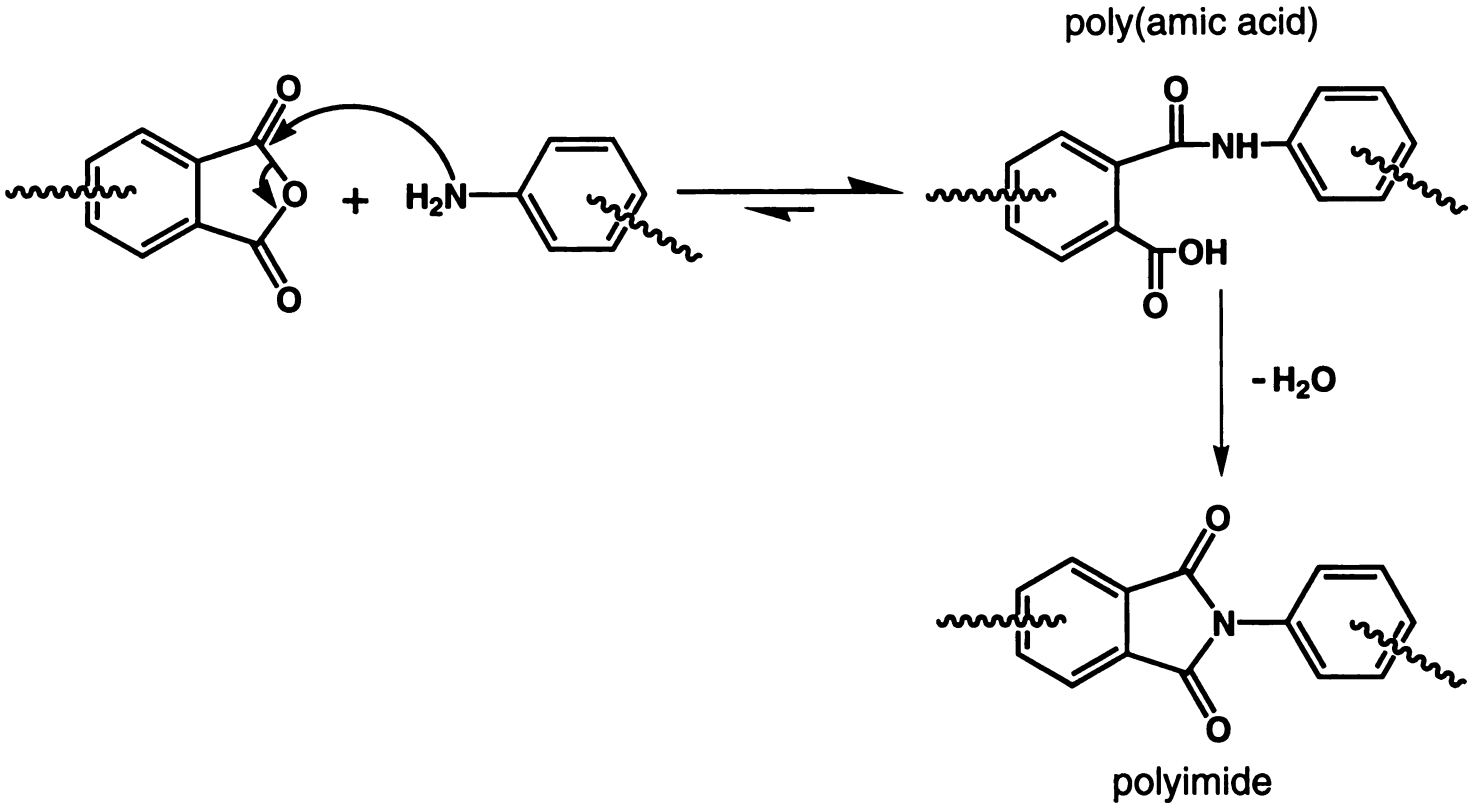

Figure 1.1: Polyimide synthesis via a two step polycondensation reaction. An equimolar mixture of dianhydride and diamine reacts to form a poly(amic acid) that is then converted to the polyimide by removal of water.

poly(amic acids), but the imidization proceeds faster in the presence of residual dipolar, amide (e.g., N,N-dimethylformamide) solvent.[25] Chemical imidization is achieved in solution with an excess of a dehydrating agent such as acetic anhydride and is catalyzed with an amine base. Both chemical and thermal imidization techniques have been applied to thin films of polyamic acids.[35-38]

1.3 Ultrathin polyimide anti-corrosion coatings

The United States alone spends an average of $278 billion dollars per year to combat corrosion.[39] The majority of corrosion countermeasures employ either a thick organic coating (paint) or galvanization to protect steel. Nevertheless, there are some specialized areas in which an ultrathin, passivating film is attractive for protecting surfaces without completely masking substrate properties. Examples of these include passivation of heat exchangers,[40,41] electronic materials,[42] and high T_c superconductors.[43]

In Chapter 2, I show that layer-by-layer covalent deposition of Gantrez™/poly(allylamine) films on aluminum yields ultrathin amic acid-linked layers that can be imidized by heating to form cross-linked polyimide coatings that protect aluminum from Cl^--induced corrosion.[44] Although the electrical resistance of these films in water is relatively small because of their minimal thickness, they do form a passivating layer on the surface oxide and increase oxide resistance by 2 orders of magnitude. Impedances of Al electrodes coated with Gantrez™/poly(allylamine) films depend on the number of deposited bilayers and increase by an order of magnitude after imidization. These results suggest

that small increases in film resistance play a role in oxide passivation by this system.

1.4 Multilayer polyelectrolyte films

In 1966, Iler published a paper entitled "Multilayers of Colloidal Particles" which described the use of oppositely charged particles such as alumina and silica to build up multilayered films.[45] He deposited these films on glass in a layer-by-layer fashion and estimated their thickness by the color of the interference pattern they produced. It wasn't until twenty-five years later that Decher and Hong reported the use of bipolar amphiphiles and polyelectrolytes to deposit multilayered films on charged surfaces.[46,47] They showed that ultrathin polymer films could be formed by a simple dip and rinse methodology. Their work has since triggered hundreds of publications in many different fields of research.

Layer-by-layer (LBL) assembly of polyelectrolytes is a simple method to build up ultrathin polymer films. Film formation begins by the adsorption of a polyelectrolyte from solution onto an oppositely charged substrate. Useful substrates include essentially all materials that support sufficient surface charge; commonly used supports are glass,[21,48,49] quartz,[50] silicon wafers,[51,52] mica,[53] metal coatings,[44,54,55] and some polymers.[56-59] The first adsorbed polyelectrolyte layer over-compensates the charge of the substrate, leaving an excess charge for subsequent adsorption of a polyelectrolyte of opposite sign (Figure 1.2). Rinsing of the substrate with water and a second immersion in the oppositely

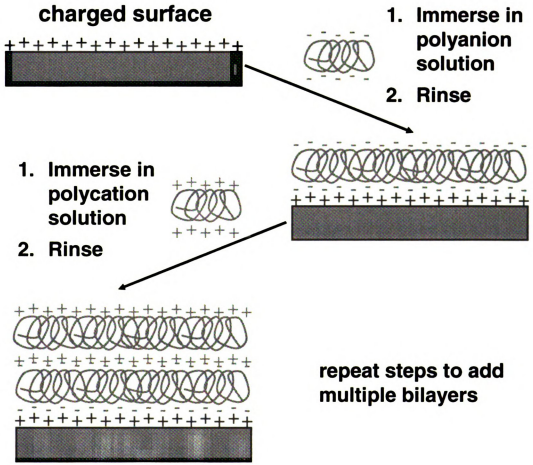

Figure 1.2: Schematic diagram of multilayer film formation using alternating polyelectrolyte deposition.

charged polyelectrolyte results in one bilayer on the substrate, and deposition of additional layers occurs similarly. The driving force for polyelectrolyte adsorption is not a change in enthalpy, but an increase in entropy.[60] When a single ionic bond is formed between two polyelectrolytes, two counter ions are displaced into the solution. Considering that each polyelectrolyte chain contains many charged groups that can undergo ionic cross-linking with an oppositely charged strand, it can easily be seen that a large increase in entropy occurs upon adsorption due to the increased freedom of many counterions.

Film thickness can be controlled over a wide range by changing either the number of bilayers in the film or by varying the deposition solution's ionic strength, pH, or solvent composition.[37,61] Increasing the ionic strength usually increases the layer thickness because the electrolyte ions screen charges on the polyelectrolytes and allow formation of coiled, rather than extended chains. The presence of many loops and tails in the film results in thicker layers. Deposition pH also has a pronounced effect on the thickness of films containing weak-acid or weak-base polyelectrolytes because protonation or deprotonation of the polyelectrolytes influences their charge density and conformation.

The layer-by-layer method is not limited to simple polyelectrolytes, and many types of charged materials such as dendrimers,[62-65] biomolecules,[52,54,62,66] dyes,[67] metal colloids,[68,69] clays,[58,70] and other inorganic particles[71,72] have been included in multilayer films. Existing polyelectrolytes can also be derivatized to incorporate desired functional groups.[73,74] This vast range of available charged materials allows tailoring of ultrathin, multilayer films for many possible

applications. Several recent papers describe attempts to apply LBL films as conducting layers,[75] active enzyme-containing films,[76] electrocatalysts,[77] electrochromic films,[77,78] sensors,[79] light-emitting thin films,[80] patterned surfaces,[81] anti-corrosion coatings,[44] and permselective membranes.[59,82,83]

1.5 Ion-selective polyimide membranes

Many industrial applications require the removal of ions from solution or selective extraction of specific ions. The removal of salt from water, for example, is important in applications such as food processing[84,85] and the production of potable water.[86-88] Salt purification methods, such as the production of table salt from sea water[89] and the removal of heavy metals from electroplating waters,[90,91] are also of great importance. Ion-separation methods that employ membranes include reverse osmosis, nanofiltration, and diffusion dialysis, but electrodialysis is the most widely used technique.[14] As an example, caustic soda is produced in the USA at a rate of 14 million tons per year, almost entirely by the electrodialysis of brine.[92] In this process chlorine is produced at the anode and NaOH at the cathode in stoichiometric quantities, and the electrodes are separated by ion-selective membranes.[14]

High fluxes are vital to any membrane application so that both the size of the membrane and energy costs can be kept to a minimum. For a particular system, flux is typically maximized by making the active separation layer of the membrane as thin as possible, as flux is usually inversely proportional to thickness.[13] However, because the separation layer is very thin, it must be

reinforced by a highly permeable support that provides mechanical strength. Fabrication of such a membrane is generally achieved by either casting an asymmetric membrane[93,94] to create a dense surface layer on an otherwise porous polymer or by forming a composite membrane through deposition of a thin polymer coating on a porous support.[13,95] Unfortunately, the formation defect-free selective skins less than 100 nm is often difficult.

The layer-by-layer deposition method provides a new and versatile technique for fabricating the ultrathin skins of composite membranes. Because such films form by adsorption, surface roughness does not greatly affect adhesion, and defect-free films can be obtained on porous supports since each added layer covers defects in the previous layer. Polyelectrolyte films are also well suited for the separation of ions in solution since the charged nature of these films allows for Donnan (electrostatic) exclusion of ions with the same charge as the outer layer of the membrane.

Krasemann and Tieke were the first to show that multilayer polyelectrolyte films could be used to make ion-selective membranes.[59] They used some of the more common polyelectrolyte combinations to form films on polyacrylonitrile/polyethylene terephthalate (PAN/PET) supports. They reported that the addition of supporting salt to the polyelectrolyte deposition solutions greatly enhances ion-transport selectivity. Membranes composed of 60 bilayers of poly(allylamine hydrochloride)/poly(styrene sulfonate) (PAH/PSS) provided selectivities of 45 for Cl^-/SO_4^{2-} and 113 for K^+/Mg^{2+}. In another publication, Toutianoush and Tieke showed that some multiply charged ions permanently

adsorb into poly(vinyl amine)/poly(vinyl sulfate) (PVA/PVS) membranes, changing the flux of monovalent ions.[96] They later used PVA/PVS membranes to remove salts from water in reverse osmosis.[97]

Much of the ion separation work using multilayer polyelectrolyte films has come out of the Bruening group. Early studies showed that as few as 4 bilayers of PSS/PAH will cover the pores of porous alumina supports.[98] These composite membranes had Cl^-/SO_4^{2-} selectivities of only ~5, but the fluxes of KCl through such films were nearly identical to those through the bare alumina support (diffusion dialysis of single-salt solutions). Thus, even though the ultrathin PSS/PAH films were not very selective, they provided a convenient way to cover underlying pores without hindering flux. Hybrid membranes can be fabricated using PSS/PAH as a "gutter layer" and capping this layer with a selective skin composed of a few bilayers of more selective polyelectrolytes. Since the selective polyelectrolyte skin is extremely thin, the flux of monovalent species will be high. Stair et. al. reported that membranes capped with 2.5 bilayers of cross-linked poly(acrylic acid) (PAA)/PAH exhibit selectivities as high as 360 for Cl^-/SO_4^{2-} and allow fluxes of KCl that are only ~60% less than those through the bare alumina support.[83] When applied to nanofiltration, membranes containing a PAA capping layer allow water fluxes that are similar to those of current commercial membranes, with selectivities as high as 80 for Cl^-/SO_4^{2-}.[99]

As previously mentioned, Donnan exclusion is probably the major factor in the ion-transport selectivity of multilayer polyelectrolyte membranes. Therefore, high charge densities are vital to achieving large selectivities. In typical

polyelectrolyte membranes, the film surface is the major source of the membrane's fixed charge, as the interior of the film is often net neutral due to complete charge compensation in the ionic cross-links.[100] To further enhance the understanding and selectivity of these systems, two methods were developed to add charge to the interior of the polyelectrolyte film after film deposition. The first of these methods makes use of polyelectrolytes that are partially derivatized with photocleavable protecting groups.[73] Since the polyelectrolytes are only partially derivatized, there is still sufficient charge for film formation. Once the film is deposited, UV light is used to photolyze the protecting group, leaving either positive or negative charges in the bulk of the film, depending on the polyelectrolyte employed. PAA/PAH membranes containing PAA with 0, 33, 50, and 63% of it carboxylic acid groups converted to negative groups only after film formation show Cl^-/SO_4^{2-} selectivities of 9, 100, 150, and 170, respectively. The second method for forming net charge in the bulk of films involves the deposition of PAA partially complexed with Cu^{2+}.[101] Removal of the Cu^{2+} after deposition can yield Cl^-/SO_4^{2-} selectivities as high as 610 for cross-linked PAA/PAH membranes. Both of these methods show that Donnan exclusion plays a large part in the selectivity of these membranes.

Chapter 3 of this dissertation describes highly selective ion separations, which are achieved primarily by size selectivities, and not by Donnan exclusion.[102] The membranes that effect these separations are formed using layer-by-layer adsorption of a poly(amic acid) and PAH on porous alumina, and subsequent heat-induced imidization yields ultrathin, polyimide films (Figure 1.3).

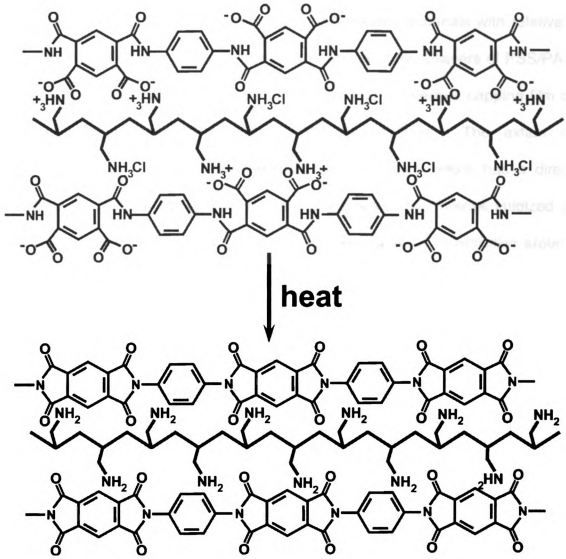

Figure 1.3: Heat-induced imidization of multilayer poly(amic acid)/poly(allylamine) films.

These membranes allow remarkably selective transport of singly over doubly charged ions, and their minimal thickness permits high flux of the monovalent species. However, selectivity is based primarily on the larger size of the divalent ions because the polyimide films are essentially neutral materials with relatively low free volume. The membranes consist of a base of five bilayers of PSS/PAH attached electrostatically to the alumina support and a selective capping film of poly (p-phenylenepyromellitamic acid) (PMDA-PDA)/PAH. The extent of imidization can be controlled by the heating temperature, which has a direct impact on the flux of the ions through the membrane. Membranes imidized at temperatures ranging between 150 to 180 °C have Cl^-/SO_4^{2-} selectivities around 1000 and K^+/Mg^{2+} selectivities of 300. Increasing the number of PMDA-PDA/PAH layers results in increases in selectivity and decreases in ion fluxes.

1.6 Ultrathin polyimide membranes for gas separations

In the past 20 years, membranes have been widely investigated for the separation of gases for potential applications such as oxygen enrichment for medicinal use or enhanced combustion, carbon dioxide removal from natural gas streams, and large scale purification of hydrogen for fuel cells.[12] The solution-diffusion mechanism of selective gas permeation that generally operates in these films is based on the solubility and diffusion of a gas within a polymeric membrane. Differences in solubilities and diffusivities among gases result in separation. Such differences depend on the polymer used to make the

membrane, and the gas permeability of a polymer is often inversely related to its selectivity.[103]

There have been some investigations of polyelectrolyte multilayers as gas separation membranes. Polyelectrolyte films can increase the gas selectivity of *non*-porous supports,[58,104,105] but deposition of these films on porous supports yields little increase in selectivity.[105,106] The earliest work was reported by Stroeve et al., in which they coated porous Celgard™ (polypropylene) and non-porous silicone membranes with up to 50 bilayers of PSS/PAH.[105] Transport through the coated Celgard™ membranes was still dominated by Knudsen diffusion, and the coated silicone membranes showed at most a 20% increase in CO_2/N_2 selectivity over the bare silicone. This small selectivity enhancement may be due to coverage of defects in the support. Leväsalmi and McCarthy later showed that PSS/PAH films could increase the selectivity of *non*-porous poly(4-methyl-1-pentene) membranes.[104] Krasemann and Tieke prepared films composed of PSS and various polycations and applied these to gas permeation experiments.[107] The best selectivity they achieved was only 1.5 (CO_2/N_2 using PSS/poly(4-vinylpyridine) multilayers). Standard gas-separation membranes with similar permeability would have selectivity values greater than 20 for CO_2/N_2. We suspect that the lack of gas-transport selectivity in polyelectrolyte films is inherent in the structure and packing of the polyelectrolytes thus far employed.

As mentioned in section 1.2, polyimide membranes can provide highly selective gas separations. The selectivity results from a combination of low free volume, low segmental motion and small interchain distances. Some general

trends relate structure to gas permeability and selectivity, but there is no clear methodology to predict these properties.[34] One such trend is that m,m' imide linkages (determined by the diamine) within the polymer generally decrease the permeability and increase the selectivity relative to p,p' linkages. This is most likely a result of a differences in the segmental motion of the glassy polymer, as m,m' linkages put a kink in the polymer chain and do not allow for rotational motion. Increasing the rigidity of the monomers has a similar effect. Permeability increases when bulky CF_3 or dimethylsiloxyl groups are incorporated into polyimides, but dimethylsiloxyl groups also significantly reduce the selectivity. The bulky groups likely disrupt packing and increase the free volume of the membrane. The CF_3 groups still allow selectivity because the rotational mobility about the flexible linkages is also slightly inhibited.[108]

Chapter 4 of this dissertation describes the formation of gas-selective, fluorinated polyimide membranes on porous alumina supports by the alternating electrostatic deposition of poly(amic acid) salts and PAH followed by heat-induced imidization.[109] These membranes are appealing because of the stability and selectivity of polyimides and the fact that alternating polyelectrolyte adsorption allows formation of ultrathin (as low as 35-40 nm), defect-free membranes that allow high flux. FTIR spectroscopy shows that heating of poly(amic acid)/PAH films at 250 °C for two hours completely converts the poly(amic acid) to the corresponding polyimide, and scanning electron microscopy reveals uniform films with minimal deposition in substrate pores. Permeability coefficients and selectivities (O_2/N_2 up to 6.9 and CO_2/CH_4 up to 68)

of three different imidized poly(amic acid)/PAH membranes are comparable to literature values for the corresponding bulk polyimides, provided that the ratio of poly(amic acid) to PAH in the film is high (9:1).

1.7 Pervaporation separations using cross-linkable polyimides.

Pervaporation is a relatively new membrane-based technique for the separation of liquid mixtures.[110] In this process, a liquid mixture is exposed to the surface of a membrane whose permeate side is at reduced pressure, and selective transport of one component through the membrane allows for solvent purification or analyte collection. Pervaporation is attractive because it allows for the separation of azeotropic mixtures and often requires less energy than conventional distillation.[111,112] Many of the successes with pervaporation involve the removal of water from organic solvents, but the reverse separation has also been demonstrated.[113-115] Even with advances in pervaporation technology, however, there is still a need for membrane systems with increased selectivity and flux.

Tieke and coworkers were the first to show that multilayer polyelectrolytes could serve as selective pervaporation membranes.[116,117] Their membranes consisted of 60 bilayers of polyelectrolytes deposited on PAN/PET, and an ethanol solution containing 6.2 wt% water was used as the feed for pervaporation. They found that selectivities and flux values varied greatly with the polyelectrolytes used to form the film and that deposition pH had a large effect on the performance of the membrane. They suggested that the optimal

deposition pH is the mean pK_a value of the cationic and anionic groups of the polyelectrolytes. The larger selectivity values at these pH values may occur because of a high ionic cross-link density that results in a very compact film structure. Although not specifically stated, this high degree of ionic cross-linking should keep film swelling to a minimum. Additionally, annealing of films at 90 °C increases the selectivity of all of polyelectrolyte pervaporation membranes, presumably because it allows for formation of even more ionic cross-links.

Tieke and coworkers also investigated how the membrane performance depends on the addition of supporting salt to the polyelectrolyte deposition solutions. They found that addition of 1 M NaCl yields a 4-fold decrease in membrane flux, presumably because film thickness increases with ionic strength in deposition solutions. The selectivity also increased with the ionic strength. For example, PVA/PVS films deposited without and with 1 M NaCl had selectivity values of 35 and 280, respectively. I think that the large variations in the selectivity of the different films may be to due incomplete pore coverage or defects in thinner films. No SEM images or thickness data for films deposited on PAN/PET supports are given, so it is difficult to know whether films are thick enough to cover the 20 to 200 nm-diameter pores in the underlying supports.

Meier-Haack and coworkers deposited polyelectrolytes on an asymmetric membrane composed of carboxyl-functionalized polyamide-6.[82] This support membrane contains a dense, 0.5 μm-thick skin layer, but it provides little selectivity in pervaporation of alcoholic solutions. Deposition of as few as 6-bilayers of polyelectrolytes on the support completely covers the substrate, to

give very high water/alcohol selectivities. Membranes coated with poly(ethylenimine)/alginic acid films exhibit the highest selectivities; 90% ethanol feed solutions had a water/alcohol selectivity of 1400. They credited the selectivities to the hydrophilicity of the film and the high degree of ionic cross-links.

In Chapter 5, I describe the formation of covalently cross-linked polyimide membranes that have high pervaporation selectivities and fluxes for the removal of water from alcohol solutions.[118] These films were produced using the alternating deposition of poly(amic acids) and polycations as described in sections 1.4 and 1.5. Moreover, incorporation of additional carboxylic acid groups in the poly(amic acid) allows cross-linking via reaction of these groups with the amines of the polycation. A similar cross-linking reaction was previously shown in PAA/PAH films.[55,83] FTIR spectroscopy confirms both full imidization and formation of amide cross-links after heating at 250 °C for 2 h, while scanning electron microscopy reveals uniform, ~50 nm thick films (7.5 to 12.5 poly(amic acid)/polycation bilayers). Pervaporation was investigated as a function of cross-linking by varying either the polycation (PAH, polyethylenimine, or poly(diallyldimethylammonium chloride)) or the number of cross-linkable groups in the polyamic acid. Maximum cross-linking and selectivities occur with imidized films prepared from PAH and a poly(amic acid) that contains diaminobenzoic acid in every repeat unit. Such membranes exhibit water/alcohol selectivities of 1100 and 6100 for solutions containing 10% and 90% isopropanol, respectively,

and the minimal thickness of the multilayer films still allows these selectivities to occur at fluxes of 11 and 2 $kg \cdot m^{-2} \cdot h^{-1}$, respectively.

1.8 References.

(1) Spencer, M.; Ruben, K.; Li, C.; Williams, P.; Flaim, T. D. *Proceedings of SPIE-The International Society for Optical Engineering* **2003**, *4979*, 79-86.

(2) Delucchi, M.; Barbucci, A.; Cerisola, G. *Mater. Eng.* **1999**, *10*, 223-235.

(3) De Rosa, R. L.; Wagner, S. R. *J. Adhesion* **2002**, *78*, 113-127.

(4) Jovanovic, R.; Dube, M. A. *J. Macromol. Sci. Polym. R.* **2004**, *C44*, 1-51.

(5) Yamada, S.; Mrozek, T.; Rager, T.; Owens, J.; Rangel, J.; Willson, C. G.; Byers, J. *Macromolecules* **2004**, *37*, 377-384.

(6) Riehn, R.; Charas, A.; Morgado, J.; Cacialli, F. *Appl. Phys. Lett.* **2003**, *82*, 526-528.

(7) Nguyen, T. P.; Le Rendu, P.; Long, P. D.; De Vos, S. A. *Surf. Coat. Tech.* **2004**, *180-181*, 646-649.

(8) Fujita, K.; Ishikawa, T.; Tsutsui, T. *Mol. Cryst. Liq. Cryst.* **2003**, *405*, 83-88.

(9) Levit, N.; Pestov, D.; Tepper, G. *Sensors Actuat. B-Chem.* **2002**, *B82*, 241-249.

(10) Matsumoto, T.; Ohashi, A.; Ito, N.; Fujiwara, H. *Biosens. Bioelectron.* **2001**, *16*, 271-276.

(11) Shepherd, R. L.; Barisci, J. N.; Collier, W. A.; Hart, A. L.; Partridge, A. C.; Wallace, G. G. *Electroanalysis* **2002**, *14*, 575-582.

(12) Koros, W. J. In *Membrane Separation Systems Recent Developments and Future Directions*; Baker, R. W., Cussler, E. L., Eykamp, W., Koros, W. J., Riley, R. L., Strathmann, H., Eds.; Noyes Data Corp.: Park Ridge, New Jersey, 1991, pp 189-241.

(13) Pinnau, I.; Freeman, B. D. In *Membrane Formation and Modification*; Pinnau, I., Freeman, B. D., Eds.; American Chemical Society: Washington, D.C., 2000, pp 1-22.

(14) Mulder, M. *Basic Principles of Membrane Technology*; 2 ed.; Kluwer Academic Publishers: Dordrecht, The Netherlands 1997.

(15) Masson, F.; Decker, C.; Andre, S.; Andrieu, X. *Prog. Org. Coat.* **2004**, *49*, 1-12.

(16) Toyooka, T.; Kobori, Y. *J. Photopolym. Sci. Technol.* **2000**, *13*, 301-306.

(17) Van Zant, P. *Microchip Fabrication: A Practical Guide to Semiconductor Processing*; 4 ed.; McGraw-Hill Professional, 2000.

(18) Roberts., G. G. *Langmuir-Blodgett Films*; Plenum Press: New York, 1990.

(19) Li, T.; Mitsuishi, M.; Miyashita, T. *Thin Solid Films* **2004**, *446*, 138-142.

(20) Budianto, Y.; Aoki, A.; Miyashita, T. *Macromolecules* **2003**, *36*, 8761-8765.

(21) Decher, G. *Science* **1997**, *277*, 1232-1237.

(22) Zhou, Y.; Bruening, M. L.; Bergbreiter, D. E.; Crooks, R. M.; Wells, M. *J. Am. Chem. Soc.* **1996**, *118*, 3773-3774.

(23) Major, J. S.; Blanchard, G. J. *Langmuir* **2001**, *17*, 1163-1168.

(24) Liu, Y.; Bruening, M. L.; Bergbreiter, D. E.; Crooks, R. M. *Angew. Chem. Int. Ed. Engl.* **1997**, *36*, 2114-2116.

(25) Sroog, C. E. *Prog. Polym. Sci.* **1991**, *16*, 561-694.

(26) Senturia, S. D. *Polym. Mater. Sci. Eng.* **1986**, *55*, 385-389.

(27) Duran, J.; Viswanathan, N. S. *Organic Coatings and Applied Polymer Science Proceedings* **1983**, *48*, 283-286.

(28) Baek, S. H.; Kang, J.-W.; Li, X.; Lee, M.-H.; Kim, J.-J. *Opt. Lett.* **2004**, *29*, 301-303.

(29) Miyadera, N.; Kuroda, T.; Takahashi, T.; Yamamoto, R.; Yamaguchi, M.; Yagi, S.; Koibuchi, S. *Mol. Cryst. Liq. Cryst.* **2003**, *406*, 233-243.

(30) Johnson, W. S.; Cobb, T. Q.; Lowther, S.; St. Clair, T. L. *Proceedings of the Annual Meeting of the Adhesion Society* **1998**, *21st*, 33-35.

(31) Kourtides, D. A. *Flame Retard. Polym. Mater., Proc. Conf. Recent Adv. Flame Retard. Polym. Mater.* **1990**, 285-292.

(32) da Silva, L. F. M.; Adams, R. D.; Gibbs, M. *Int. J. Adhes. Adhes.* **2004**, *24*, 69-83.

(33) Millington, S.; Shaw, S. J. *MRS Bull.* **2003**, *28*, 428-433.

(34) Langsam, M. In *Polyimides Fundamentals and Applications*; Ghosh, M. K., Mittal, K. L., Eds.; Marcel Dekker: New York, 1996, pp 697-741.

(35) Kilian, H.-G.; Bronnikov, S.; Sukhanova, T. *J. Phys. Chem. B* **2003**, *107*, 13575-13582.

(36) Cho, D.; Yang, G.; Drzal, L. T. *Macromol. Res.* **2003**, *11*, 297-302.

(37) Baur, J. W.; Besson, P.; O'Connor, S. A.; Rubner, M. F. *Mater. Res. Soc. Symp. Proc.* **1996**, *413*, 583-588.

(38) Srinivasan, M. P.; Gu, Y.; Begum, R. *Colloid Surface A* **2002**, *198-200*, 527-534.

(39) Koch, G. H.; Brongers, M. P. H.; Thompson, N. G.; Virmani, Y. P.; Payer, J. H. "Corrosion Cost and Preventive Strategies in the United States," CC Technologies Laboratories, Inc., 2001.

(40) Flemming, H.-C.; Schaule, G. *Werkst. Korros.* **1994**, *45*, 29-39.

(41) Melo, L. F.; Bott, T. R. *Exp. Therm. Fluid Sci.* **1997**, *14*, 375-391.

(42) Bellucci, F.; Nicodemo, L.; Monetta, T.; Kloppers, M. J.; Latanision, R. M. *Corros. Sci.* **1992**, *33*, 1203-1226.

(43) Ritchie, J. E.; Wells, C. A.; Zhou, J.-P.; Zhao, J.; McDevitt, J. T.; Ankrum, C. R.; Jean, L.; Kanis, D. R. *J. Am. Chem. Soc.* **1998**, *120*, 2733-2745.

(44) Dai, J.; Sullivan, D. M.; Bruening, M. L. *Ind. Eng. Chem. Res.* **2000**, *39*, 3528-3535.

(45) Iler, R. K. *J. Colloid Interface Sci.* **1966**, *21*, 569-594.

(46) Decher, G.; Hong, J. D. *Ber. Bunsen-Ges. Phys. Chem.* **1991**, *95*, 1430-1434.

(47) Decher, G.; Hong, J. D. *Makromol. Chem., Macromol. Symp.* **1991**, *46*, 321-327.

(48) Ferreira, M.; Rubner, M. F. *Macromolecules* **1995**, *28*, 7107-7114.

(49) Klitzing, R. v.; Möhwald, H. *Macromolecules* **1996**, *29*, 6901-6906.

(50) Yang, X.; Johnson, S.; Shi, J.; Holesinger, T.; Swanson, B. *Sensors and Actuators* **1997**, *45*, 87-92.

(51) Sukhishvili, S. A.; Granick, S. *J. Chem. Phys.* **1998**, *109*, 6861-6868.

(52) Lvov, Y.; Ariga, K.; Ichinose, I.; Kunitake, T. *J. Am. Chem. Soc.* **1995**, *117*, 6117-6123.

(53) Moriguchi, I.; Teraoka, Y.; Kagawa, S.; Fendler, J. H. *Chem. Mater.* **1999**, *11*, 1603-1608.

(54) Caruso, F.; Niikura, K.; Furlong, D. N.; Okahata, Y. *Langmuir* **1997**, *13*, 3422-3426.

(55) Harris, J. J.; DeRose, P. M.; Bruening, M. L. *J. Am. Chem. Soc.* **1999**, *121*, 1978-1979.

(56) Delcorte, A.; Bertrand, P.; Wischeroff, E.; Laschewsky, A. *Langmuir* **1997**, *13*, 5125-5136.

(57) Chen, W.; McCarthy, T. J. *Macromolecules* **1997**, *30*, 78-86.

(58) Kotov, N. A.; Magonov, S.; Tropsha, E. *Chem. Mater.* **1998**, *10*, 886-895.

(59) Krasemann, L.; Tieke, B. *Langmuir* **2000**, *16*, 287-290.

(60) Arys, X.; Jonas, A. M.; Laschewsky, A.; Legras, R. In *Supramolecular Polymers*, 2000, pp 505-563.

(61) Shiratori, S. S.; Rubner, M. F. *Macromolecules* **2000**, *33*, 4213-4219.

(62) Anzai, J.; Kobayashi, Y.; Nakamura, N.; Nishimura, M.; Hoshi, T. *Langmuir* **1999**, *15*, 221-226.

(63) Bergbreiter, D. E.; Franchina, J. G.; Kabza, K. *Macromolecules* **1999**, *32*, 4993-4998.

(64) Dermody, D. L.; Peez, R. F.; Bergbreiter, D. E.; Crooks, R. M. *Langmuir* **1999**, *15*, 885-890.

(65) Watanabe, H.; Regen, S. L. *J. Am. Chem. Soc.* **1994**, *116*.

(66) Caruso, F.; Furlong, D. N.; Ariga, K.; Ichinose, I.; Kunitake, T. *Langmuir* **1998**, *14*, 4559-4565.

(67) Lindsay, G. A.; Roberts, M. J.; Chafin, A. P.; Hollins, R. A.; Merwin, L. H.; Stenger-Smith, J. D.; Yee, R. Y.; Zarras, P.; Wynne, K. J. *Chem. Mater.* **1999**, *11*, 924-929.

(68) Yonezawa, T.; Onoue, S.; Kunitake, T. *Adv. Mater.* **1998**, *10*, 414-416.

(69) Liu, Y.; Claus, R. O. *J. Appl. Phys.* **1999**, *85*, 419-424.

(70) Fendler, J. J. *Std. Surf. Sci. Catal.* **1997**, *103*, 261-276.

(71) Kovtyukhova, N. I.; Ollivier, P. J.; Martin, B. R.; Mallouk, T. E.; Chizhik, S. A.; Buzaneva, E. V.; Gorchinskiy, A. D. *Chem. Mater.* **1999**, *11*, 771-778.

(72) Cassagneau, T.; Fendler, J. H. *Adv. Mater.* **1998**, *10*, 877-881.

(73) Dai, J.; Balachandra, A. M.; Lee, J. I.; Bruening, M. L. *Macromolecules* **2001**, *35*, 3164-3170.

(74) Dai, J.; Jensen, A. W.; Mohanty, D. K.; Erndt, J.; Bruening, M. L. *Langmuir* **2001**, *17*, 931-937.

(75) Cheung, J. H.; Fou, A. F.; Rubner, M. F. *Thin Solid Films* **1994**, *244*, 985-989.

(76) Onda, M.; Lvov, Y.; Ariga, K.; Kunitake, T. *Biotechnol. Bioeng.* **1996**, *51*, 163-167.

(77) Stepp, J.; Schlenoff, J. B. *J. Electrochem. Soc.* **1997**, *144*, L155-L157.

(78) Laurent, D.; Schlenoff, J. *Langmuir* **1997**, *13*, 1552-1557.

(79) Sun, Y.; Zhang, X.; Sun, C.; Shen, J. *Macromol. Chem. .Physic* **1996**, *197*, 147-153.

(80) Fou, A. C.; Onitsuka, O.; Ferreira, M.; Rubner, M. F.; Hsieh, B. R. *J. Appl. Phys.* **1996**, *79*, 7501-7509.

(81) Hammond, P. T.; Whitesides, G. M. *Macromolecules* **1995**, *28*, 7569-7571.

(82) Meier-Haack, J.; Lenk, W.; Lehmann, D.; Lunkwitz, K. *J. Membrane Sci.* **2001**, *184*, 233-243.

(83) Stair, J. L.; Harris, J. J.; Bruening, M. L. *Chem. Mater.* **2001**, *13*, 2641-2648.

(84) Wang, X.; Spencer, H. G. *Trends in Polym. Sci.* **1997**, *5*, 38-39.

(85) Pothakamury, U. R.; Barbosa-Canovas, G. V. *Fluid Part. Sep. J.* **1993**, *6*, 110-118.

(86) Meier-Haack, J.; Booker, N. A.; Carroll, T. *Water Res.* **2003**, *37*, 585-588.

(87) Fusaoka, Y.; Inoue, T.; Murakami, M.; Kurihara, M. *Membrane Technology Conference: The Future of Purer Water, Proceedings, San Antonio, TX, United States, Mar. 4-7, 2001* **2001**, 1369-1373.

(88) Weber, W. J., Jr.; LeBoeuf, E. J. *Water Sci. Technol.* **1999**, *40*, 11-19.

(89) Saracco, G.; Zanetti, M. C. *Ind. Eng. Chem. Res.* **1994**, *33*, 96.

(90) Ventura, X. A. *Proceedings - AESF SUR/FIN Annual International Technical Conference* **2003**, 477-492.

(91) Li, H.; He, X.; Liang, Y. *Sep. Sci. Technol.* **2003**, *38*, 1633-1648.

(92) Genders, J. D.; Hartsough, D.; Thompson, J. *Proc. - Electrochem. Soc.* **1994**, *94-22*, 457-466.

(93) Kim, S.-G.; Kim, Y.-I.; Yun, H.-G.; Lim, G.-T.; Lee, K.-H. *J. Appl. Polym. Sci.* **2003**, *88*, 2884-2890.

(94) Loeb, S.; Sourirajan, S. *Adv. Chem. Ser.* **1963**, *38*, 117-132.

(95) Polotskaya, G. A.; Kuznetsov, Y. P.; Goikhman, M. Y.; Podeshvo, I. V.; Maricheva, T. A.; Kudryavtsev, V. V. *J. Appl. Polym. Sci.* **2003**, *89*, 2361-2368.

(96) Toutianoush, A.; Tieke, B. In *Novel Methods to Study Interfacial Layers*; Elsevier: Amsterdam, 2001, pp 416-425.

(97) Jin, W.; Toutianoush, A.; Tieke, B. *Langmuir* **2003**, *19*, 2550-2553.

(98) Harris, J. J.; Stair, J. L.; Bruening, M. L. *Chem. Mater.* **2000**, *12*, 1941-1946.

(99) Stanton, B. W.; Harris, J. J.; Miller, M. D.; Bruening, M. L. *Langmuir* **2003**, *19*, 7038-7042.

(100) Riegler, H.; Essler, F. *Langmuir* **2002**, *18*, 6694-6698.

(101) Balachandra, A. M.; Dai, J.; Bruening, M. L. *Macromolecules* **2001**, *35*, 3171-3178.

(102) Sullivan, D. M.; Bruening, M. L. *J. Am. Chem. Soc.* **2001**, *123*, 11805-11806.

(103) Robeson, L. M. *J. Membrane Sci.* **1991**, *62*, 165-185.

(104) Leväsalmi, J.-M.; McCarthy, T. J. *Macromolecules* **1997**, *30*, 1752-1757.

(105) Stroeve, P.; Vasquez, V.; Coelho, M. A. N.; Rabolt, J. F. *Thin Solid Films* **1996**, *284-285*, 708-712.

(106) van Ackern, F.; Krasemann, L.; Tieke, B. *Thin Solid Films* **1998**, *327-329*, 762-766.

(107) Krasemann, L.; Tieke, B. *Mat. Sci. & Eng. C* **1999**, *8-9*, 513-518.

(108) Coleman, M. R.; Koros, W. J. *J. Polym. Sci., Part B: Polym. Phys.* **1994**, *32*, 1915-1926.

(109) Sullivan, D. M.; Bruening, M. L. *Chem. Mater.* **2003**, *15*, 281-287.

(110) Huang, R. Y. M. *Pervaporation Membrane Separation Processes*; Elsevier Science: Amsterdam, 1991; Vol. 1.

(111) Lipnizki, F.; Field, R. W. *Environ. Prog.* **2002**, *21*, 265-272.

(112) Aminabhavi, T. M.; Khinnavar, R. S.; Harogoppad, S. B.; Aithal, U. S. *J. Macromol. Sci. R. M. C.* **1994**, *C34*, 139-204.

(113) Liu, Q.-L.; Xiao, J. *J. Membrane Sci.* **2004**, *230*, 121-129.

(114) Volkov, V. V.; Fadeev, A. G.; Khotimsky, V. S.; Litvinova, E. G.; Selinskaya, Y. A.; McMillan, J. D.; Kelley, S. S. *J. Appl. Polym. Sci.* **2004**, *91*, 2271-2277.

(115) Slater, C. S.; Hickey, P. J.; Juricic, F. P. *Sep. Sci. Technol.* **1990**, *25*, 1063-1077.

(116) Krasemann, L.; Tieke, B. *J. Membrane Sci.* **1998**, *150*, 23-30.

(117) Krasemann, L.; Toutianoush, A.; Tieke, B. *J. Membrane Sci.* **2001**, *181*, 221-228.

(118) Sullivan, D. M.; Bruening, M. L. *submitted to Langmuir* **2004**.

Chapter 2

Ultrathin, Layered Polyimide Coating on Aluminum

2.1 Introduction

In 1999, Harris and Bruening reported the synthesis of ultrathin, nylon-like coatings through cross-linking of poly(acrylic acid)/poly(allylamine hydrochloride) (PAA/PAH) films deposited on gold surfaces.[1] They showed that such films have the potential to passivate surfaces, and subsequent studies examined protection of aluminum by these coatings.[2,3] Here, I report on the possibility of using similar ultrathin polyimide coatings to protect Al from corrosion. In contrast to PAA/PAH films, these coatings are constructed using a layer-by-layer method based on formation of covalent, rather than ionic, bonds. Such polyimide films protect the native oxide layer of Al, and even a 30 nm-thick film increases the impedance of Al by 2 orders of magnitude.

Nevertheless, passivation by the films employed in this work is significantly less than that of typical coatings because surface passivation generally increases with coating thickness. However, there are applications where ultrathin coatings are required. In heat exchangers, for example, coatings should be thin enough that they do not drastically reduce heat-transfer coefficients.[4,5] Thin coatings are also important for protecting electronic materials[6] and high T_c superconductors.[7]

In spite of the fact that thin films are not as passivating as thick coatings, they can provide substantial protection. This should not be too surprising, as

thin-film formation is the mechanism of corrosion prevention by inhibitors such as 1H-benzotriazole on copper.[8] In a similar way, fatty acids can form a protective layer on Al,[9-11] and alkanethiolates form protective monolayers on copper.[12-14] The ultrathin cross-linked films discussed here should have a stability advantage over monolayer films, but they do have the disadvantage of needing a heat treatment. Such heat treatments are common, however, in the deposition of practical epoxy coatings.[15]

I should note that the film-formation method used in this work is similar to a procedure reported by Liu and co-workers. They described a covalent process in which polyamidoamine (PAMAM) dendrimers and Gantrez™ (poly(methyl vinyl ether-*alt*-maleic anhydride)) are covalently deposited in a layer-by-layer fashion.[16] Heating of these films produces a passivating polyimide film.[17] In this study, I utilize poly(allylamine) and Gantrez™ in an analogous fashion to prepare layered polyimide films (Figure 2.1). Although such films provide some protection for Al, under the conditions of this study, they are slightly less protective than ultrathin nylon-like films prepared from multilayer PAA/PAH films.

2.2 Experimental Section

2.2.1 Materials. Poly(allylamine hydrochloride) (M_w ~ 70 000), sodium metal, methanol, tetrahydrofuran, and dimethyl sulfoxide were obtained from Aldrich. The Gantrez™ (M_w ~1,100,000, M_n ~310,000) was a gift from ISP Technologies (Wayne, NJ). THF and DMSO were dried using molecular sieves. Al-coated substrates were made by sputtering 200 nm of Al on Si(100) wafers. This

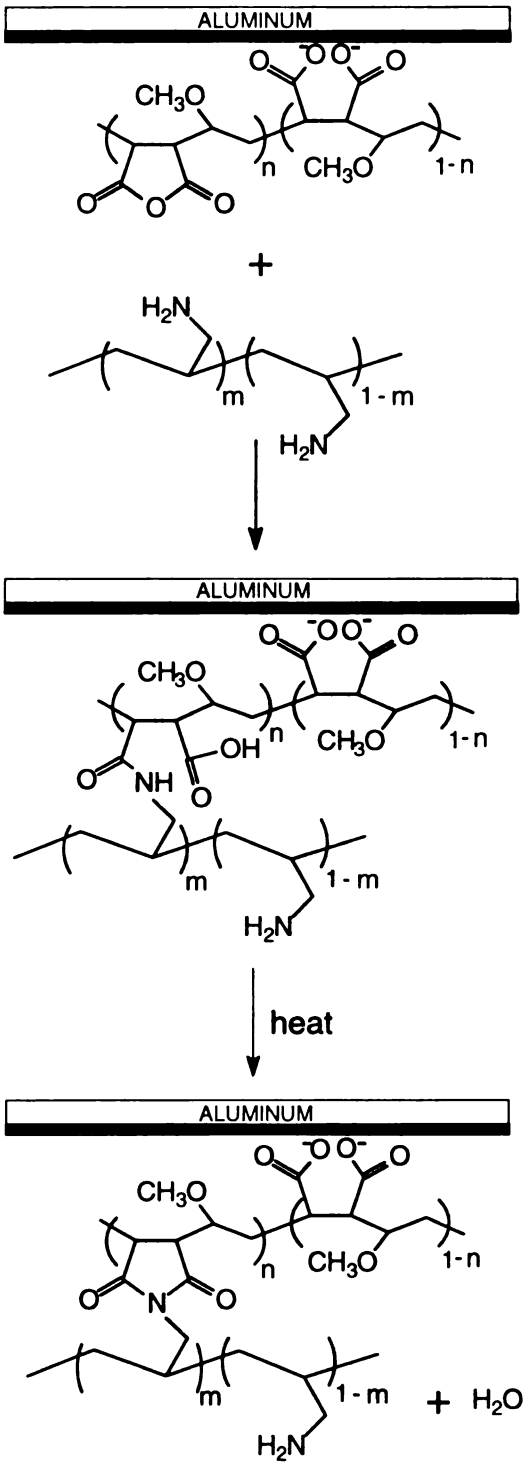

Figure 2.1: Synthesis of a Gantrez™/poly(allylamine) bilayer on Al and subsequent conversion to an imide-containing film.

substrate has a native oxide layer with an ellipsometric thickness of about 40 Å after 15 min of cleaning in a UV/O_3 cleaner. In this chapter, when we refer to Al or "bare" Al, we mean Al with its native oxide.

Poly(allylamine hydrochloride) was converted to the unprotonated poly(allylamine) (PAAm) by reacting it with freshly generated sodium methoxide. In a typical procedure, 1g of sodium metal was placed into a nitrogen-purged three-neck round-bottom flask fitted with a condenser. Then, 70 mL of methanol was added dropwise while stirring and cooling in an ice bath. After dissolution of the sodium, a stoichiometric amount of PAH (4.07 g) was added to the solution and allowed to react at room temperature for 1 h. The resulting solution was then filtered to remove some of the insoluble sodium chloride. The methanol was removed in a vacuum and the product was dissolved in chloroform. This solution was filtered to remove the remaining sodium chloride, and the chloroform was removed to yield the product. The complete conversion to poly(allylamine) is confirmed by NMR studies: ^1H NMR (300 MHz, D_2O): δ 0.8-1.45 (m), 2.25-2.55 (s).

2.2.2 Gantrez™/PAAm Film Synthesis. The Al substrate was placed in a UV/O_3 cleaner for 15 min and then immersed in the Gantrez™ solution (25 wt % in THF) for 20 min. Next, the wafer was rinsed with 3 mL of THF, placed into a 20-mL THF bath, sonicated for 3 min, and dried with N_2. The wafer was then put into a PAAm solution (0.1 wt % in DMSO) for 30 min, rinsed with 3 mL of DMSO, and sonicated in DMSO for 3 min. Residual DMSO was removed by rinsing thoroughly with THF. The procedure was repeated until the desired ellipsometric

thickness or number of bilayers was achieved. To convert amic acid groups to imides, the samples were heated at 150 °C under N_2 for 2 h.[18]

2.2.3 Film Characterization. External reflectance FTIR spectra of films were obtained with a Nicolet Magna-IR 560 spectrometer using a Pike grazing angle (80°) attachment. Film thicknesses were measured with a M-44 rotating analyzer spectroscopic ellipsometer (J. A. Woollam), assuming a film refractive index of 1.5.

2.2.4 Electrochemical Studies. Impedance data and polarization curves were obtained with a CH Instruments electrochemical analyzer (Model 604). Measurements were made using a Ag/AgCl (3 M KCl) reference electrode and a platinum wire counter electrode. The working electrode was "bare" or coated Al contained within an O-ring holder that exposed 2.2 cm^2 of the sample. We intentionally used a rather corrosive electrolyte solution (0.5 M NaCl adjusted to pH 3.0 with HCl) for impedance measurements to differentiate between the impedances of bare and film-coated Al. At neutral pH, the impedance of bare Al is as high as 10^7 Ω cm^2 after a 4 h immersion in 0.5 M NaCl due to the native aluminum oxide layer. Acquisition of impedance data started only after 4 h of immersion in NaCl solutions in order to achieve stable values. For bare Al, the impedance data were acquired at the open circuit potential (ca. -1.20 V vs Ag/AgCl) using a sinusoidal voltage of 5 mV. Other impedance measurements were made at a dc potential of -0.75 V vs Ag/AgCl because coated Al has a much more positive open circuit potential (-0.48 to -0.75 V) than bare Al. Applying potentials higher than -0.7 V (pitting potential of Al[6]) causes rapid

corrosion in some cases. The frequency range for impedance measurements was 10^5 Hz to 10 mHz. Impedance data fits were performed using LEVM 7.0 software written by J. Ross MacDonald (available from Solatron).[19] All electrochemical experiments were performed on at least three different electrodes.

2.3 Results and Discussion

2.3.1 Synthesis of Gantrez™/PAAm Films. Synthesis of Gantrez™/PAAm films occurs by alternating deposition of the two polymers as shown in Figure 2.1. In the initial deposition of Gantrez™ on Al, we speculate that anhydride groups react with the surface to form carboxylate salts. The presence of large anhydride peaks (1860 and 1790 cm^{-1}) in the FTIR spectrum of the first Gantrez™ layer (Gz 1, Figure 2.2a) shows that most of the anhydride groups did not react with the surface and are available for subsequent attachment of PAAm. Upon exposure to PAAm, most of the anhydride groups on the surface react with amine groups, covalently linking PAAm to the surface. FTIR spectroscopy (spectrum PAAm 1, Figure 2.2b) gives evidence for this reaction as the peaks corresponding to cyclic anhydrides diminish after reaction with PAAm, and amide peaks (1630 and 1540 cm^{-1}) appear. Deposition of multilayers proceeds by alternating reactions of Gantrez™ with surface amine groups and PAAm with unreacted surface anhydride groups as shown by FTIR spectra (Figure 2.2). This chemistry is analogous to that used previously in preparing films containing alternating layers of Gantrez™ and PAMAM dendrimers.[16]

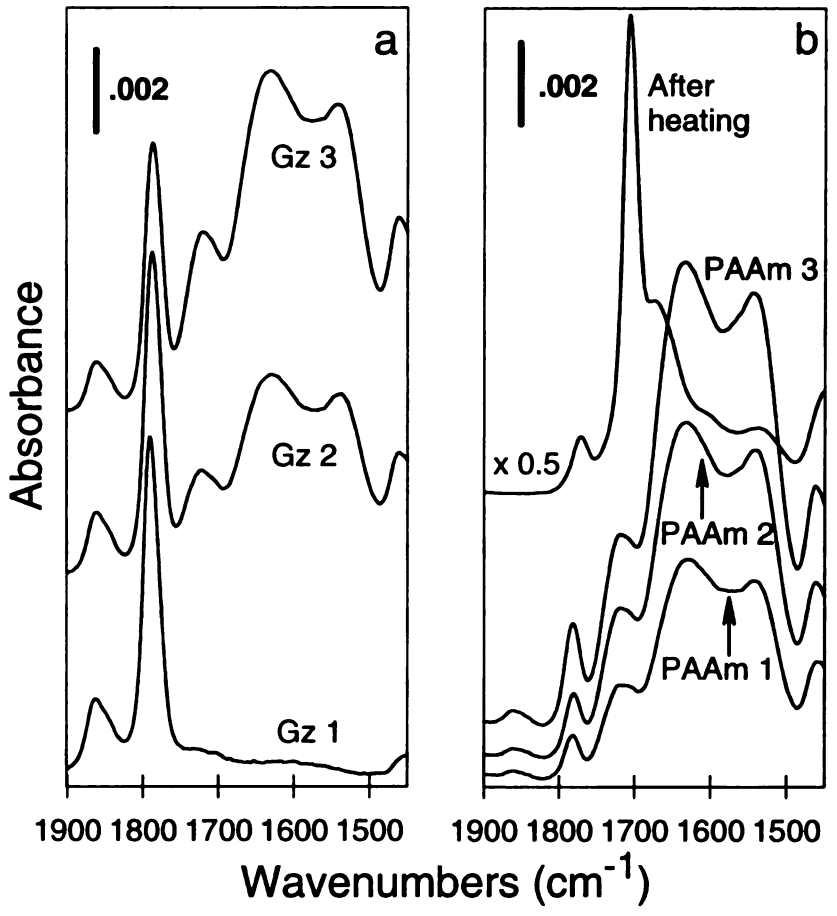

Figure 2.2: Reflectance FTIR spectra of Gantrez™/PAAm films. Figure A shows spectra after the deposition of Gantrez™ on Al (Gz 1) and on one (Gz 2) and two (Gz 3) Gantrez™/PAAm bilayers. Figure B shows the spectra after deposition of PAAm (1, 2, and 3 Gantrez™/PAAm bilayers) as well as the spectrum of a 3-bilayer film after heating. The spectrum of the heated film is multiplied by 0.5 for clarity.

Conversion of Gantrez™/PAAm films to polyimides occurs by heating of the film to convert amic acids to imides as shown in Figure 2.1. Reflectance FTIR spectra confirm this conversion as seen from the appearance of the cyclic imide bands at 1770 and 1710 cm^{-1} and the disappearance of amide bands at 1630 and 1540 cm^{-1} (Figure 2.2b). In addition to creating a polyimide film, this process likely anneals the structure, resulting in a more passivating film. Unlike previous studies with heated dendrimer/Gantrez™ films,[16,18] Gantrez™/PAAm films will not undergo retro-Michael additions to form additional internal cross-links. This is because PAAm does not contain the secondary and tertiary amines that exist in PAMAM dendrimers.

2.3.2 Electrochemical Impedance Spectroscopy. Electrochemical impedance spectroscopy is one of the most powerful methods for studying corrosion because it often provides mechanistic information about corrosion processes.[20-29] In this technique, one determines the impedance of an electrochemical cell over a wide range of frequencies and then uses an equivalent circuit to describe impedance as a function of frequency. Various equivalent circuit models were proposed to simulate the impedance behavior of coated aluminum,[22,26-28,30-32] and most of these are similar to the circuits shown in Figure 2.3. For bare Al, the insulating oxide film forms a leaky capacitor, resulting in circuit A. The presence of an organic coating that is highly blocking complicates the circuit by the introduction of another leaky capacitor as shown in circuit B. As a parallel RC component results in a semicircle in a plot of real versus imaginary components of impedance, the introduction of an organic coating often results in a plot with

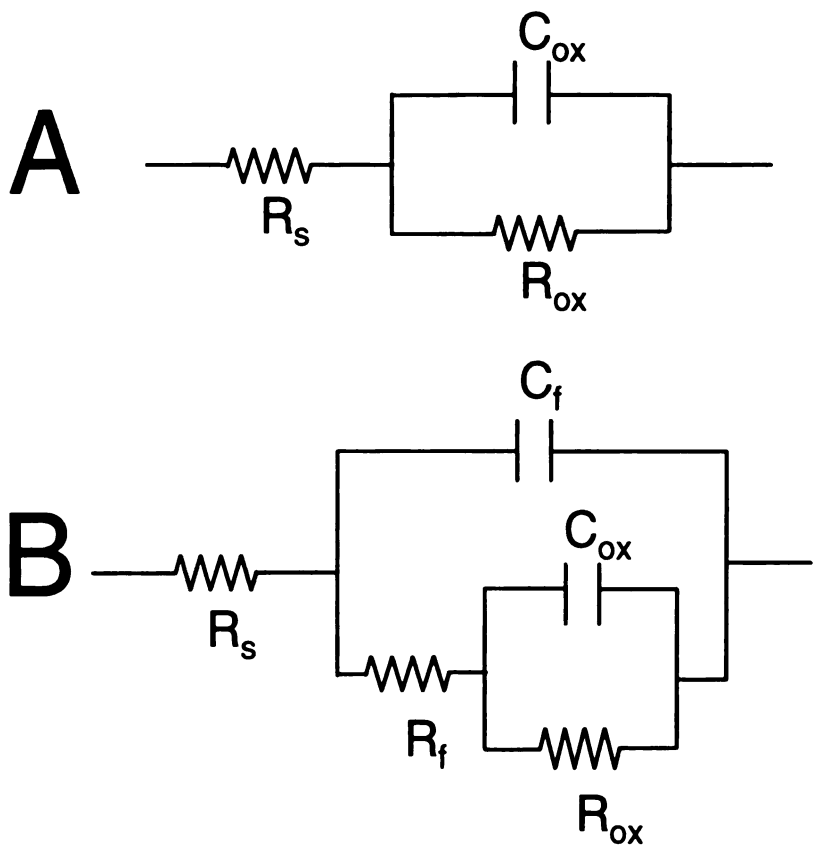

Figure 2.3: Equivalent circuits for impedance data. Circuit A was used to fit "bare" Al and Al coated with Gantrez™/PAAm films. Circuit B would be used if the organic film were highly resistive. The physical meaning of the different symbols is R_s, solution resistance, R_{ox}, oxide resistance, R_f, film resistance, C_f, film capacitance, and C_{ox}, oxide capacitance.

two partial semicircles.[20,21,26] Note that the magnitude of the diameter of each semicircle is proportional to the resistance in the parallel RC circuit.[33] Thus, larger semicircles in impedance plots represent better corrosion protection. Scully and Hensley suggest that coating resistances need to be at least 10^7 Ω cm^2 to provide effective protection of Al.[34]

2.3.3 Protection of Al by Gantrez™/PAAm Coatings. Heated Gantrez™/PAAm films protect the underlying oxide (Table 2.1), but average values for R_{ox} are a factor of 5 to 10 lower for 2- and 3-layer films than for related, heated PAA/PAH films with similar thicknesses.[3] The heated PAA/PAH films form amide cross-links upon heating rather than imides. Additiionally, the Gantrez™/PAAm films may yield less surface protection because of a lower cross-linking density or weaker binding to the Al surface. Figure 2.4 shows representative impedance plots for Al coated with a 3-bilayer Gantrez™/PAAm film before and after heating. Unlike heated PAA/PAH films, there is only one semicircle in the impedance plot for imidized Gantrez™/PAAm.[3] Plots of phase angle versus frequency also show only one RC time constant for these electrodes. This suggests that R_f values for Gantrez™/PAAm systems are minimal, so we used circuit A (Figure 2.3) to model these data.[35]

The impedance data explain why even ultrathin films may reduce the rate of Al corrosion. Binding of a monolayer of Gantrez™ to the surface passivates the oxide layer and, in turn, protects Al (Table 2.1) by increasing the oxide resistance. The film resistance due to a single Gantrez™ layer or unheated Gantrez™/PAAm films should be small, but the film still apparently inhibits

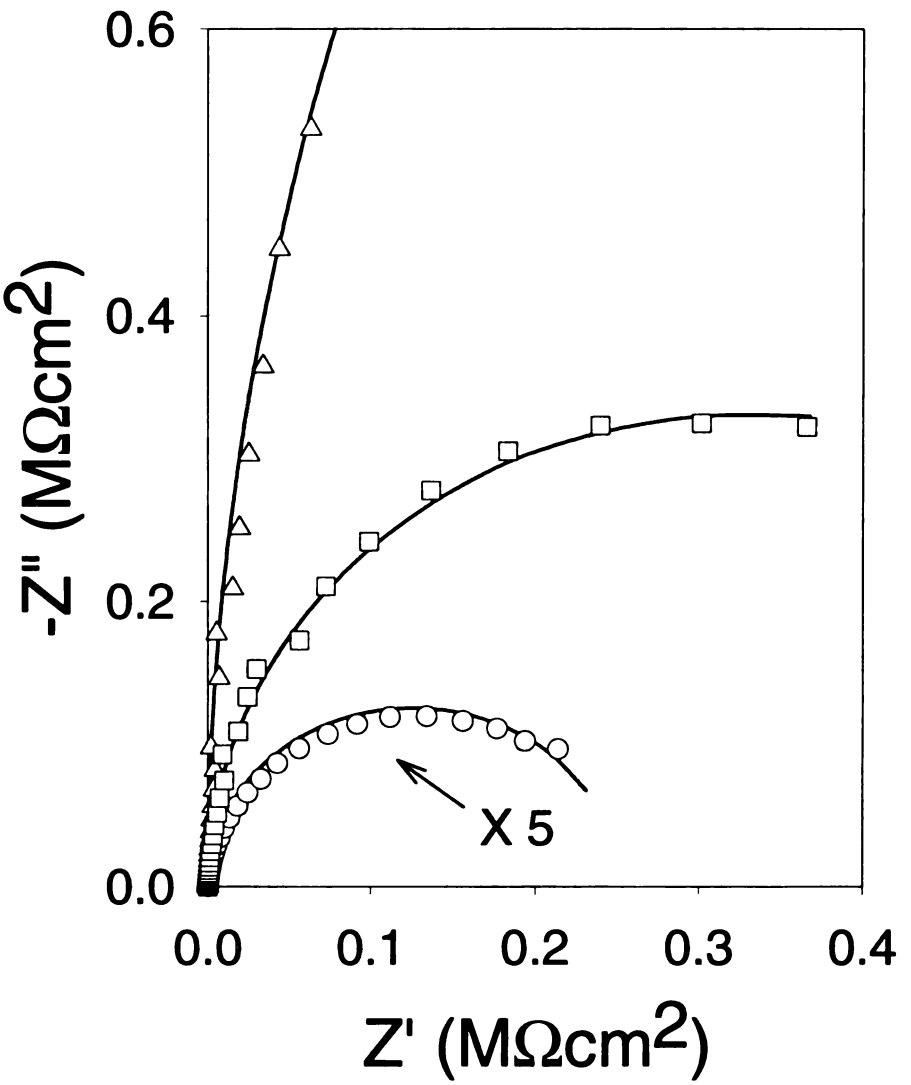

Figure 2.4: Impedance plots for bare Al (circles, both Z' and Z' ' were multiplied by 5 for clarity) and Al coated with 3 bilayers of Gantrez™/PAAm before (squares) and after heating (triangles). All impedance data were measured in 0.5 M NaCl at pH 3 after a 4 h immersion time.

Table 2.1: Coating thicknesses and equivalent circuit parameters for Al electrodes coated with various layers of Gantrez^{TM}/poly(allylamine) films.

	bare Al	monolayer, Gantrez^{TM}	1 bilayer	1.5 bilayer	2 bilayer	2.5 bilayer	3 bilayer
Coating thickness before heating (Å)	-	20	95	103	160	180	290
Coating thickness after heating (Å)	-	-	77	85	120	140	270
R_{ox} (MΩ-cm^2), unheated	-	2.5 ± 0.5	0.2 ± 0.1	0.1 ± 0.1	0.3 ± 0.2	0.7 ± 0.4	0.7 ± 0.4
R_{ox} (MΩ-cm^2), heated	0.07 ± 0.02	-	1.3 ± 0.2	1.1 ± 0.6	6 ± 4	8 ± 3	13 ± 2
C_{ox} (μF/cm^2), unheated	-	4.4 ± 0.4	5.1 ± 0.7	5.7 ± 0.5	6.2 ± 0.6	5.0 ± 0.2	4.6 ± 0.2
C_{ox} (μF/cm^2), heated	7.5 ± 1.0	-	4.1 ± 0.1	3.6 ± 0.2	3.6 ± 0.1	5.9 ± 0.3	4.5 ± 0.5

dissolution of the oxide. Thus, the oxide resistance is equivalent to what it would be in a less corrosive, neutral solution. Previous studies showed that copolymers of maleic acid and styrene protect pigments in solution,[36] but it is somewhat surprising that pure Gantrez™ provides protection because it is not particularly hydrophobic (the 4 h immersion time in water should convert the remaining anhydrides to diacids). We surmise that a protective layer of Al carboxylates is forming on the surface similar to protective layers formed by corrosion inhibitors.[8,10] The layer inhibits Cl^- adsorption,[37] thus protecting the oxide. This layer will not be as ordered as protective films of self-assembled monolayers, but it does passivate the oxide film

Oxide resistances of Al electrodes coated with Gantrez™/PAAm films depend substantially on the number of layers in the film and whether the film is imidized. Interestingly, reaction of the Gantrez™ with a layer of PAAm results in a 12-fold decrease in oxide resistance (unheated films, Table 2.1). This may be due to the fact that PAAm is more hydrophilic than Gantrez™. Imidization of Gantrez™/PAAm films increases R_{ox} by an order of magnitude.

As the number of Gantrez™/PAAm layers increases, oxide resistance increases significantly (Table 2.1). For heated films, R_{ox} increases by an order of magnitude on going from 1 to 3 bilayers of Gantrez™/PAAm. Multilayers increase R_{ox} values because they protect the oxide from degradation, even though their resistance may not be extremely high. An increasing number of layers may result in fewer defects in the coating. C_{ox} does not vary much with

the number of layers because the thickness and dielectric constant of the aluminum oxide are relatively independent of coating thickness.

2.4 Conclusions

Gantrez™/PAAm films can be synthesized on Al by a simple "dip and rinse", layer-by-layer method. Each added layer binds covalently to the previous layer via reaction of an anhydride (Gantrez™) with a primary amine (PAAm). Heating of these films results in imidation of Gantrez™/PAAm, and even a single monolayer of Gantrez™ attached to the surface protects the aluminum oxide and increases the oxide resistance by 35-fold. For Gantrez™/PAAm films on Al, electrode impedance depends on both the number of bilayers and whether the film is imidized. Imidization increases oxide resistance by an order of magnitude over unheated films.

2.5 References

(1) Harris, J. J.; DeRose, P. M.; Bruening, M. L. *J. Am. Chem. Soc.* **1999**, *121*, 1978-1979.

(2) Harris, J. J.; Bruening, M. L. *Langmuir* **2000**, *16*, 2006-2013.

(3) Dai, J.; Sullivan, D. M.; Bruening, M. L. *Ind. Eng. Chem. Res.* **2000**, *39*, 3528-3535.

(4) Flemming, H.-C.; Schaule, G. *Werkst Korros* **1994**, *45*, 29-39.

(5) Melo, L. F.; Bott, T. R. *Exp. Therm. Fluid Sci.* **1997**, *14*, 375-391.

(6) Bellucci, F.; Nicodemo, L.; Monetta, T.; Kloppers, M. J.; Latanision, R. M. *Corros. Sci.* **1992**, *33*, 1203-1226.

(7) Ritchie, J. E.; Wells, C. A.; Zhou, J.-P.; Zhao, J.; McDevitt, J. T.; Ankrum, C. R.; Jean, L.; Kanis, D. R. *J. Am. Chem. Soc.* **1998**, *120*, 2733-2745.

(8) Brusic, V.; Frisch, M. A.; Eldridge, B. N.; Novak, F. P.; Kaufman, F. B.; Rush, B. M.; Frankel, G. S. *J. Electrochem. Soc.* **1991**, *138*, 2253-2259.

(9) Allara, D. L.; Nuzzo, R. G. *Langmuir* **1985**, *1*, 45-52.

(10) Ogawa, H.; Chihera, T.; Taya, K. *J. Am. Chem. Soc.* **1985**, *107*, 1365-1369.

(11) Fischer, E. R.; Parker, J. E., III *Corrosion* **1997**, *53*, 62-64.

(12) Haneda, R.; Nishihara, H.; Aramaki, K. *J. Electrochem. Soc.* **1997**, *144*, 1215-1221.

(13) Jennings, G. K.; Laibinis, P. E. *Colloid Surface A* **1996**, *116*, 105-114.

(14) Jennings, G. K.; Munro, J. C.; Yong, T.-H.; Laibinis, P. E. *Langmuir* **1998**, *14*, 6130-6139.

(15) Grandle, J. A.; Taylor, S. R. *Corrosion* **1994**, *50*, 792-803.

(16) Liu, Y.; Bruening, M. L.; Bergbreiter, D. E.; Crooks, R. M. *Angew. Chem. Int. Ed. Engl.* **1997**, *36*, 2114-2116.

(17) Zhao, M.; Liu, Y.; Crooks, R. M.; Bergbreiter, D. E. *J. Am. Chem. Soc.* **1999**, *121*, 923-930.

(18) Zhao, M.; Zhou, Y.; Bruening, M. L.; Bergbreiter, D. E.; Crooks, R. M. *Langmuir* **1997**, *13*, 1388-1391.

(19) Macdonald, J. R. *Solid State Ionics* **1992**, *58*, 97-107.

(20) Deflorian, F.; Fedrizzi, L.; Bonora, P. L. *Prog. Org. Coat.* **1993**, *23*, 73-88.

(21) Deflorian, F.; Miskovic-Stankovic, V. B.; Bonora, P. L.; Fedrizzi, L. *Corrosion* **1994**, *50*, 438-446.

(22) Kendig, M.; Scully, J. *Corrosion* **1990**, *46*, 22-29.

(23) Mansfeld, F.; Chen, C.; Lee, C. C.; Xiao, H. *Corros. Sci.* **1996**, *38*, 497-513.

(24) Bonora, P. L.; Deflorian, F.; Fedrizzi, L. *Electrochim. Acta* **1996**, *41*, 1073-1082.

(25) Griffin, A. J. J.; Brotzen, F. R. *J. Electrochem. Soc.* **1994**, *141*, 3473-3479.

(26) Su, P.-C.; Devereux, O. F. *Corrosion* **1998**, *54*, 419-427.

(27) Mertens, S. F.; Xhoffer, C.; DeCooman, B. C.; Temmerman, E. *Corrosion* **1997**, *53*, 381-388.

(28) Scholl, H.; Jimenez, M. M. D. *Corros. Sci.* **1992**, *33*, 1967-1978.

(29) Lin, S.; Shih, H.; Mansfeld, F. *Corros. Sci.* **1992**, *33*, 1331-1349.

(30) Bessone, J.; Mayer, C.; Jüttner, K.; Lorentz, W. J. *Electrochim. Acta.* **1983**, *28*, 171-175.

(31) Bellucci, F.; Kloppers, M.; Latanision, R. M. *J. Electrochem. Soc.* **1991**, *138*, 40-48.

(32) Mansfeld, F.; Kendig, M. W.; Tsai, S. *Corrosion* **1982**, *38*, 478-485.

(33) Bard, A. J.; Faulkner, L. R. *Electrochemical Methods Fundamentals and Applications*; John Wiley & Sons, Inc.: New York, 1980.

(34) Scully, J. R.; Hensley, S. T. *Corrosion* **1994**, *50*, 705-716.

(35) There is a small possibility that film resistance is high, but the time constants (τ = 1/RC) for the two parallel RC components in circuit B (Figure 2.3) are similar. This would also result in only one semicircle in impedance plots

(36) Mueller, B.; Mebarek, D. *Angew. Makromol. Chem.* **1994**, *221*, 177-185.

(37) El-Awady, A. A.; Abd-El-Nabey, B. A.; Aziz, S. G. *J. Chem. Soc., Faraday Trans.* **1993**, *89*, 795-802.

Chapter 3

Ultrathin, Ion-Selective Polyimide Membranes Prepared from Layered Polyelectrolytes

3.1 Introduction

Membrane-based separations are attractive because of their convenience and low energy costs.[1,2] Separation occurs by simply flowing a mixture past a membrane, and by either a pressure or concentration gradient, primarily one component of the mixture will permeate through the membrane. In spite of the appeal of such separations, development of highly selective membranes that allow practical fluxes is an ongoing challenge. This is particularly true because flux is often inversely proportional to selectivity.[3]

The tradeoff between flux and selectivity generally requires that practical membrane systems consist of an ultrathin, selective skin on a highly permeable support. The minimal thickness of the selective layer allows a reasonable flux, while the support provides needed mechanical strength. Such membranes are often prepared by phase-inversion processes that result in a polymeric material with a dense surface layer and a highly porous bulk.[4,5] Composite membranes provide an appealing alternative to phase inversion, because deposition of a thin, selective layer on an inexpensive support allows use of more expensive, and potentially more discriminating, skin materials.[6,7]

This chapter describes the formation of selective polyimide skins on porous alumina by alternating polyelectrolyte deposition (APD) and subsequent

imidization (Figure 3.1). Deposition of the polyimide film on a relatively permeable PSS/PAH base layer allows coverage of the surface with an extremely thin (4 – 9 nm) polyimide film. Additionally, the APD/heating method is convenient and affords control over the selectivity of the polyimide film.[8-10] Such polyimide membranes show remarkably selective transport of singly over doubly charged ions (Cl^-/SO_4^{2-} selectivities reach values as high as 1000), and their minimal thickness permits high flux of the monovalent species.

Aromatic polyimides are, in general, attractive membrane materials because of their mechanical strength, thermal stability, selectivity, and wide tunability.[11-13] With common processing techniques, however, it is difficult to form ultrathin selective membranes with thickness less than 40 nm. APD, on the other hand, offers an easy way to deposit ultrathin multilayered films. A few previous studies combined APD of poly(amic acids) and a polycation with post-deposition heating to form polyimide films.[14-16] Here we utilize this approach to form highly selective, ultrathin polyimide membranes on porous supports coated with multilayered polyelectrolyte gutter layers. Because the polyimide portion of such systems is ultrathin, these membranes simultaneously allow high flux and high selectivity. Although several groups studied layered polyelectrolyte membranes for various applications,[17-23] the polyimide films described here show unique ion-transport selectivities with deposition of only a few layers.

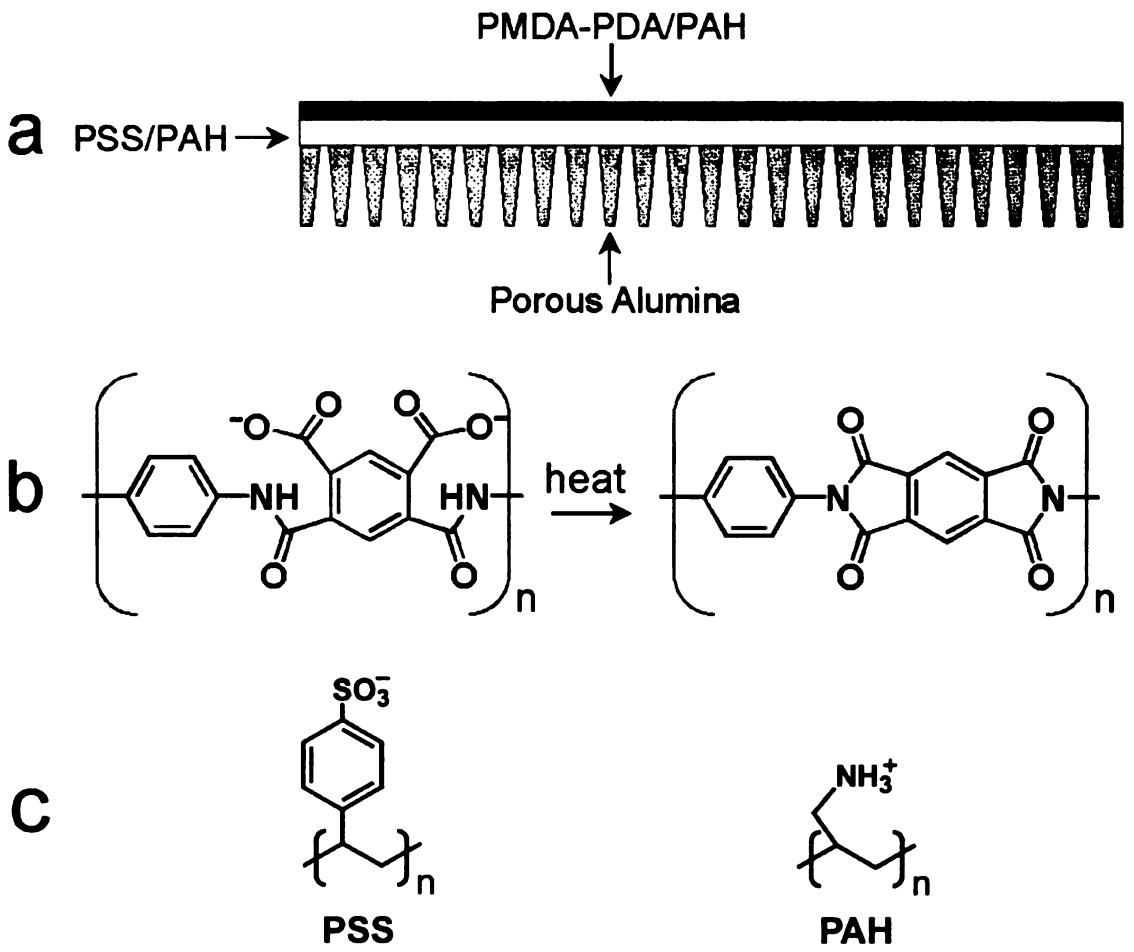

Figure 3.1: (a) Membrane consisting of a porous alumina support, a PSS/PAH base layer, and a PMDA-PDA/PAH selective capping layer (b) PMDA-PDA structure and heat induced imidization and (c) PSS and PAH structures.

3.2 Experimental

3.2.1 Chemicals and Materials. Poly(sodium 4-styrenesulfonate) (PSS, M_W = 70,000), poly(allylamine hydrochloride) (PAH, M_W = 70,000), pyromellitic dianhydride, 1,4 phenylenediamine, *N,N*-dimethylacetamide, and mercaptopropionic acid (MPA) were used as received from Aldrich. Solutions of KCl, K_2SO_4, $K_3Fe(CN)_6$, $BaCl_2$, $CaCl_2$, and $MgCl_2$ were prepared to 0.1 M in 18.2 MΩ-cm deionized (Milli-Q) water. Alumina support membranes (Whatman Anopore, 0.02 μm pore diameter skin layer, 25 mm diameter) were purchased from Fisher. Silicon(100) wafers (Silicon Quest) sputter coated with either 200 nm of Al or 20 nm of Cr and then 200 nm of Au were used as supports for ellipsometry and reflectance FTIR measurements.

3.2.2 Substrate Preparation. In the case of porous alumina supports, the polypropylene support ring on the alumina was removed to prevent it from melting into substrate pores during heat-induced imidization. This was accomplished by cutting off as much of the polymer as possible with scissors, and then burning off the remaining ring at 400 °C for 18 h in a furnace. Subsequently, the alumina supports were rinsed with acetone, dried with N_2, and cleaned for 15 min in a UV/O_3 cleaner (Boekel Industries, model 135500). Au-coated wafers were first cleaned with "piranha" solution (70% H_2SO_4(conc)/30% H_2O_2(aq): *caution*: piranha is a strong oxidizer and should not be stored in closed containers), rinsed in water, and dried with N_2. They were then immersed into a 2 mM MPA in ethanol solution for 30 min, rinsed with ethanol, and dried with N_2. Al-coated wafers were simply cleaned by UV/O_3 prior to use.

3.2.3 Synthesis of PMDA-PDA. The poly(amic acid), poly(pyromellitic dianhydride- phenylenediamine) (PMDA-PDA),[24] was prepared using a typical literature procedure.[25] 1,4 phenylenediamine (0.66 g) was dissolved in *N,N*-dimethylacetamide (50 mL) and pyromellitic dianhydride (1.34 g) was added to the solution in small increments over a ~15 min period. This mixture was purged with nitrogen and stirred for 24 h. The PMDA-PDA was precipitated into 1.5 L of ethanol and was subsequently filtered. The product was dried by vacuum, dissolved in an additional 50 ml of *N,N*-dimethylacetamide, and precipitated into ethanol once again. The final product was dried by vacuum overnight and stored in a desiccator until needed.

3.2.4 Film Characterization. Ellipsometric thickness measurements on Al-coated silicon wafers were made using a rotating analyzer ellipsometer (model M-44, J. A. Woollam) and WVASE32 software. A film refractive index of 1.5 was assumed in all thickness determinations. Reflectance FTIR spectra were obtained using a Nicolet Magna-560 FTIR spectrophotometer and a Pike grazing angle (80º) attachment. A UV/O_3-cleaned substrate was used as a background. Field-emission scanning electron microscopy (FESEM) images were obtained with a Hitachi S-4700 II instrument using an acceleration voltage of 15 kV. Samples were fractured in liquid nitrogen and sputter-coated with 5 nm of gold before imaging.

3.2.5 Membrane Preparation. Specially designed holders that expose only one side of the membrane to solution were used during the deposition of the polyelectrolytes. This limits film growth to the top of the membrane and keeps

polymer from filling the pores from the back side. Film preparation starts with exposure of the cleaned membrane surface to a solution of PSS (20 mM, with respect to the repeating unit, in 0.5 M $MnCl_2$, pH adjusted to 2.3, Figure 3.1c) for 2 minutes. A single layer of negatively charged PSS remains on the surface after rinsing with deionized water for 1 minute. Exposure to a PAH solution (20 mM in 0.5 M NaBr, pH adjusted to 2.3, Figure 3.1c) for 5 min followed by water rinsing for 1 min yields a second, positively charged layer on the alumina. This procedure was repeated until 5 PSS/PAH bilayers were deposited.

PMDA-PDA solutions for APD were made by first dissolving ~16 mg PMDA-PDA in 1 ml of 0.15 M triethylamine. This solution was then diluted to 10 ml (5 mM), with 0.5 M NaCl, and the pH was adjusted to 4.5. This solution was prepared only when needed to reduce the risk of hydrolysis of the poly(amic acid). The PMDA-PDA solution was deposited on the 5 bilayers of PSS/PAH for 3 min and rinsed to yield the first PMDA-PDA layer. PAH (0.02 M, 0.5 M NaCl, pH adjusted to 4.5) was added in the same manner. This procedure was repeated until 1.5, 2.5, or 3.5 bilayers were built up. The extra half bilayer indicates that the membranes terminated in the poly(amic acid). The samples were dried with N_2 only after all of the layers were added.

3.2.6 Membrane Transport. Dialysis was performed using a holder composed of two identical glass cells (100 ml volume) connected by a flange with a 2.1 cm^2 hole (Figure 3.2). The membrane was centered over the hole and an O-ring was placed on its top side to provide a seal and some cushion. The membrane separates a source phase solution (0.1 F salt, unbuffered, pH 5.3-6.2) from a

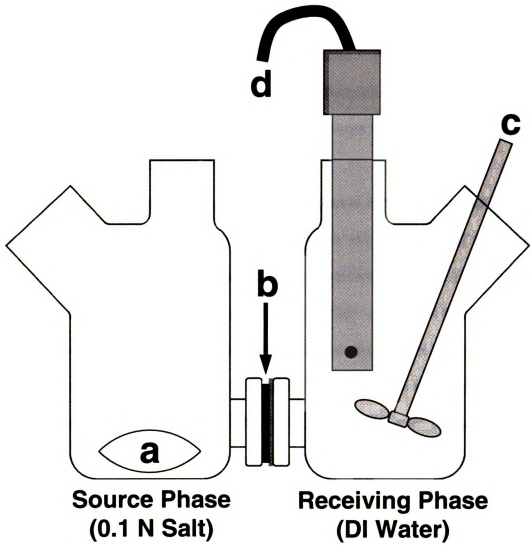

Figure 3.2: Dialysis setup used to measure ion-permeability of polyelectrolyte membranes: magnetic stir bar (a), O-ring and membrane (b), mechanical stir prop, motor not shown (c), and conductivity probe (d).

receiving phase that initially contains deionzed water.[26] Both phases were stirred vigorously to reduce concentration polarization at the two membrane surfaces. The receiving phase conductivity was measured at 5 min intervals for 45 min to monitor the change in concentration, and these values were divided by the source phase conductivity to normalize the data. The conductivity data were converted to concentration via fitting to conductivity calibration curves of standard salt solutions ($5e^{-7}$ to 0.1 M). Selectivity coefficients were determined by dividing KCl flux values by those of another salt.

In diffusion dialysis experiments, membrane conditioning was required to obtain steady flux values. (We witnessed an increase in KCl flux for initial transport experiments.) We repeated measurements of KCl, K_2SO_4, $K_3Fe(CN)_6$, $BaCl_2$, $CaCl_2$, and $MgCl_2$ fluxes twice in this order, with one final KCl measurement. The last two KCl flux measurements differed by less then 10%, so we utilized the second set of flux values to calculate selectivity. Additionally, experiments were performed in which the flux of KCl was measured between experiments with each of the above salts, and the incremental change in KCl flux values did not indicate an effect from the salts used. The increase in flux during conditioning is most likely due to swelling and reorganization of the polymers.

3.3 Results and Discussion

3.3.1 Deposition of PMDA-PDA/PAH Films on Al and Au. One challenge in depositing PMDA-PDA/PAH films by APD is making a poly(amic acid) solution for deposition. Poly(amic acids) are not water soluble as synthesized, so extra steps

are needed to make the polyelectrolyte solution. One method is to first dissolve the poly(amic acid) in an organic solvent, such as DMF, and then dilute with water.[14] Another way to do this (without organic solvents) is to convert the protonated poly(amic acid) into the readily water soluble salt form (Figure 3.1b).[15,16] We accomplished this by simply dissolving the polymer in a solution containing a base (0.15 M triethylamine), and then further diluting this mixture with water. The solution properties, such as pH and salt concentration, can then be adjusted to control the thickness of the film. We found that the PMDA-PDA would precipitate out of a 0.5 M NaCl solution when the pH was lowered below 4.0. Therefore, we made these solutions at pH 4.5 to minimize the risk of non-electrostatic polymer adsorption at the membrane surface.

We first investigated the alternating deposition of PMDA-PDA and PAH directly on Al-coated Si wafers. These substrates are convenient to use for APD because the oxide layer is net positively charged and therefore does not require treatment to introduce charged groups on its surface. Film preparation begins with an immersion into the poly(amic acid) solution, during which a layer of PMDA-PDA attaches electrostatically to the oxide surface. After rinsing the substrate with water, immersion into a PAH solution yields another layer (two layers, PMDA-PDA/PAH, are referred to as one bilayer). Subsequent alternating immersions into PMDA-PDA and PAH solutions produce a multilayer film. Reflectance FTIR spectra demonstrate the layer-by-layer growth of these films, as absorbances increase regularly with the number of deposited bilayers (Figure 3.3). Ellipsometric studies also indicate a linear growth for PMDA-PDA/PAH

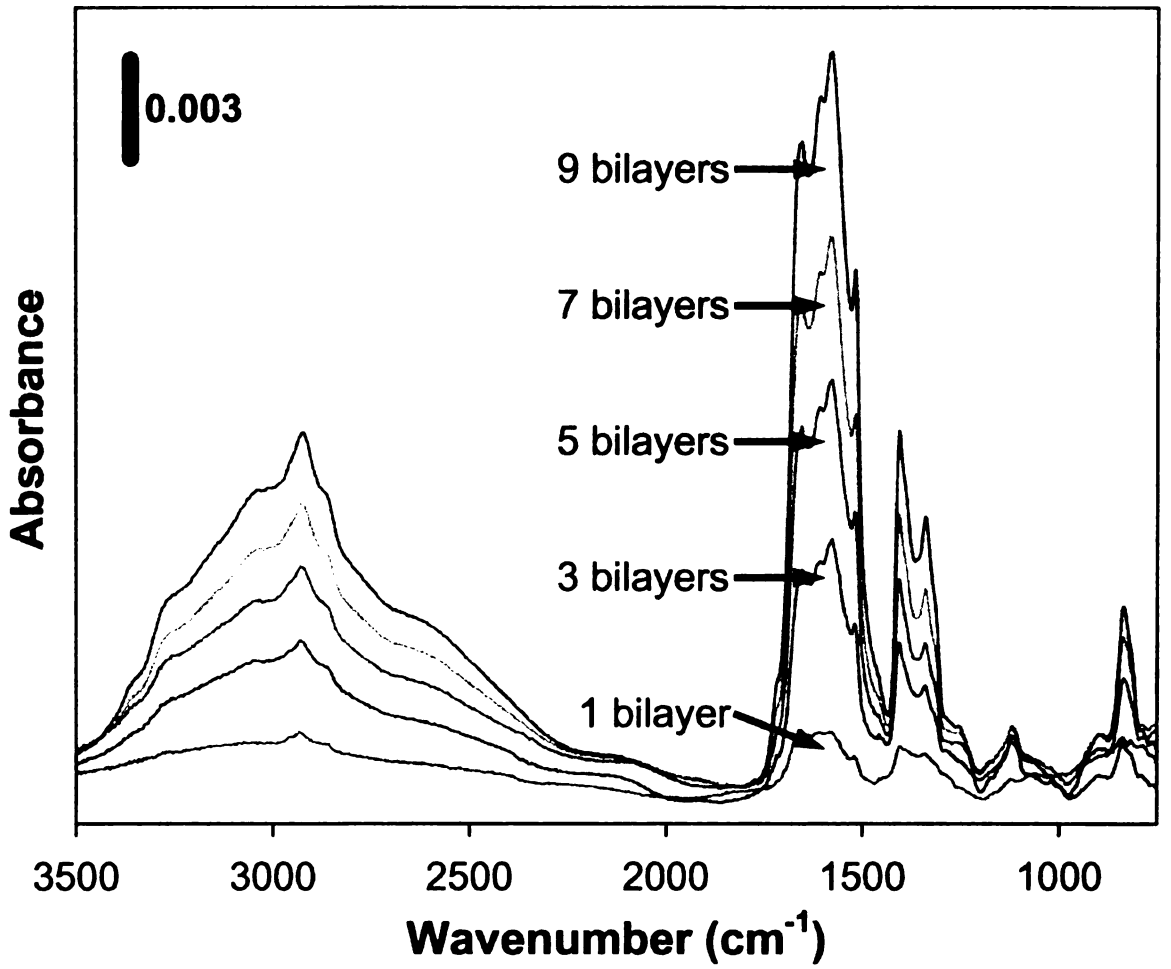

Figure 3.3: Reflectance FTIR spectra of 1, 3, 5, 7, and 9 bilayers of PMDA-PDA/PAH on Al-coated Si wafters.

films with a 26 Å increase in thickness per bilayer (Figure 3.4). Heating of these films at 150 °C reduces the bilayer thickness to 23 Å.

We also investigated whether PMDA-PDA/PAH films will deposit on top of a PSS/PAH coated substrate. We used Au-coated Si wafers modified with a monolayer of MPA because the lower pH solutions employed in PSS/PAH film deposition corroded the Al-coated substrates. Deprotonation of the carboxylic acid groups of MPA yields a negatively charged surface, so deposition began with PAH. The ~170 Å thick PSS/PAH films (4.5 bilayers) terminate with PAH, so PMDA-PDA/PAH deposition occurred as described above. Figure 3.5 shows the separate spectra of both PMDA-PDA and PSS/PAH films, and a spectrum of a composite PSS/PAH + PMDA-PDA/PAH film.

Heating PMDA-PDA under N_2 yields a polyimide membrane (Figure 3.1b). To examine the extent of imidization, we prepared PAH/PSS (4.5-bilayers) + PMDA-PDA/PAH films on gold supports and measured their reflectance FTIR spectra. Figure 3.6 shows spectra of films containing a 2.5-bilayer top coat of PMDA-PDA/PAH before and after heating for 2 h under a N_2 atmosphere. Unheated films have a broad absorbance band from 1680 to 1520 cm^{-1}, primarily due to the overlap of the amide and asymmetric $-COO^-$ stretches of the poly(amic acid). The symmetric $-COO^-$ stretch appears at 1407 cm^{-1}. Heating of these films results in the appearance of asymmetric and symmetric imide carbonyl peaks (1775 and 1730 cm^{-1}, respectively) and the disappearance of amide and carboxylate peaks. Higher heating temperatures result in higher intensities of imide peaks, showing that one can control the extent of imidization.

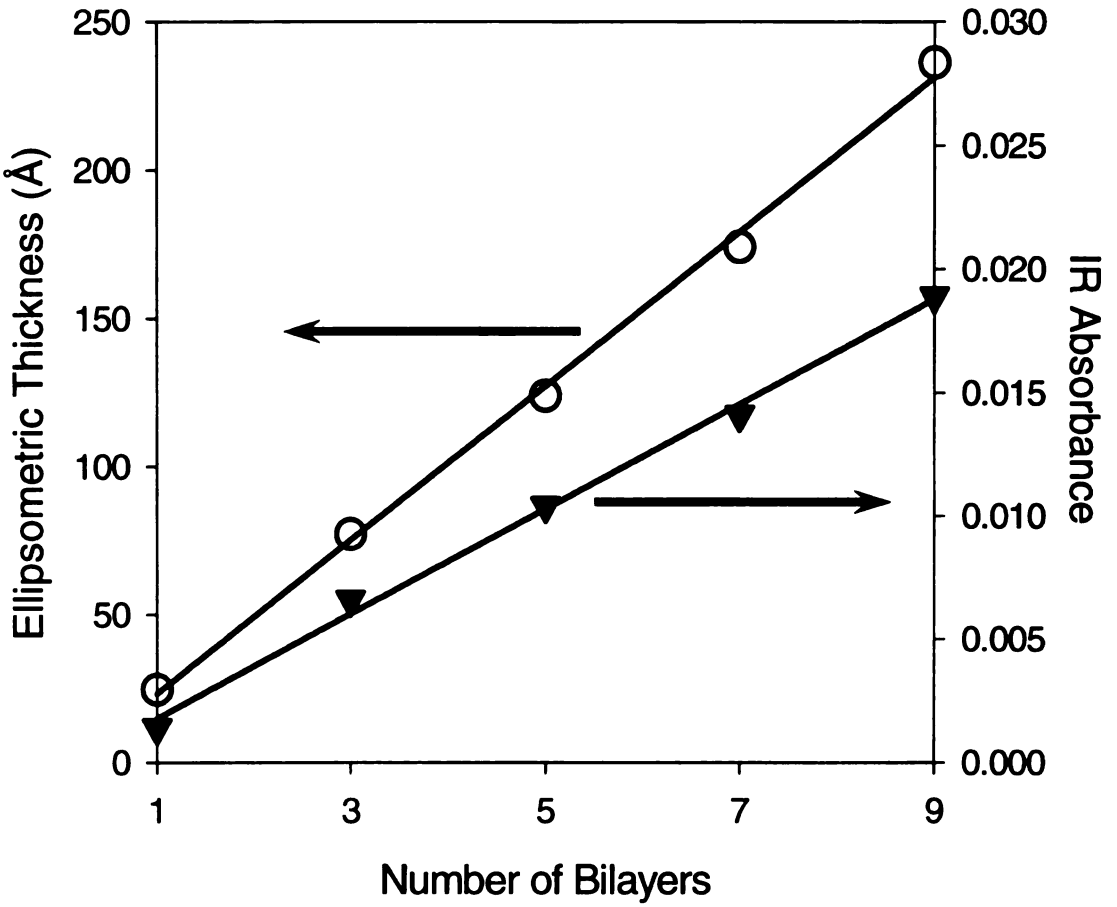

Figure 3.4: Ellipsometric thickness and absorbance at 1580 cm^{-1} of PMDA-PDA/PAH films on Al-coated Si wafers as a function of the number of bilayers in the film.

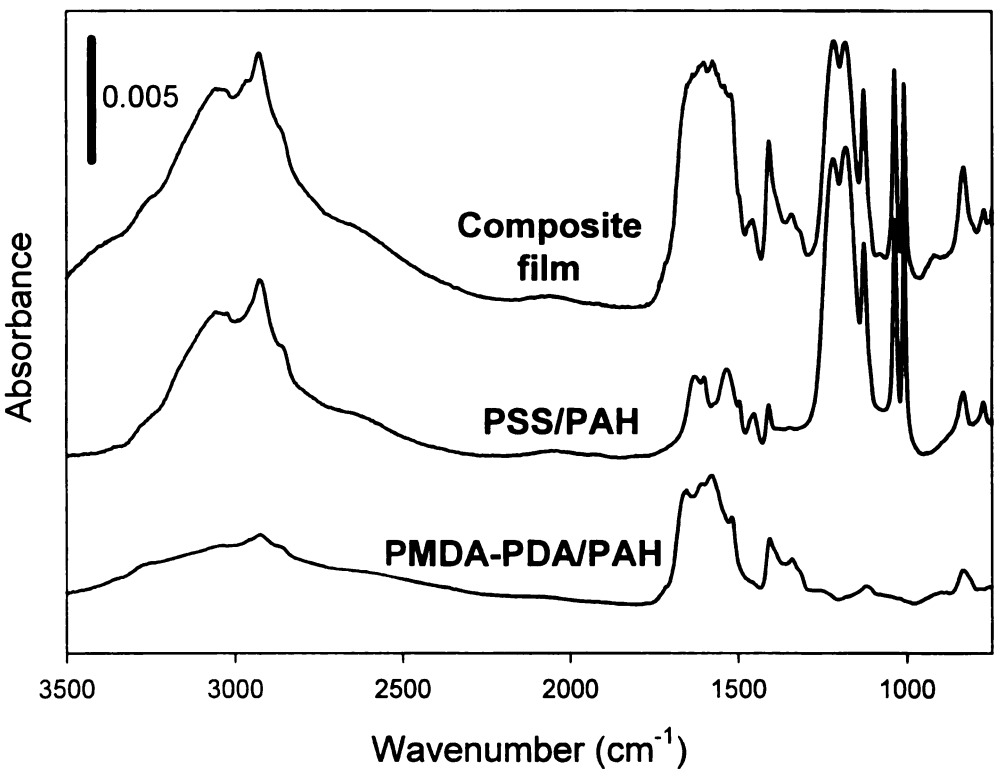

Figure 3.5: Reflectance FTIR spectra of 2.5 bilayers of PMDA-PDA/PAH, 4.5 bilayers of PSS/PAH, and the composite film (same number of bilayers for each) deposited on gold-coated substrates modified with MPA.

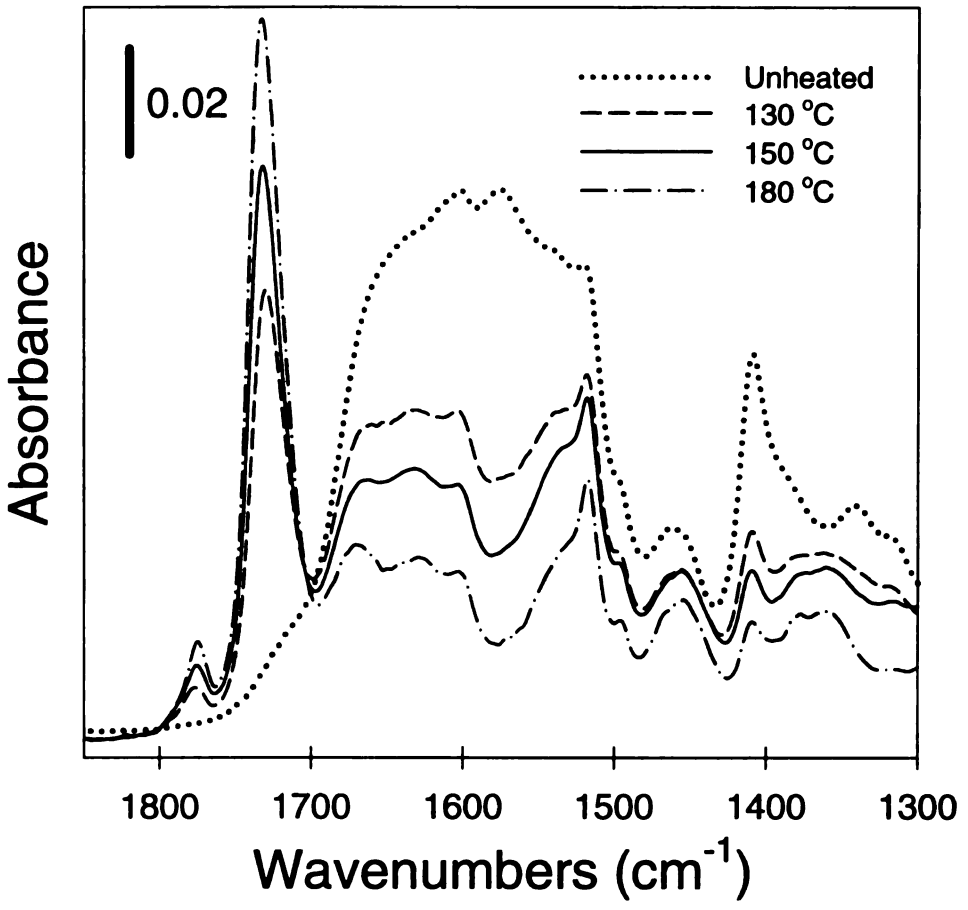

Figure 3.6: Reflectance FTIR spectra of films containing a PAH/PSS base of 4.5 bilayers and a PMDA-PDA/PAH topcoat of 2.5 bilayers before and after heating for 2 h at several temperatures. Films were deposited on gold-coated substrates modified with MPA.

3.3.2 Coverage of porous alumina. The first challenge in forming ultrathin polyelectrolyte membranes is to show that they completely cover a porous substrate without filling underlying pores. Previous FESEM studies of 5-bilayer PSS/PAH coatings attached electrostatically to porous alumina supports showed complete pore coverage with little penetration of polymer into the underlying cavities.[26] Figure 3.7 shows examples of typical top-down and cross-sectional FESEM images of porous alumina coated with 5 bilayers of PSS/PAH and capped with PMDA-PDA/PAH. Top-down images (Figure 3.7a) suggest complete pore coverage (no pores are visible), and since the film deposition was restricted to the top-side, images of the uncoated alumina backside show completely open pores (not shown). There also appear to be cracks in the membrane surface, but these are likely a result of the gold that was sputter-coated onto the surface to provide a conductive layer for imaging or contraction of the film in the SEM vacuum. Cross-sectional images (Figure 3.7b) show 40 to 50 nm-thick films and, this and other images suggest that films are relatively uniform across the support. These images show very little, if any, deposition of polyelectrolytes on the walls of the 0.2-μm-diameter pores that make up the majority of the porous alumina.

3.3.3 PSS/PAH base layer. Previous diffusion dialysis studies on PSS/PAH films show little difference in the flux of singly charged ions through film-coated and bare alumina supports. The porous alumina substrate is effectively covered with as few as 4.5 bilayers of PSS/PAH (anionic top layer), but KCl flux only

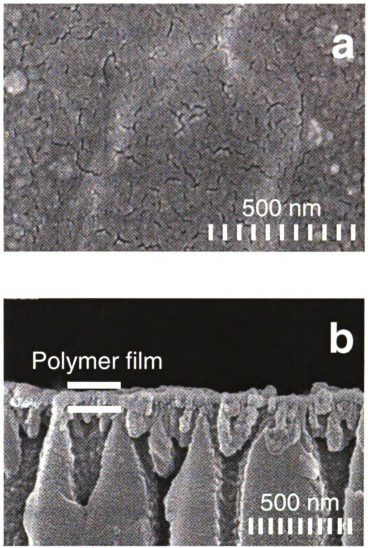

Figure 3.7: Top-down (a) and cross-sectional (b) FESEM images of porous alumina coated with 5 bilayers of PSS/PAH and capped with 2.5 bilayers of PMDA-PDA/PAH.

decreases by 25% relative to the bare support. Addition of more bilayers has little effect on the flux, as 9.5-bilayer films reduce KCl flux by only 33%. In the case of K_2SO_4, flux drops by ~80% compared to bare alumina for both 4.5 and 9.5 bilayer PSS/PAH films. The difference in KCl and K_2SO_4 fluxes results in a Cl^-/SO_4^{2-} selectivity of 5 to 7. The relatively small changes in flux that occur when doubling the thickness of the film suggest that Donnan exclusion near the surface is the major factor in the selectivity. The excess charge at the surface hinders transport of divalent ions whose charge is of the same sign as the surface charge, and this explains the larger flux for singly charged Cl^- relative to doubly charged SO_4^{2-}.

The Donnan exclusion model is also consistent with the fact that if the outer layer is changed to the positively charged PAH (changing from a 4.5 to 5 bilayer membrane) the K_2SO_4 flux increases by 120%. Therefore, we think these PSS/PAH films have a large free-volume that permits high fluxes, while their highly charged surface allows for Donnan selectivity between single and multiply charged ions. Thus, when using PSS/PAH as a gutter layer, the polyimide portion of the membrane will still be the dominant factor in controlling transport, as PSS/PAH provides little resistance to mass transport . A similar approach was previously used to form a thin, discriminating skin layer of poly(acrylic acid)/PAH on top of PSS/PAH.[18]

3.3.4 Unheated PMDA-PDA/PAH membranes. When membrane skins are composed entirely of imidized PMDA-PDA/PAH (9.5 bilayers), salt flux is about 2 orders of magnitude lower than that through bare alumina supports. These

results are similar to those for heated PAA/PAH membranes.[18] Therefore, we used PSS/PAH as a highly permeable gutter-layer to allow for a reduction in the polyimide film thickness. Since the pores in the alumina are already covered by PSS/PAH, only a very thin skin of PMDA-PAH/PAH is needed form a defect-free, selective coating that controls transport properties.

We prepared alumina membranes coated with 5 bilayers of PSS/PAH (terminating with PAH) and capped these systems with 1.5, 2.5, or 3.5 bilayers of PMDA-PDA/PAH (terminating with PMDA-PAH). The KCl flux for these unheated membranes is essentially the same as that through the PSS/PAH gutter-layer and is independent of the thickness of the PMDA-PDA/PAH film (Table 3.1).[18] The Cl^-/SO_4^{2-} and $Cl^-/Fe(CN)_6^{3-}$ selectivities are also similar to those of PSS/PAH films.[18,26] ($Cl^-/Fe(CN)_6^{3-}$ selectivities are high because the $Fe(CN)_6^{3-}$ is large and triply charged.). An intriguing aspect of unheated membranes with PMDA-PDA/PAH layers is that they are highly cation selective (Table 3.2). The K^+/Mg^{2+} selectivity value for unheated films is relatively high at 120, and somewhat lower for K^+/Ca^{2+} and K^+/Ba^{2+} at about 40 and 27, respectively. This value for K^+/Mg^{2+} selectivity is comparable to that achieved previously with a 60 bilayer PSS/PAH membrane.[22] Cation selectivity seems to also be independent of the number of PMDA-PDA/PAH bilayers. However, capping an unheated film with an amine rather than the poly(amic acid) (3-bilayer film, Table 3.2) does give a 2-fold increase in cation-transport selectivity. I should note that other studies suggest that termination of films with a polycation rather than a polyanion yields tighter films.[27,28]

Table 3.1: Fluxes and anion selectivity coefficients for diffusion dialysis through porous alumina[a] coated with a 5-bilayer PSS/PAH base and capped with 1.5 to 3.5 bilayers of PMDA-PDA/PAH.[b]

Heating Temp.	KCl flux 10^{-8} mole·cm^{-2}·s^{-1}			α, Cl^-/SO_4^{2-}				α, $Cl^-/Fe(CN)_6^{3-}$		
	1.5 bilayers	2.5 bilayers	3.5 bilayers	1.5 bilayers	2.5 bilayers	3 bilayers	3.5 bilayers	1.5 bilayers	2.5 bilayers	3.5 bilayers
Unheated	3.5 ± 0.2	3.7 ± 0.3	3.5 ± 0.5	4.2 ± 0.2	4.7 ± 1	3.2 ± 0.2	6 ± 0.5	640 ± 260	2100 ± 1700	880 ± 360
130 °C	4.3 ± 0.8	3.8 ± 0.9	3.4 ± 0.1	16 ± 1.4	24 ± 5.3	-	100 ± 46	760 ± 47	1300 ± 170	1500 ±420
150 °C	4.1 ± 0.5	2.8 ± 0.3	2.2 ± 0.9	51 ± 8	680 ± 153	390 ± 23	790 ± 120	1200 ± 400	2800 ± 750	2600 ± 1300
165 °C	2.8 ± 0.2	2.9 ± 0.6	1.5 ± 0.1	680 ± 33	820 ± 220	-	1000 ± 580	3200 ± 3500	4000 ± 4600	1400 ± 610
180 °C	3.0 ± 0.7	1.6 ± 0.2	0.5 ± 0.03	590 ± 85	1100 ± 150	-	310 ± 140	1000 ± 700	1500 ± 1000	240 ± 50

[a] Porous alumina Cl^- flux of 5.3 x 10^{-8} mole·cm^{-2}·s^{-1} (from reference 18).
[b] The source phase contained 0.1 M salt.

Table 3.2: Cation selectivity coefficients for diffusion dialysis through porous alumina coated with a 5-bilayer PSS/PAH base and capped with 1.5 to 3.5 bilayers of PMDA-PDA/PAH.[a]

Heating Temp.	α, K^+/Mg^{2+}				α, K^+/Ca^{2+}			α, K^+/Ba^{2+}		
	1.5 bilayers	2.5 bilayers	3 bilayers	3.5 bilayers	1.5 bilayers	2.5 bilayers	3.5 bilayers	1.5 bilayers	2.5 bilayers	3.5 bilayers
Unheated	120 ± 12	120 ± 31	210 ± 3.7	110 ± 25	38 ± 5.9	39 ± 8.8	43 ± 11	25 ± 1	26 ± 7.2	31 ± 11
130 °C	91 ± 19	100 ± 4.5	-	130 ± 21	26 ± 7	27 ± 2.5	33 ± 2.8	19 ± 3.3	22 ± 2.7	30 ± 5.9
150 °C	94 ± 24	110 ± 22	130 ± 5	310 ± 73	27 ± 5	42 ± 2	100 ± 8	24 ± 4	51 ± 8	120 ± 2
165 °C	110 ± 20	170 ± 30	-	190 ± 55	39 ± 8	77 ± 15	120 ± 2	37 ± 9	92 ± 13	140 ± 24
180 °C	41 ± 13	93 ± 12	-	60 ± 11	34 ± 7	33 ± 3	64 ± 10	33 ± 7.4	48 ± 5	69 ± 9.6

[a] All experiments were performed with 0.1 M chloride salts.

3.3.5 Heated membranes. Heating of membranes converts the poly(amic acid) to the polyimide (Figure 3.1b), and the extent of imidization has a large effect on the membrane selectivity and flux. Tables 3.1 and 3.2 show the selectivity coefficients, α, for membranes top-coated with 1.5, 2.5, 3, and 3.5 PMDA-PDA/PAH bilayers that were heated at various temperatures. Heating membranes increases Cl^-/SO_4^{2-} selectivities to values as high as 1100. For comparison, Neosepta membranes coated with a single layer of polyanion showed a maximum Cl^-/SO_4^{2-} selectivity of 20.[29] In contrast, the K^+/Mg^{2+} selectivity is relatively high (120) for unheated films, but heating does not increase this selectivity to the same degree as seen for anions. Figure 3.8 shows typical normalized conductivity vs. time plots for KCl, K_2SO_4, and $MgCl_2$.

Donnan exclusion due to surface charge, which is a major factor in the selectivity of some polyelectrolyte membranes,[18,22,26] is not the main reason for the large selectivity values in the present case. This can be seen by changing the sign of the outer-layer charge through termination with PAH rather than PMDA-PDA (Tables 3.1 and 3.2, 3-bilayer PMDA-PDA/PAH). This change in sign has only a small effect (at most a factor of 2) on selectivity with either cations or anions.

The selectivity among ions most likely reflects differences in hydration energies and ion sizes. Both hydration energy and hydrated ion radius decrease in the order $Mg^{2+} > Ca^{2+} > Ba^{2+} > SO_4^{2-} > Cl^- > K^+$ (Table 3.3).[30] Either loss of waters of hydration upon partitioning into the membrane or slower diffusion of large hydrated ions would result in K^+/Mg^{2+} and Cl^-/SO_4^{2-} selectivity. The K^+/Mg^{2+}

Table 3.3: Ionic and hydrated radii and hydration energies of the ions used in the diffusion dialysis experiments.[a]

Ion	Ionic Radius	Hydrated Radius	Hydration Energy
Cl^-	181	223	340
SO_4^{2-}	240	278	1080
$Fe(CN)_6^{3-}$	380	396	-
K^+	138	212	295
Mg^{2+}	72	299	1830
Ca^{2+}	100	271	1505
Ba^{2+}	136	254	1250

[a] Data from reference 30.

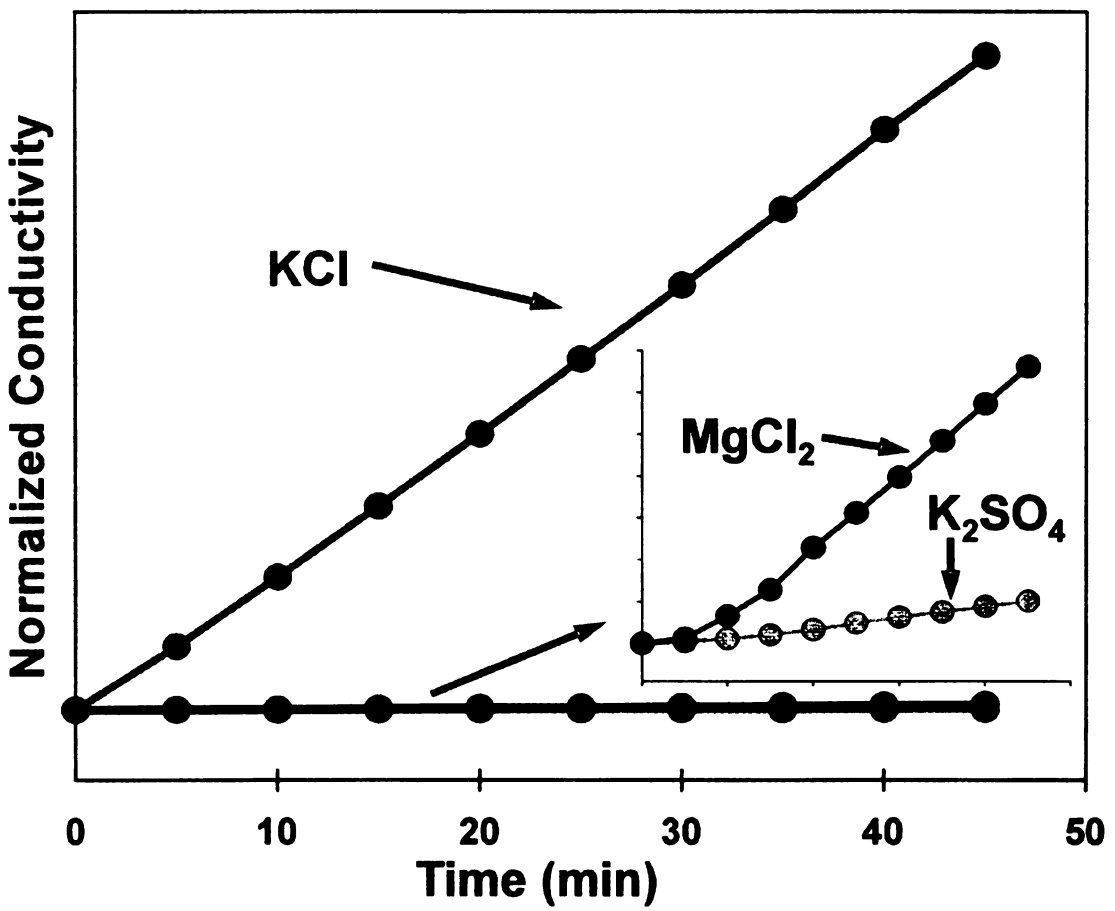

Figure 3.8: Plots of normalized receiving phase conductivity vs. time for diffusion dialysis experiments in which a heated 2.5-bilayer PMDA-PDA/PAH + 5-bilayer PSS/PAH membrane separates a 0.1 M source phase from the receiving phase. The inset shows $MgCl_2$ and K_2SO_4 plots magnified by 2 orders of magnitude.

selectivity should also be greater than that for Cl^-/SO_4^{2-}, as is seen for unheated films, because K^+/Mg^{2+} hydration energy differences are greater than those of Cl^-/SO_4^{2-}. Selective transport of K^+ over Ba^{2+} or Ca^{2+} also occurs through unheated membranes, but these selectivity values are only about 30% of those for K^+/Mg^{2+}, as would be expected from trends in hydrated radii and hydration energies.

After heating and imidization, the membrane should become denser and more hydrophobic. This would explain the increase in Cl^-/SO_4^{2-} selectivity upon heating. However, we would expect the K^+/Mg^{2+} selectivity to increase with heating to an even greater extent. We speculate that Mg^{2+} may be diffusing through the membrane with only a few waters of hydration, and thus increases in film density may not slow its diffusion as much as that of SO_4^{2-}, which has a larger unhydrated radius.

The selectivity depends greatly on the heating temperature applied. A plot of the flux vs. heating temperature (Figure 3.9) shows that the SO_4^{2-} flux decreases rapidly with heating temperature up to 150 °C and levels off after this temperature. For Cl^-, flux usually decreases over the entire heating range we tested. The selectivity, therefore, reaches a maximum point at a particular heating temperature and decreases at higher heating temperatures because Cl^- flux is further reduced with higher heating temperature while SO_4^{2-} flux is constant.

Membrane selectivity also varies with the number of PMDA-PDA/PAH bilayers. Adding more bilayers appears to decrease the heating temperature at which the onset of high Cl^-/SO_4^{2-} selectivity occurs. Due to interpenetration of

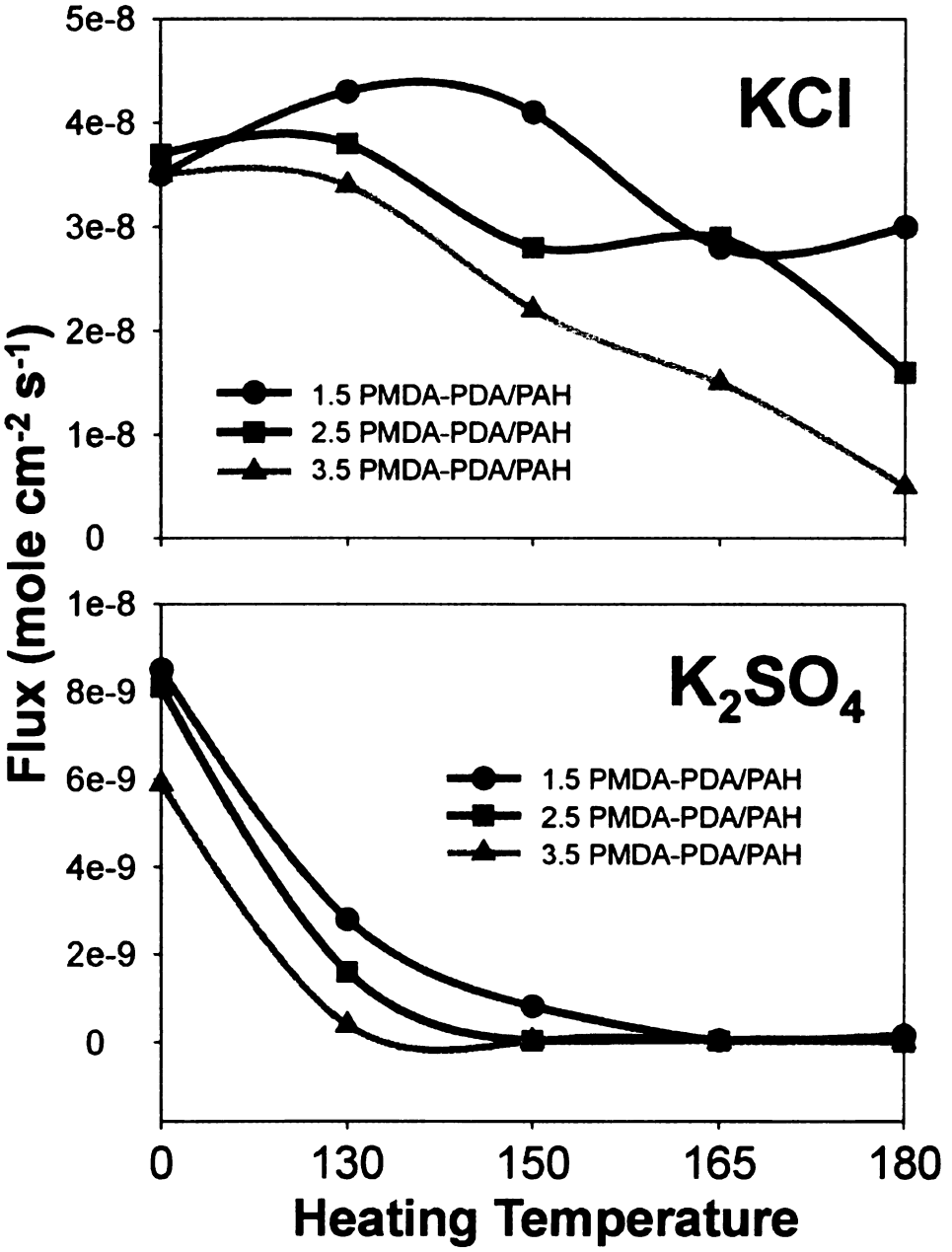

Figure 3.9: Plots of the diffusion dialysis flux of KCl (top) and K_2SO_4 (bottom) as a function of the imidization temperature of composite membranes consisting of 5 bilayers of PSS/PAH and a capping layer of 1.5 (circles), 2.5 (squares), and 3.5 (triangles) bilayers of PMDA-PDA.

polymers, the 1.5-bilayer PMDA-PDA/PAH top-coat likely contains some PSS and may be less selective than thicker top-coats. Remarkably, even a 2.5-bilayer PMDA-PDA/PAH top-coating that is only 70 Å thick can give Cl^-/SO_4^{2-} selectivities of over 1000 after heating at 180 °C. Selectivities as high as 680 for Cl^-/SO_4^{2-} can be achieved with Cl- flux that is still 50% of that through bare alumina.

3.4 Conclusion.

In summary, ultrathin polyimide membranes can be formed on porous alumina supports coated with a polyelectrolyte gutter layer, and these membranes exhibit extremely large selectivity coefficients for separation of monovalent and divalent ions. The selectivity varies with both the thickness of the selective skin layer and the extent of imidization. Also, these polyimide membranes are selective for both anions and cations. This phenomenon may be best explained by the differences in the hydration energies and sizes of the ions, as well as a small amount of selectivity due to the negative membrane surface.

3.5 References.

(1) Lipnizki, F.; Field, R. W. *Environ. Prog.* **2002**, *21*, 265-272.

(2) Koros, W. J. *Chem. Eng. Prog.* **1995**, *91*, 68-81.

(3) Robeson, L. M. *J. Membrane Sci.* **1991**, *62*, 165-185.

(4) Loeb, S.; Sourirajan, S. *Adv. Chem. Ser.* **1963**, *38*, 117-132.

(5) Kim, S.-G.; Kim, Y.-I.; Yun, H.-G.; Lim, G.-T.; Lee, K.-H. *J. Appl. Polym. Sci.* **2003**, *88*, 2884-2890.

(6) Pinnau, I.; Freeman, B. D. In *Membrane Formation and Modification*; Pinnau, I., Freeman, B. D., Eds.; American Chemical Society: Washington, D.C., 2000, pp 1-22.

(7) Polotskaya, G. A.; Kuznetsov, Y. P.; Goikhman, M. Y.; Podeshvo, I. V.; Maricheva, T. A.; Kudryavtsev, V. V. *J. Appl. Polym. Sci.* **2003**, *89*, 2361-2368.

(8) Decher, G. *Science* **1997**, *277*, 1232-1237.

(9) Shiratori, S. S.; Rubner, M. F. *Macromolecules* **2000**, *33*, 4213-4219.

(10) Dubas, S. T.; Schlenoff, J. B. *Macromolecules* **1999**, *32*, 8153-8160.

(11) Huang, R. Y. M.; Feng, X. *J. Membrane Sci.* **1993**, *84*, 15-27.

(12) Clausi, D. T.; Koros, W. J. *J. Membrane Sci.* **2000**, *167*, 79-89.

(13) Sroog, C. E. In *Polyimides*; Wilson, D., Stenzenberger, H. D., Hergenrother, P. M., Eds.; Chapman and Hall: New York, 1990, pp 252-284.

(14) Baur, J. W.; Besson, P.; O'Connor, S. A.; Rubner, M. F. *Mater. Res. Soc. Symp. Proc.* **1996**, *413*, 583-588.

(15) Liu, Y.; Wang, A.; Claus, R. O. *Appl. Phys. Lett.* **1997**, *71*, 2265-2267.

(16) Moriguchi, I.; Teraoka, Y.; Kagawa, S.; Fendler, J. H. *Chem. Mater.* **1999**, *11*, 1603-1608.

(17) Harris, J. J.; Bruening, M. L. *Langmuir* **2000**, *16*, 2006-2013.

(18) Stair, J. L.; Harris, J. J.; Bruening, M. L. *Chem. Mater.* **2001**, *13*, 2641-2648.

(19) Stroeve, P.; Vasquez, V.; Coelho, M. A. N.; Rabolt, J. F. *Thin Solid Films* **1996**, *284-285*, 708-712.

(20) Leväsalmi, J.-M.; McCarthy, T. J. *Macromolecules* **1997**, *30*, 1752-1757.

(21) Kotov, N. A.; Magonov, S.; Tropsha, E. *Chem. Mater.* **1998**, *10*, 886-895.

(22) Krasemann, L.; Tieke, B. *Langmuir* **2000**, *16*, 287-290.

(23) Krasemann, L.; Tieke, B. *Chem. Eng. Technol.* **2000**, *23*, 211-213.

(24) Li, Q.; Yamashita, T.; Horie, K.; Yoshimoto, H.; Miwa, T.; Maekawa, Y. *J. Polym. Sci., Part A: Polym. Chem.* **1998**, *36*, 1329-1340.

(25) Sroog, C. E. *J. Polym. Sci., Macromol. Rev.* **1976**, *11*, 161-208.

(26) Harris, J. J.; Stair, J. L.; Bruening, M. L. *Chem. Mater.* **2000**, *12*, 1941-1946.

(27) Smith, R. N.; Reven, L.; Barrett, C. J. *Macromolecules* **2003**, *36*, 1876-1881.

(28) Stanton, B. W.; Harris, J. J.; Miller, M. D.; Bruening, M. L. *Langmuir* **2003**, *19*, 7038-7042.

(29) Sata, T.; Yamaguchi, T.; Matsusaki, K. *J. Membrane Sci.* **1995**, *100*, 229-238.

(30) Marcus, Y. *Biophys. Chem.* **1994**, *51*, 111-127.

Chapter 4

Ultrathin, Gas-selective Polyimide Membranes Prepared from Multilayer Polyelectrolyte Films

4.1 Introduction

Polyimides are attractive membrane materials because of their mechanical and thermal stability,[1,2] and compared with other polymers, certain polyimides exhibit a favorable combination of permeability and gas-transport selectivity.[3-9] Practical application of these materials, however, requires formation of a defect-free polyimide layer on a highly permeable support, and this layer should be as thin as possible to allow high flux through the membrane. Methods for creating ultrathin polyimide skins include phase-inversion processes and formation of composite membranes by deposition of polyimide films on highly permeable substrates. For example, Koros and coworkers prepared cast-sheet[10,11] and hollow-fiber polyimide membranes[12] by a phase-inversion process that yields a dense, selective layer at the surface of a porous material.

Composite membranes offer the advantage that only a thin, selective film of the separation material is used, and thus more expensive, and hopefully more selective, polymers can be employed.[13] In the case of polyimides, composite membranes can be prepared by deposition of a poly(amic acid) followed by imidization to form a selective film. Ding and coworkers coated porous polysulfone hollow fibers with a solution of a poly(amic acid) salt and showed that

heating the fibers at 150 °C for 24 h yields fully imidized films that are as thin as 50 nm.[14]

Even with these successes in creating ultrathin membranes, deposition of defect-free polyimide skins that are less than 50 nm thick is still difficult.[15,16] New methods for forming ever-thinner skins will allow creation of membrane systems with higher fluxes, and the recently developed technique of alternating polyelectrolyte deposition (APD) may prove useful in this regard. This method simply involves alternating immersions of a charged substrate into oppositely charged polyelectrolytes,[17] and thus film thickness is easily controlled by changing either the number of adsorbed polyelectrolyte layers or deposition variables such as pH, supporting salt concentration, and solvent.[18-20] Because the films self-assemble, surface roughness does not greatly affect adhesion, and defect-free films can be obtained on porous supports since each added layer covers defects in the previous layer.[17,21]

A few recent studies demonstrate membrane formation using APD on permeable supports. Successful separation of monovalent and divalent ions with such membranes occurs with various polyelectrolytes and deposition conditions,[22-24] and highly selective separations by pervaporation are also possible.[25-27] In contrast, gas-transport selectivities due to multilayer polyelectrolyte films are relatively modest. Polyelectrolyte films can increase the gas selectivity of non-porous supports,[28-30] but deposition of these films on porous supports yields little increase in selectivity.[30,31] We suspect that the lack

of gas-transport selectivity in polyelectrolyte films is inherent in the structure and packing of the polyelectrolytes thus far employed.

In this work, we utilize poly(amic acids) as polyelectrolytes for APD so that these materials can be imidized to produce polyimides that are known to exhibit high gas-transport selectivities and permeabilities. Several previous studies combined APD of poly(amic acids) and a polycation with postdeposition heating to form polyimide films or ion-selective membranes,[22,32-35] but this chapter represents the first utilization of this method to form membranes for gas separations. Ionized precursor poly(amic acids) serve as polyanions that form films with poly(allylamine hydrochloride) (PAH) on porous alumina[36] (Figure 4.1), and subsequent heating yields the polyimide membrane. We chose to study the three polyimides shown in Figure 4.2 because their gas-transport properties were previously investigated.[7-9] (In this chapter, we use the acronyms in Figure 4.2 to refer to both the imidized and poly(amic acid) forms of the polymers.) One of the main points that we demonstrate in this study is that the presence of a small amount of PAH in the membrane does not alter the selectivity of the polyimide films. Gas-transport studies clearly demonstrate that 35 to 50 nm-thick polyimide films prepared using APD have selectivities and permeabilities that are the same as those of the corresponding bulk polyimides. Thus APD indeed provides a new tool for development of ultrathin, gas-selective membranes.

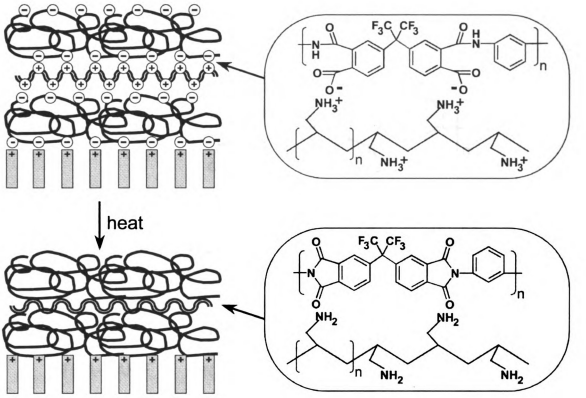

Figure 4.1: Heat-induced imidization of a poly(amic acid)/PAH film on a porous support. Neutralization of PAH occurs when it contributes a proton for the formation of water. Intertwining of neighboring layers is not shown for figure clarity.

6FDA-mPDA

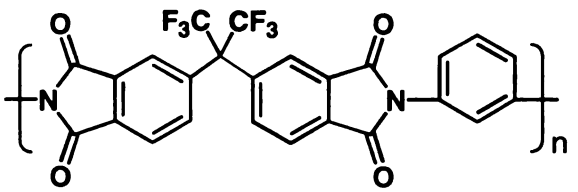

6FDA-BAHF

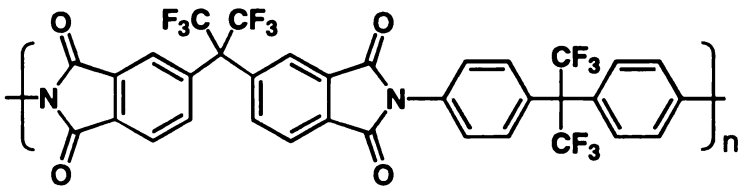

BTDA-BAHF

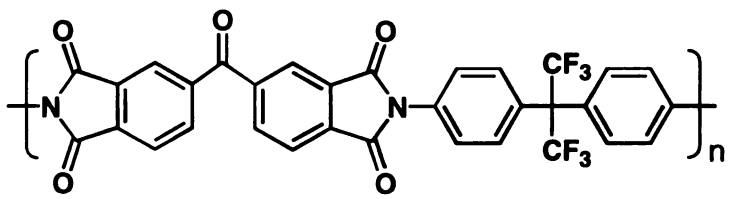

Figure 4.2: Structures of the polyimides used in this study.

4.2 Experimental Section

4.2.1 Materials. 4,4'–(hexafluoroisopropylidene)diphthalic anhydride (6FDA), 3,3',4,4'-benzophenonetetracarboxylic dianhydride (BTDA), 4,4'-(hexafluoroisopropylidene) dianiline (BAHF), 1,3-phenylenediamine (mPDA), (3-aminopropyl)triethoxysilane and poly(allylamine hydrochloride) were purchased from Aldrich. DMF (Spectrum) was dried with molecular sieves for at least 24 h, and the 3,3',4,4'-benzophenonetetracarboxylic dianhydride was purified by vacuum sublimation prior to use. All other chemicals were used as received. Acetone (Vorpak), ethanol (Pharmco, 200 proof) and deionized water (Milli-Q, 18.2 MΩcm) were used for rinsing and preparation of polymer-containing solutions. Porous alumina supports were 25 mm Whatman Anodiscs with 0.02 μm-diameter surface pores (Fisher Scientific), and silicon(100) wafers (Silicon Quest) were used as supports for ellipsometry (single-side polished) and Brewster-angle transmission FTIR spectroscopy (double-side polished).

4.2.2 Substrate Preparation. Prior to film deposition, silicon wafers were silanized with (3-aminopropyl)-triethoxysilane to prepare a controlled surface capable of supporting a positive charge. Silanization was accomplished using the method of Petri et al.[37] In the case of porous alumina supports, the polypropylene support ring on the alumina was removed to prevent it from melting into substrate pores during heat-induced imidization. This was accomplished by cutting off as much of the polymer as possible with scissors, and then burning off the remaining ring at 400 °C for 18 h. Subsequently, the

alumina supports were rinsed with acetone, dried with N_2, and cleaned for 10 min in a UV/ozone cleaner (Boekel Industries, model 135500). Film formation occurred directly on the alumina, so silanization was not necessary.

4.2.3 Polymer Synthesis. The poly(amic acids) were prepared using a typical literature procedure.[38] First, the diamine was dissolved in an appropriate solvent (acetone for 6FDA-BAHF and DMF for both 6FDA-mPDA and BTDA-BAHF). A stoichiometric quantity of the dianhydride was then added to this solution gradually over a ~15 min period, and the 15% by weight (total dissolved solids) solution was stirred for 24 h. The poly(amic acids) were precipitated twice in either 1:1 hexanes/ethyl acetate (6FDA-BAHF and BTDA-BAHF) or 3:1 chloroform/hexanes (6FDA-mPDA), filtered, and then dried under vacuum for 24 h.

4.2.4 Solution Preparation and Film Deposition. Due to the insolubility of the poly(amic acid) in water, solutions containing 0.005 M 6FDA-BAHF and 0.5 M NaCl were prepared by dissolving 0.039 g of 6FDA-BAHF in 7 mL of ethanol, and then adding 3 mL of 1.67 M aqueous NaCl. The molarities of the polyelectrolytes are given with respect to the repeating unit. The pH was adjusted to 5.0 by adding 0.2 M triethylamine in 7:3 (v:v) ethanol/water. Film deposition began with immersion of the substrate (silanized silicon or porous alumina) into the poly(amic acid) solution for 3 min. (The alumina membrane was placed in an o-ring holder so that only the face with 0.02 μm-diameter pores was exposed to solutions.) The substrate was removed from solution and rinsed with copious amounts of ethanol and then Milli-Q water. Subsequently, the substrate was

immersed in an aqueous 0.02 M PAH solution (0.02 M NaCl, adjusted to pH 5.0 with NaOH) for 3 min and rinsed with Milli-Q water and then ethanol. This process was repeated until the desired number of bilayers was deposited, and all films were terminated with a poly(amic acid) layer. 6FDA-mPDA/PAH films were prepared similarly except that the rinsing solvent was a 1:1 mixture of ethanol and water, and the PAH solution did not contain NaCl. BTDA-BAHF solutions were made by first dissolving BTDA-BAHF in acetone, and then adding water to make 0.005 M BTDA-BAHF in 7:3 (v:v) acetone/water. The pH of this solution was adjusted to 5.0 by adding 0.2 M triethylamine in 7:3 acetone/water. For BTDA-BAHF/PAH films, the poly(amic acid) layers were rinsed with acetone and neither solution contained NaCl.

4.2.5 Film Imidization. Films were heated using a home-built apparatus consisting of a temperature controller, thermocouple, glass chamber, and heating mantle. The heating apparatus was purged with nitrogen for 2 h prior to heating as well as during heating and cooling. The temperature was ramped at a rate of 5 °C per min and was held at the desired heating temperature for 2 h.

4.2.6 Film Characterization. Ellipsometric thickness measurements on amine-terminated silicon wafers were made using a rotating analyzer ellipsometer (model M-44, J. A. Woollam) and WVASE32 software. Approximate film compositions were determined by measuring the change in thickness upon adsorption of each polymer and assuming that each polyelectrolyte layer had the same density. (For layer-by-layer monitoring of growth, films had to be dried with N_2 after deposition of each layer, but in all other cases films were dried only after

deposition of the entire film.) A film refractive index of 1.5 was assumed in all thickness determinations. Transmission FTIR spectra of films on double-side polished Si wafers were measured using a Nicolet Magna-550 FTIR spectrophotometer with a Brewster angle attachment set at 75º (p-polarized light). A UV/O_3-cleaned Si substrate was used as a background. Field-emission scanning electron microscopy (FESEM) images were obtained with a Hitachi S-4700 instrument using an acceleration voltage of 15 kV. Samples were fractured in liquid nitrogen and sputter-coated with 5 nm of Au before imaging.

4.2.7 Gas-Transport Studies. Room-temperature (23-24 °C) gas-transport measurements were carried out using a home-built permeation cell containing of a chamber that sealed onto a membrane via an o-ring. The membrane was supported by a stainless-steel frit (Mott), and gas flux was measured using a soap-bubble flow meter (Fisher Scientific, model 420). Using a pressure relief valve, the permeation cell was purged many times with the gas of interest and all measurements with that gas were then taken after a steady-state flux was observed. Fluxes were measured at pressures of 5 – 45 psig (in 5 psig intervals), and the area of the membrane exposed to the gas was 2.0 cm^2. The fluxes of O_2, N_2, H_2, CH_4, and CO_2 (in that order) were determined for each membrane, and O_2 and N_2 were then tested again to insure that membrane properties did not change upon exposure to different gases. Permeabilities of the individual gases were calculated for each pressure and then averaged.

4.3 Results and Discussion

4.3.1 Film Formation and Composition. The selective layer of gas-separation membranes usually consists of a single, gas-selective polymer,[39] while formation of membranes by APD, in contrast, requires two oppositely charged polymers. In the present case, the polyanion is a poly(amic acid) that can be heated to form a gas-selective polyimide, while the cation, PAH, is probably not a selectively permeable material. Thus formation of gas-selective polyimide/PAH membranes will likely require keeping the amount of PAH in the film to a minimum. One of the goals of this study was to obtain multilayer polyelectrolyte films that contain as much as 90% polyimide. We wanted to make the poly(amic acid) layer as thick as possible to both reduce the number of layers that need to be deposited and increase the overall fraction of polyimide in the final film.

Poly(amic acid) layer thickness can be controlled by varying the solvent composition, deposition pH, and supporting salt concentration in deposition solutions. The fluorinated poly(amic acids) employed in this study must first be dissolved in a good solvent (e.g. ethanol or acetone) and then some water can be added to the solution to enhance the deprotonation of –COOH groups. Addition of too much water, however, results in precipitation of the polymer if it is not fully deprotonated. Thus we deposited films from solutions containing 30% water. Although the addition of salt to polyelectrolyte deposition solutions increased the thickness of some multilayer polyelectrolyte films by as much as an order of magnitude,[19,40] in the poly(amic acid) case, film thickness increased by

at most 50% with the addition of up to 0.5 M NaCl. Although small, this difference can increase the overall fraction of poly(amic acid) in the film by 5-10%. Unfortunately, added salt can also change the solubility of the poly(amic acid). This was most apparent for solutions of BTDA-BAHF. When these solutions contained 0.5 M salt, they quickly became cloudy if any of the solvent evaporated. Without the added salt, the solution would stay clear for over two hours if left uncapped. Thus BTDA-BAHF was deposited in the absence of salt while 6FDA-BAHF and 6FDA-mPDA were deposited in the presence of 0.5 M NaCl.

For weakly acidic or basic polyelectrolyte systems, adjusting the deposition pH can also have a large effect on layer thickness.[20,41] In the case of poly(amic acids) lower pH values should decrease the fraction of acid groups that are ionized and reduce the number of charged groups per polymer chain. With fewer available charged sites, more polymer strands are required to compensate the charge on the substrate surface, and hence more polymer will be deposited.[20,41] For fluorinated poly(amic acids), pH also affects film thickness by altering polymer solubility. Because deposition solutions are composed of both a good solvent (ethanol or acetone) and water, the polymer is soluble in both the fully protonated and the fully deprotonated forms. However, at intermediate pH values, fluorinated poly(amic acids) are partially protonated and only sparingly soluble. At points near solubility limits, the driving force for film deposition is greatest,[19] and the thickest poly(amic acid) layers form. Thus we deposited

poly(amic acid) films at a pH of 5, because this is the lowest intermediate pH at which polymers reproducibly remain in solution.

The same thought process applies to deposition of PAH, except that we wanted to deposit as little PAH as possible. In this case, the ideal solution might be one that contains the polycation dissolved in a very good solvent, water, at a low pH in the absence of supporting electrolyte. [20,41] However, at some point the amount of PAH deposited is too small to permit deposition of the next poly(amic acid) layer. Thus for controlled film formation with minimal PAH adsorption, we adjusted the pH of the PAH solution to be the same as that of the poly(amic acid). Also, in the case of films containing 6FDA-BAHF, a small amount of NaCl (0.02 M) was necessary to form layers with consistent thicknesses.

Overall, control over pH and solvent yielded bilayer thicknesses of 34, 38, and 50 Å for 6FDA-BAHF/PAH, BTDA-BAHF/PAH, and 6FDA-mPDA/PAH, respectively. Increases in film thickness after adsorption of PAH were about 11% of those resulting from adsorption of poly(amic acid). Thus, control over deposition conditions allowed formation of films that were ~90% poly(amic acid).

4.3.2 Film Imidization. To examine the extent of imidization after heating, we measured the Brewster-angle transmission FTIR spectra of poly(amic acid)/PAH films on amine-modified double-side polished Si supports. Figure 4.3 shows the spectra of films before and after heating at 150 or 250 °C. Unheated films have a broad absorbance band from 1670 to 1520 cm^{-1} primarily due to the overlap of amide and asymmetric $-COO^-$ stretches of the poly(amic acid). Heating of these films results in the appearance of asymmetric and symmetric imide carbonyl

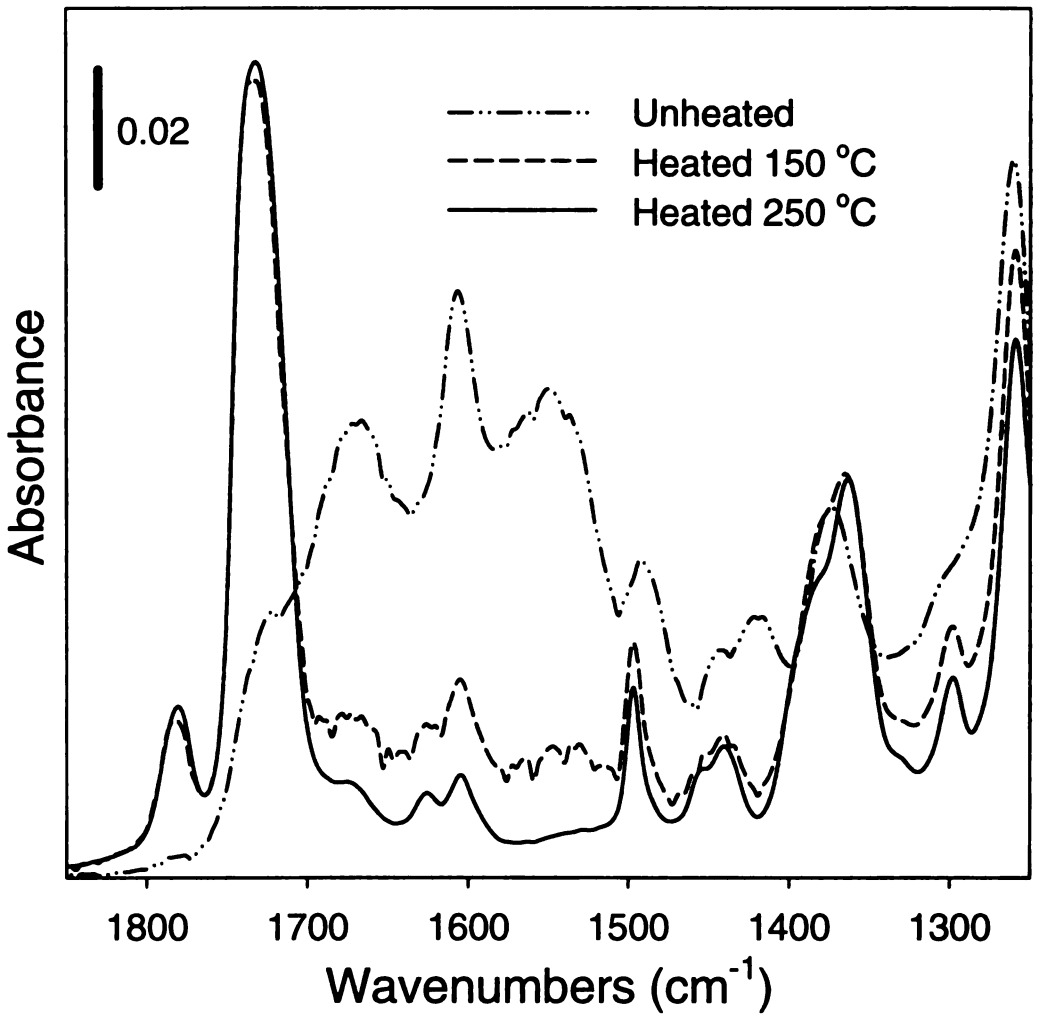

Figure 4.3: Brewster-angle transmission FTIR Spectra of 9.5-bilayer 6FDA-mPDA/PAH films on Si before and after heating at 150 °C or 250 °C for 2 h to induce imidization.

peaks (1775 and 1730 cm^{-1}) and the reduction of amide and carboxylate peaks. In principle, a few amide bonds could form by reaction of the amine groups of PAH and the carboxylate groups of the poly(amic acid), but we see no spectral evidence for this reaction.

Decreases in the carboxylate and amide peak intensities suggest that ~50% and ~85% imidization occur for samples heated at 100 °C (not shown) and 150 °C, respectively. Spectra obtained after heating at 250 and 300 °C were essentially identical, implying that full imidization occurs at 250 °C. Thus complete imidization takes place at temperatures lower than the glass transition temperature of the polyimides (298 °C for 6FDA-mPDA, 298 °C for 6FDA-BAHF, and 305 °C for BTDA-BAHF),[7,8] which is typically considered to be the temperature needed to induce full imidization.[42] Several studies show that complexation of poly(amic acids) with an amine base lowers imidization temperatures and decreases the time needed for full imidization.[14,43] Similarly, we form poly(amic acid) salts when electrostatically attaching the layers, and thus lower imidization temperatures occur. Low heating temperatures will prove essential if poly(amic acid) films are to be imidized on temperature-sensitive polymeric supports.

For most gas-transport studies, we employed heating temperatures of 250 °C to achieve full imidization. Temperatures above 250 °C present some risk of decomposition of PAH, which may lead to membrane defects. After heating at 250 °C, film thickness decreases by ~30%, and this change is probably due to both imidization and removal of adsorbed water from the film.

4.3.3 FESEM Studies of Membrane Formation. Figure 4.4 shows cross-sectional FESEM images of porous alumina substrates before and after deposition of 6FDA-mPDA/PAH films. These images show very little, if any, deposition of polyelectrolytes on the walls of the 0.2-μm pores that make up the majority of the alumina support. There may be some film penetration (10 – 20 nm) into the 0.02 μm pores at the alumina surface. Cross-sectional images taken at several points along the diameter of the membrane indicate a uniform film thickness, while top-view images of the membrane show complete coverage of surface pores. The uncoated back side of the alumina exhibited open pores with no evidence of polyelectrolyte deposition.

Using FESEM images we were able to estimate polyimide film thicknesses to within ~5 nm. The thicknesses of 6FDA-mPDA/PAH (9.5 bilayers), 6FDA-BAHF/PAH (14.5 bilayers), and BTDA-BAHF/PAH (10.5 bilayers) films were all about 50 nm. These thicknesses are about 30% higher than ellipsometric thicknesses of similar films deposited on amine-functionalized silicon wafers. The higher thicknesses on the porous alumina support may be due to a small amount of deposition in the surface pores or differences between charge distributions and roughnesses of the two substrates. The similarity of permeability coefficients determined using these thicknesses and permeability coefficients of bulk polyimides suggests that the thickness values are reasonable (see below).

4.3.4 Gas-Transport Measurements. Table 4.1 lists gas permeability coefficients and the ideal O_2/N_2 and CO_2/CH_4 selectivities for polyimide

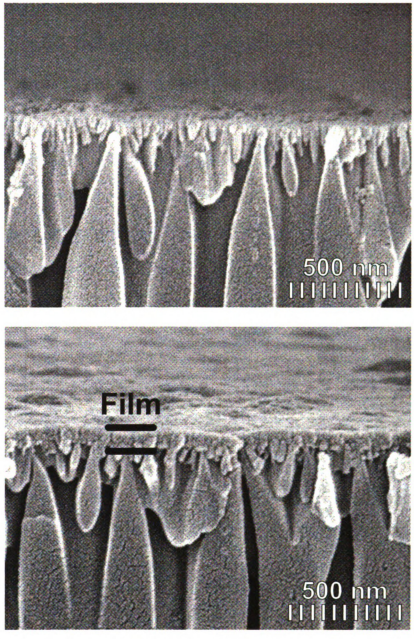

Figure 4.4: Cross-sectional field-emission scanning electron microscopy images of (a) a bare alumina support and (b) an alumina support coated with an imidized 9.5-bilayer 6FDA-mPDA/PAH film.

Table 4.1: Permeability (barrers)[a] and selectivity coefficients for the transport of various gases through several polyimide membranes containing ~10% PAH.

Polymer	P_{O_2}	P_{N_2}	P_{H_2}	P_{CH_4}	P_{CO_2}	P_{O_2}/P_{N_2}	P_{CO_2}/P_{CH_4}
6FDA-mPDA/PAH [b] (9.5 bilayers)	2.8 ± 0.50	0.40 ± 0.08	42 ± 4	0.16 ± 0.06	11 ± 1	6.9	68
Bulk 6FDA-mPDA [c,8]	3.0	0.45	40	0.16	9.2	6.7	58
6FDA-BAHF/PAH [b] (14.5 bilayers)	14 ± 0.7	2.6 ± 0.5	110 ± 9	1.4 ± 0.5	53 ± 4	5.2	38
Bulk 6FDA-BAHF [c,7]	14	3.1	110	1.3	51	4.6	38
Bulk 6FDA-BAHF [c,9]	16	3.5	-	1.6	64	4.7	40
BTDA-BAHF/PAH [b] (10.5 bilayers)	2.2 ± 0.4	0.38 ± 0.09	28 ± 3	0.17 ± 0.06	8.8 ± 1.2	5.8	52
Bulk BTDA-BAHF [c,7]	2.5	0.45	31	0.23	10	5.6	45

[a]barrers = 10^{10}·cm^3 (STP)·cm/(cm^2·s·cm(Hg))
[b]measured at 24 °C
[c]measured at 35 °C

membranes formed by alternating polyelectrolyte deposition and imidization at 250 °C. Permeabilities are presented in barrers (10^{10}·cm^3 (STP)·cm/(cm^2·s·cm(Hg)) and were determined using film thicknesses obtained by FESEM. Selectivities were calculated by dividing the permeabilities of two different gases. All of the membranes were made to be about 50 nm thick, and all data shown represent an average of measurements on 3 replicate membranes.

Within experimental uncertainty, the permeability and selectivity values of the tested membranes are the same as those of cast, pure polyimide membranes with μm thicknesses. We should note that the transport experiments with the membranes prepared by APD were performed at 24 °C, while the literature data for bulk polyimides were acquired at 35 °C. However, the 10 °C difference in the present case should have little effect on permeability.[44] The high selectivities in these membranes (Table 4.1) clearly show that the films are free of defects, as even a small fraction of defects would negate selectivity.[45] Annealing that occurs during heat-induced imidization may help to heal defects in these films.

The agreement between the permeability of membranes prepared by APD and analogous bulk polyimide membranes is somewhat surprising considering that the films prepared by APD contain a mixture of the polyimide and PAH. One would expect lower selectivities and different permeabilities if the two layers were as interpenetrated as is the case for other polyelectrolyte films.[17] Interpenetration may not be as prevalent in these films because each polyelectrolyte is insoluble in the deposition solvent of the other polyelectrolyte.

Phase segregation could also occur during heating. Further experiments are required to determine if phase segregation occurs.

4.3.5 Gas Transport as a Function of Film Composition and the Degree of Imidization. To investigate the relationship between extent of imidization and gas transport, we measured gas fluxes through 6FDA-mPDA/PAH membranes before and after heating at 150 °C or 250 °C (Table 4.2). The unheated membranes exhibited Knudsen diffusion-like selectivities and relatively low permeabilities for O_2 and CO_2 (5- and 18-fold less, respectively, than through membranes heated at 250 °C). Knudsen diffusion occurs in pores with diameters smaller than the mean free path of the gas, and flux in such a system is inversely proportional to the square root of the molecular mass of the gas.[46] Thus Knudsen diffusion selectivities suggest that transport occurs primarily through a few small defects in unheated films. The relatively low flux through unheated membranes may be due to the ionic cross-links in the film or the presence of residual solvent.

Heating at 150 °C for 2 h increased selectivity relative to unheated films (Table 4.2), but not to the level found in similar films heated at 250 °C. Fluxes of O_2 and CO_2 were also 5-10-fold lower than for films heated at 250 °C. Increasing heating time (150 °C) to 12 or 24 h did not yield increases in flux, but selectivity appeared to increase. (The fluxes of N_2 and CH_4 through the films heated at 150 °C for 12 or 24 h were too low to be measured with our system, so we could only determine limits for O_2/N_2 and CO_2/CH_4 selectivities.) The differences between membranes heated at 150 and 250 °C could result from a lower (10-15%) degree

Table 4.2: Gas permeability[a] and selectivity values for 6FDA-mPDA/PAH membranes prepared with different heating temperatures and thicknesses.

Membrane	P_{O_2}	P_{N_2}	P_{CH_4}	P_{CO_2}	P_{O_2}/P_{N_2}	P_{CO_2}/P_{CH_4}
9.5 bilayer 6FDA-mPDA/PAH unheated	0.59	0.68	0.92	0.61	0.86	0.66
9.5 bilayer 6FDA-mPDA/PAH heated at 150 °C for 2 h	0.57	0.30	0.30	1.4	1.9	4.6
9.5 bilayer 6FDA-mPDA/PAH heated at 150 °C for 12 h	0.49	<0.2[b]	<0.2[b]	1.8	>2.5	>9
9.5 bilayer 6FDA-mPDA/PAH heated at 150 °C for 24 h	0.49	<0.2[b]	<0.2[b]	2.1	>2.5	>11
5.5 bilayer 6FDA-mPDA/PAH heated at 250 °C for 2 h	2.9	1.5	1.5	6.1	1.9	4.1
7.5 bilayer 6FDA-mPDA/PAH heated at 250 °C for 2 h	2.9	0.43	0.25	13	6.7	51
9.5 bilayer 6FDA-mPDA/PAH heated at 250 °C for 2 h[c]	2.8	0.40	0.16	11	6.9	68

[a]Data are averages of measurements on two membranes. The difference between the two measurements was <10%.
[b]Fluxes were lower that the limit of the flow meter.
[c]Data from Table 4.1.

of imidization, caged solvent that cannot be completely removed at 150 °C, or a change in film structure (polymer segregation) at the higher heating temperature.

To better understand the effect of the polycation on gas transport, we prepared 6FDA-mPDA membranes that contained a higher fraction of PAH (25 – 30%). This was accomplished by increasing the deposition pH for PAH to 9.0 and adding NaCl (0.5 M) to this solution. In relation the 6FDA-mPDA/PAH membranes containing only 10% PAH and having the same total thickness, O_2/N_2 selectivity decreased from 6.9 to 2.2 and CO_2/CH_4 selectivity decreased from 68 to 5.8, although the permeabilities of O_2 and CO_2 did not change by an appreciable extent. This change in selectivity could result from a greater extent of interpenetration between the layers due to the higher thickness of PAH. The high pH of the PAH solution should also deprotonate the remaining –COOH groups in the poly(amic acid) layer on the surface, allowing for a greater degree of interpenetration.

4.3.6 Gas Transport as a Function of Film Thickness. Although ion-transport studies suggested that as little as 25 nm of polyelectrolyte film is required to cover the pores of alumina supports,[47] the gas-selectivity of polyimide membranes decreased for films less than 35 nm thick. When polyimide thickness was reduced from 50 nm to 25-30 nm by reducing the number of 6FDA-mPDA/PAH bilayers from 9.5 to 5.5, O_2/N_2 selectivity decreased from 6.9 to 1.9 and CO_2/CH_4 selectivity decreased from 68 to 4.1 (Table 4.2). Decreases in selectivity result primarily from increases in N_2 and CH_4 flux. The presence of

some selectivity suggests that the density of defects is not high enough for transport to occur simply by diffusion through pores, but we think that a few defects result in greatly reduced selectivity by increasing N_2 and CH_4 transport. By making the film two layers thicker (7.5 bilayers), we achieved the selectivities similar to those of 9.5-bilayer films, presumably because defects are covered. Thus we find that a minimum thickness of 35 – 40 nm is necessary to achieve the highest selectivities. Even thinner selective films might be constructed if non-porous supports or gutter layers are used.

4.4 Conclusion

Alternating electrostatic adsorption of poly(amic acids) and PAH followed by post-deposition heating provides a convenient method for forming ultrathin, gas-selective polyimide films at the surface of porous alumina. By controlling deposition conditions, films can be tailored to contain primarily polyimide, and fully imidized membranes exhibit permeability coefficients and selectivities that are comparable to literature values for the corresponding bulk polyimides. These selectivities can be achieved even with films as thin as 35-40 nm. Future work aims at further reducing the minimum film thickness required for high selectivity and developing gentler imidization conditions that will allow use of polymeric substrates.

4.5 References

(1) Feng, X.; Huang, R. Y. M. *J. Membrane Sci.* **1996**, *109*, 165-172.

(2) Sroog, C. E. In *Polyimides*; Wilson, D., Stenzenberger, H. D., Hergenrother, P. M., Eds.; Chapman and Hall: New York, 1990, pp 252-284.

(3) Liu, Y.; Pan, C.; Ding, M.; Xu, J. *Polym. Int.* **1999**, *48*, 832-836.

(4) Robeson, L. M.; Burgoyne, W. F.; Langsam, M.; Savoca, A. C.; Tien, C. F. *Polymer* **1994**, *35*, 4970-4978.

(5) Koros, W. J.; Fleming, G. K. *J. Membrane Sci.* **1993**, *83*, 1-80.

(6) Maier, G. *Angew. Chem. Int. Edit.* **1998**, *37*, 2961-2974.

(7) Tanaka, K.; Kita, H.; Okano, M.; Okamoto, K. *Polymer* **1992**, *33*, 587-592.

(8) Tanaka, K.; Okano, M.; Toshino, H.; Kita, H.; Okamoto, K. *J. Polym. Sci., Part B: Polym. Phys.* **1992**, *30*, 907-914.

(9) Koros, W. J.; Walker, D. R. B. *Polym. J.* **1991**, *23*, 481-490.

(10) Pinnau, I.; Koros, W. J. *J. Appl. Polym. Sci.* **1992**, *46*, 1195-1204.

(11) Pinnau, I.; Koros, W. J. *Ind. Eng. Chem. Res.* **1991**, *30*, 1837-1840.

(12) Clausi, D. T.; Koros, W. J. *J. Membrane Sci.* **2000**, *167*, 79-89.

(13) Pinnau, I.; Freeman, B. D. In *Membrane Formation and Modification*; Pinnau, I., Freeman, B. D., Eds.; American Chemical Society: Washington, D.C., 2000, pp 1-22.

(14) Ding, Y.; Bikson, B.; Nelson, J. K. *Macromolecules* **2002**, *35*, 912-916.

(15) Chung, T. S.; Teoh, S. K.; Hu, X. D. *J. Membrane Sci.* **1997**, *133*, 161-175.

(16) Hachisuka, H.; Ohara, T.; Ikeda, K. In *Membrane Formation and Modification*; Pinnau, I., Freeman, B. D., Eds.; American Chemical Society: Washington, D. C., 2000, pp 65-78.

(17) Decher, G. *Science* **1997**, *277*, 1232-1237.

(18) Bertrand, P.; Jonas, A.; Laschewsky, A.; Legras, R. *Macromol. Rapid Comm.* **2000**, *21*, 319-348.

(19) Dubas, S. T.; Schlenoff, J. B. *Macromolecules* **1999**, *32*, 8153-8160.

(20) Shiratori, S. S.; Rubner, M. F. *Macromolecules* **2000**, *33*, 4213-4219.

(21) Kleinfeld, E. R.; Ferguson, G. S. *Chem. Mater.* **1996**, *8*, 1575-1578.

(22) Sullivan, D. M.; Bruening, M. L. *J. Am. Chem. Soc.* **2001**, *123*, 11805-11806.

(23) Krasemann, L.; Tieke, B. *Langmuir* **2000**, *16*, 287-290.

(24) Stair, J. L.; Harris, J. J.; Bruening, M. L. *Chem. Mater.* **2001**, *13*, 2641-2648.

(25) Krasemann, L.; Tieke, B. *J. Membrane Sci.* **1998**, *150*, 23-30.

(26) Krasemann, L.; Tieke, B. *Chem. Eng. Technol.* **2000**, *23*, 211-213.

(27) Meier-Haack, J.; Lenk, W.; Lehmann, D.; Lunkwitz, K. *J. Membrane Sci.* **2001**, *184*, 233-243.

(28) Leväsalmi, J.-M.; McCarthy, T. J. *Macromolecules* **1997**, *30*, 1752-1757.

(29) Kotov, N. A.; Magonov, S.; Tropsha, E. *Chem. Mater.* **1998**, *10*, 886-895.

(30) Stroeve, P.; Vasquez, V.; Coelho, M. A. N.; Rabolt, J. F. *Thin Solid Films* **1996**, *284-285*, 708-712.

(31) van Ackern, F.; Krasemann, L.; Tieke, B. *Thin Solid Films* **1998**, *327-329*, 762-766.

(32) Baur, J. W.; Besson, P.; O'Connor, S. A.; Rubner, M. F. *Mater. Res. Soc. Symp. Proc.* **1996**, *413*, 583-588.

(33) Anderson, M. R.; Davis, R. M.; Taylor, C. D.; Parker, M.; Clark, S.; Marciu, D.; Miller, M. *Langmuir* **2001**, *17*, 8380-8385.

(34) Moriguchi, I.; Teraoka, Y.; Kagawa, S.; Fendler, J. H. *Chem. Mater.* **1999**, *11*, 1603-1608.

(35) Liu, Y.; Wang, A.; Claus, R. O. *Appl. Phys. Lett.* **1997**, *71*, 2265-2267.

(36) Martin, C. R. *Science* **1994**, *266*, 1961-1966.

(37) Petri, D. F. S.; Wenz, G.; Schunk, P.; Schimmel, T. *Langmuir* **1999**, *15*, 4520-4523.

(38) Sroog, C. E. *J. Polym. Sci., Macromol. Rev.* **1976**, *11*, 161-208.

(39) Merkel, T. C.; Freeman, B. D.; Spontak, R. J.; He, Z.; Pinnau, I.; Meakin, P.; Hill, A. J. *Science* **2002**, *296*, 519-522.

(40) Arys, X.; Jonas, A. M.; Laguitton, B.; Legras, R.; Laschewsky, A.; Wischerhoff, E. *Prog. Org. Coat.* **1998**, *34*, 108-118.

(41) Yoo, D.; Shiratori, S. S.; Rubner, M. F. *Macromolecules* **1998**, *31*, 4309-4318.

(42) Harris, F. W. In *Polyimides*; Wilson, D., Stenzenberger, H. D., Hergenrother, P. M., Eds.; Chapman and Hall: New York, 1990, pp 1-37.

(43) Zhou, Y.; He, P.; Chen, K.; Li, C.; Hong, K. *Zhongguo Kexue Jishu Daxue Xuebao* **1995**, *25*, 21-26.

(44) Kim, T.-H.; Koros, W. J.; Husk, G. R. *J. Membrane Sci.* **1989**, *46*, 43-56.

(45) Henis, J. M. S.; Tripodi, M. K. *Science* **1983**, *220*, 11-17.

(46) Kesting, R. E.; Fritzche, A. K. *Polymeric Gas Separation Membranes*; John Wiley & Sons: New York, 1993.

(47) Harris, J. J.; Stair, J. L.; Bruening, M. L. *Chem. Mater.* **2000**, *12*, 1941-1946.

Chapter 5

Ultrathin, Cross-linked Polyimide Pervaporation Membranes Prepared from Polyelectrolyte Multilayers

5.1 Introduction

Pervaporation is a promising, membrane-based technique for the separation of liquid mixtures. In this process, the liquid is exposed to the surface of a membrane whose permeate side is at reduced pressure, and selective transport of one component through the membrane allows for solvent purification or analyte collection.[1] Pervaporation is attractive because it allows for the separation of azeotropic mixtures and often requires less energy than conventional distillation.[2,3] Many of the successes with pervaporation involve the removal of water from organic solvents, but the reverse separation has also been demonstrated.[4-6] Even with advances in pervaporation technology, however, there is still a need for membrane systems with increased selectivity and flux.

Membranes with high water-pervaporation selectivities generally contain hydrophilic materials that preferentially absorb water. Nevertheless, many hydrophilic polymers swell dramatically in aqueous solutions to give large fluxes but little or no transport selectivity.[7-9] Hence, to achieve selective water pervaporation, several research groups reduced the extent to which hydrophilic membranes swell by using cross-linked polymers[10-13] or materials that contain both hydrophobic and hydrophilic regions.[9,14-18] The use of mildly hydrophobic polymers, e.g., polyimides, also reduces membrane swelling to yield highly

selective pervaporation membranes.[19-21] All of these strategies for decreasing swelling can increase selectivity, but at the same time, they do reduce permeate flux.

When selecting membrane materials, there generally is a compromise between selectivity and flux because highly selective materials are usually not highly permeable.[22] The most common method employed to overcome this limitation is the use of asymmetric[23,24] or composite[25,26] membranes that consist of a thin, highly selective material on a highly permeable support. Because the thin separation layer provides most of the resistance to mass transport, flux is often inversely proportional to the thickness of this layer.[25] The recently developed technique of alternating polyelectrolyte deposition (APD) provides a particularly versatile method for depositing ultrathin membrane skins whose thickness can be controlled on the nm scale.[27-32] This method involves alternating immersions of a charged substrate into polycation and polyanion solutions, and thus film thickness is easily controlled by changing either the number of adsorbed polyelectrolyte layers or deposition variables such as pH and supporting salt concentration.[33-36] To form membranes using APD, the polyelectrolyte multilayers are simply deposited on porous supports, and because each added polyelectrolyte layer covers defects in prior layers, [32,33,37] films as thin as 20 nm can completely cover underlying pores.[38]

Tieke and coworkers used typical polyelectrolyte multilayers, e.g., poly(styrene sulfonate)/poly(allylamine), to prepare pervaporation membranes for the removal of water from ethanol.[39,40] They found a direct relationship between

the separation selectivity and the charge density of the polyelectrolytes, presumably because higher charge density increases the extent of ionic cross-linking and reduces swelling. They attempted to further increase ionic cross-linking by annealing the films at 90 °C and achieved water/ethanol selectivities as high as 450. Although these membranes were very selective in the removal of water from organic solvents, they also had relatively low fluxes, most likely because of the high thickness of the separating layer (sixty bilayers were used to make these membranes). Meier-Haack and coworkers showed similar results using polyethylenimine/poly(acrylic acid) films with as few as 6 bilayers.[28] However, even in that case, fluxes in highly selective separations were less than 1 $kg \cdot m^{-2} \cdot h^{-1}$.

In this C, we combine the versatility of APD with covalent interlayer cross-linking and the use of semi-hydrophobic polymers (polyimides) to prepare high-flux, high selectivity pervaporation membranes. Ionized precursor poly(amic acids) serve as the polyanions in multilayer polyelectrolyte films, and subsequent heating yields a polyimide coating.[41-44] Using this method, we previously prepared polyimide membranes for gas and ion separations,[29,30] but the poly(amic acids) employed in this study contain diaminobenzoic acid (DABA) groups that can form amide cross-links when heated (Figures 5.1 and 5.2). DABA was previously incorporated into polyimide pervaporation membranes to increase hydrophilicity[17,45] or to allow for cross-linking upon addition of diols or diamines.[46,47] In the case of poly(amic acid)/polycation multilayers, the polycation, e.g., protonated poly(allylamine), serves as the cross-linking agent,

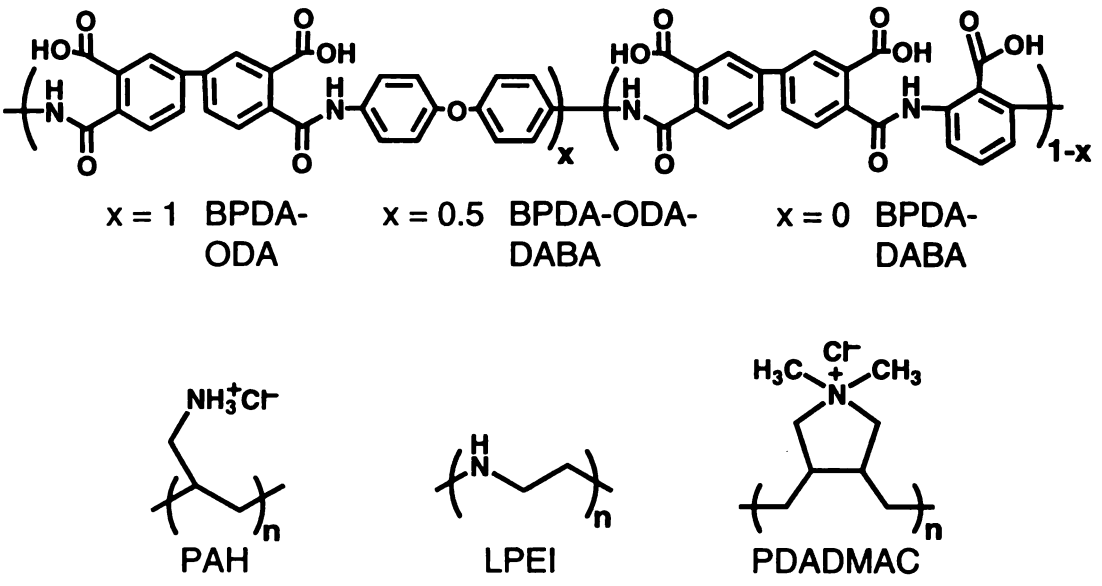

Figure 5.1. Structures of the poly(amic acids) and other polyelectrolytes used in this study.

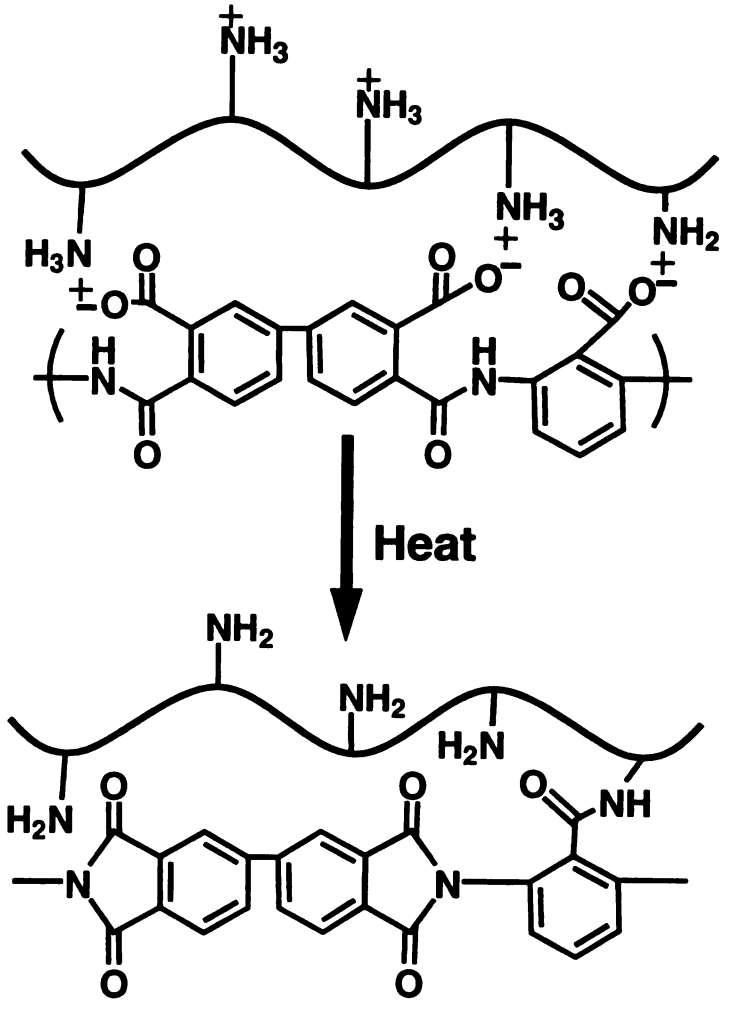

Figure 5.2. Heat-induced imidization and cross-linking of BPDA-DABA/PAH films.

and the cross-linking density can be controlled by varying the fraction of DABA groups in the poly(amic acid).

By depositing ~50 nm thick films on porous alumina supports,[48] we are able to selectively dehydrate ethanol and isopropanol solutions while maintaining high flux. Both amide cross-links and the hydrophobic polyimide backbone aid in reducing the swelling of selective films, and water-selective permeation presumably occurs because the polycation and non-cross-linked acid groups add a hydrophilic component to the membrane. We investigated the effect of imidization temperature, polyimide structure, and the amount of cross-linking on selectivity and flux. We also utilized three different polycations to examine the effects of polycation structure and composition on transport. Fully imidized membranes composed of 3,3',4,4'-biphenyltetracarboxylic dianhydride-DABA and poly(allylamine) give the largest water-pervaporation selectivities: 1100 for 10% isopropanol solutions and 6100 for 90% isopropanol, with fluxes of 11 and 2 $kg \cdot m^{-2} \cdot h^{-1}$, respectively. Such selectivities are typical of high-performance pervaporation membranes, but fluxes are, in general, several times larger. [49-51]

5.2 Experimental Section

5.2.1 Materials. 3,3',4,4'-biphenyltetracarboxylic dianhydride (BPDA), 4,4'-oxydianiline (ODA), 3,5-diaminobenzoic acid (DABA), poly(allylamine hydrochloride) (PAH), and poly(diallyldimethylammonium chloride) (PDADMAC) were purchased from Aldrich. Linear polyethylenimine (LPEI) was purchased from Polysciences. DMF (Spectrum) was dried with molecular sieves for at least 24 h before use. The ODA and BPDA were purified by vacuum sublimation, and

DABA was recrystallized twice from water and dried in vacuum prior to use. All other chemicals were used as received. ACS grade isopropanol (CCI) and 200-proof ethanol (Pharmco) were employed in pervaporation studies, and deionized water (Milli-Q, 18.2 MΩ cm) was used for rinsing and preparation of polymer-containing and pervaporation solutions. Porous alumina supports were 25 mm Whatman Anodiscs with 0.02 μm-diameter surface pores (Fisher Scientific), while silicon(100) wafers (Silicon Quest) sputter coated with 200 nm of Al served as supports for ellipsometry, reflectance FTIR spectroscopy, and contact-angle measurements.

5.2.2 Substrate Preparation. In the case of porous alumina supports, the polypropylene support ring on the alumina was removed to prevent it from melting into substrate pores during heat-induced imidization and cross-linking. This was accomplished by cutting off as much of the polymer as possible, and then burning off the remaining ring at 400 °C for 18 h in a furnace. Subsequently, the alumina supports were rinsed with acetone, dried with N_2, and cleaned for 10 min in a UV/O_3 cleaner (Boekel Industries, model 135500). Al-coated wafers were simply cleaned by UV/O_3 prior to use.

5.2.3 Polymer Synthesis. The poly(amic acids) were prepared using a typical literature procedure.[52] The diamine was dissolved in DMF, a stoichiometric quantity of the dianhydride was gradually added to this solution over a ~15 min period, and the 10% by weight (total dissolved solids) solution was stirred for 24 h under a nitrogen atmosphere. The poly(amic acids) were precipitated twice in 0.01 M HCl, filtered, and then dried under vacuum for 24 h.

5.2.4 Solution Preparation and Film Deposition. To avoid the possibility of hydrolysis, poly(amic acid) solutions were made just prior to film formation, and the dry polymers were always kept in the freezer. Due to the insolubility of the poly(amic acids) in water, solutions containing ~0.005 M poly(amic acid) and 0.5 M NaCl were prepared by dissolving the poly(amic acid) in 0.75 ml of 0.2 M triethylamine, diluting to 10 ml with water and adding 0.29 g NaCl. (The molarities of the polyelectrolytes are given with respect to the repeating unit.) The pH was adjusted to ~5.0 for DABA-containing poly(amic acids) and ~6.0 for BPDA-ODA by adding 0.1 M HCl. As mentioned in a previous publication, the deprotonated poly(amic acids) are deposited under conditions near their solubility limits to achieve films of appreciable thickness.[30] Poly(amic acids) typically precipitate out of aqueous solutions when either the pH is low enough to protonate most of the carboxylic acids or the concentration of salt is high.

Film deposition began with immersion of the substrate (Al-coated Si or porous alumina) into the poly(amic acid) solution for 3 min. (The alumina membranes were placed in an o-ring holder so that only the face with 0.02 μm-diameter pores was exposed to solutions.) The substrate was then rinsed with copious amounts of Milli-Q water for about 1 min. Subsequently, the substrate was immersed in an aqueous 0.02 M PAH, LPEI, or PDADMAC solution (adjusted to pH 5.0 with NaOH) for 3 min and rinsed with Milli-Q water. This process was repeated until the desired number of bilayers were deposited, and all films were terminated with a poly(amic acid) layer.

5.2.5 Film Imidization. Films were heated using a home-built apparatus consisting of a temperature controller, thermocouple, glass chamber, and heating mantle. The heating apparatus was purged with nitrogen for 2 h prior to heating as well as during heating and cooling. The temperature was ramped at a rate of 5 °C per min and was held at the final heating temperature for 2 h.

5.2.6 Film Characterization. Ellipsometric thickness measurements on Al-coated silicon wafers were made using a rotating analyzer ellipsometer (model M-44, J. A. Woollam) and WVASE32 software. A film refractive index of 1.5 was assumed in all thickness determinations. Reflectance FTIR spectra were obtained using a Nicolet Magna-560 FTIR spectrophotometer and a Pike grazing angle (80º) attachment. A UV/O_3-cleaned Al-substrate was used as a background. Static water contact-angle measurements (Firsttenangstroms contact angle analyzer) were also performed before and after film heating. Field-emission scanning electron microscopy (FESEM) images were obtained with a Hitachi S-4700II instrument using an acceleration voltage of 15 kV. Samples were fractured in liquid nitrogen and sputter-coated with 5 nm of gold before imaging.

5.2.7 Pervaporation Measurements. All pervaporation measurements were taken using the home-built apparatus shown in Figure 5.3a. The apparatus consists of a vacuum pump, peristaltic pump, collection traps, and a heated water bath, which is not shown in the figure. The membranes are first placed in a membrane cell (Figure 5.3b) where they are supported by a stainless steel frit

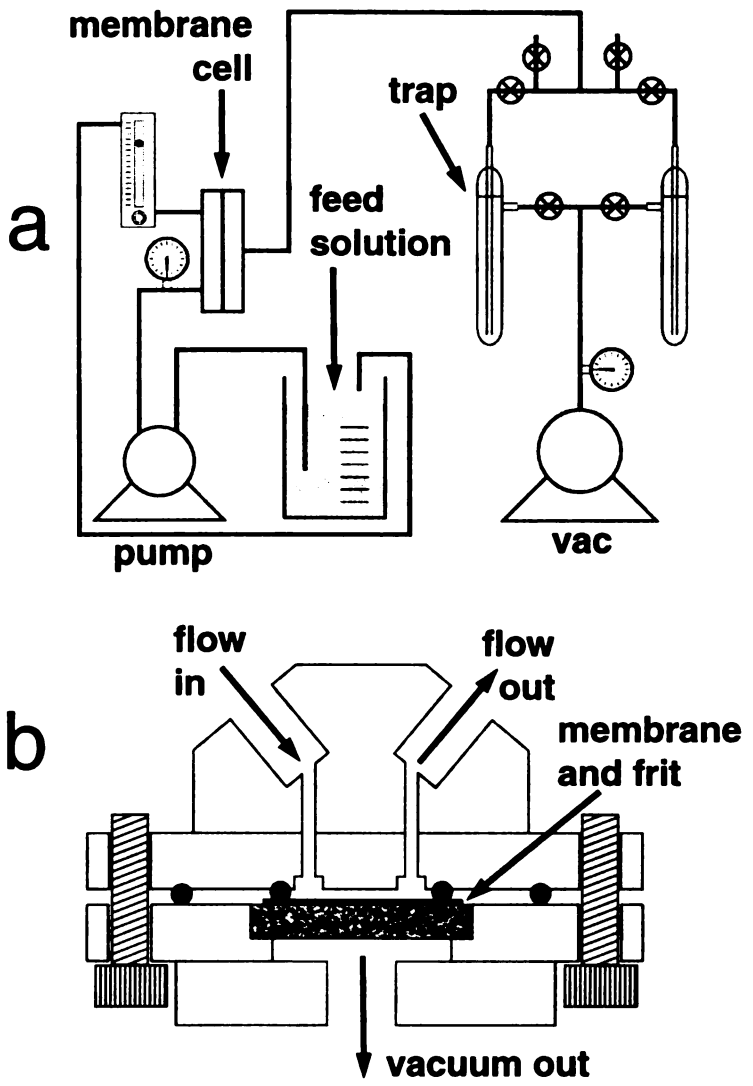

Figure 5.3. Schematic diagrams of (a) the pervaporation system and (b) a cross-sectional view of the membrane cell.

(Mott Corporation) and sealed with an o-ring. The cell is sealed with an additional o-ring to maintain vacuum, and solution is pumped across the membrane at a rate of 10 mL/min to minimize concentration polarization. The membrane cell is connected to a coiled stainless steel feed tube, and both the membrane cell and coiled tube were immersed into a thermostated water bath to control the feed solution temperature. The bath was maintained at 50 °C unless otherwise stated. Vacuum (pressure of 0.06 mbar) was applied to the backside of the membrane, and the permeate was collected in a liquid nitrogen-cooled trap. Tubing on the permeate side was warmed with heating tape to avoid any condensation. Between experiments with different concentrations of the same alcohol, the feed side of the membrane was flushed with 300 mL of the feed solution. When changing from isopropanol to ethanol, the feed side was flushed with 1.5 L of water followed by 300 mL of the next feed solution. At all times, permeate was collected in a trap. Finally, prior to sample collection, pervaporation was performed for at least 1 h to achieve stable, steady-state fluxes. The collected samples were analyzed by gas chromatography (Shimadzu GC-17A equipped with a Restek RTx-BAC1 column) using methanol as an internal standard. The selectivity,α, was calculated using equation 1 where P_W, F_W, P_A, and F_A are the concentrations of water in the permeate and the feed and alcohol in the permeate and the feed, respectively. Reported selectivities and fluxes are averages of measurements performed on at least three different membranes.

Table 5.1: Bilayer thicknesses (nm) and Water Contact Angles for Unheated and Heated (250 °C) Polyelectrolyte Films Deposited on Al-coated Si.

Polyelectrolyte Film[a]	bilayer thickness		contact angle	
	unheated	heated	unheated	heated
BPDA-ODA/PAH	4.0 ± 0.3	2.8 ± 0.3	41 ± 6	66 ± 5
BPDA-ODA-DABA/PAH	4.1 ± 0.1	3.3 ± 0.2	27 ± 3	49 ± 1
BPDA-DABA/PAH	3.5 ± 0.1	2.7 ± 0.1	27 ± 1	52 ± 4
BPDA-ODA-DABA/PDADMAC	5.2 ± 0.1	4.2 ± 0.1	39 ± 3	53 ± 5
BPDA-DABA/PDADMAC	4.2 ± 0.3	2.8 ± 0.2	29 ± 3	53 ± 2
BPDA-ODA-DABA/LPEI	6.7 ± 0.6	3.5 ± 0.1	39 ± 2	57 ± 1
BPDA-DABA/LPEI	6.3 ± 0.1	3.7 ± 0.1	31 ± 2	58 ± 3

[a] Measurements were taken on films containing 5.5 bilayers.

$$\text{eq. 1} \qquad \alpha = \frac{P_W F_A}{P_A F_W}$$

5.3 Results and Discussion

5.3.1 Film Deposition and Characterization. To evaluate how polymer structure and cross-linking affect pervaporation selectivity and flux, we prepared polyelectrolyte multilayers using three different poly(amic acids) as well as three polycations (Figure 5.1). The poly(amic acids) contain varying amounts of DABA, which is the primary cross-linking moiety in these polymers, while the polycations PAH and LPEI contain protonated primary and secondary amines, respectively. These amine groups can form amide cross-links via heat-induced reaction with the carboxylic acid groups of DABA (Figure 5.2). In contrast, PDADMAC contains permanently charged quaternary amines that do not react with carboxylic acids.

We first performed ellipsometric and reflectance FTIR studies with films deposited on Al-coated Si wafers to characterize film thickness and the heat-induced imidization reaction. Film thickness increase linearly with the number of bilayers deposited, and Table 5.1 presents the thickness per bilayer for each of the films. Bilayer thicknesses are about the same (within a factor of 2) for all of the materials. From these measurements, we determined the number of bilayers (unheated) needed to form 40 to 50 nm-thick films for each of the polyelectrolyte pairs examined. Previous FESEM images suggest that at least 20 nm of film is required to cover porous alumina, so we deposited 40 to 50 nm-thick films to

ensure full coverage of underlying pores.[38] Imidization at 250 °C results in a 20 to 50% decrease in film thickness, presumably because of the loss of water.

Thicknesses determined by ellipsometry on Al-coated Si and by FESEM on porous alumina are in reasonable agreement, although in general, the films on porous alumina appear to be about 30% thicker.[30] Cross-sectional FESEM images of *imidized* films on porous alumina showed 40 to 60 nm-thick films for all of the polyelectrolyte combinations. (Tables 5.2 and 5.3 give the number of bilayers in different films.) Figure 5.4 shows a typical image of 12.5 bilayers of imidized BPDA-DABA/PAH on alumina, and this and other images suggest that films are relatively uniform across the support. Top-down images also suggest complete pore coverage. Very little, if any, deposition of polyelectrolytes is noticeable on the walls of the 0.2-μm pores in the bulk of the alumina, and images of the uncoated backside of the membrane show completely open pores.

Reflectance FTIR spectroscopy confirmed imidization and cross-linking within polyelectrolyte multilayers. Figure 5.5 shows spectra of three different poly(amic acid)/PAH films that were heated at 250 °C as well as the spectrum of one unheated film. After imidization at 250 °C, absorbances due to amic acids vanished (1750-1500 cm^{-1}), and imide peaks appeared (1775 and 1725 cm^{-1}). The spectrum of the heated BPDA-DABA/PAH film contains a shoulder at 1670 cm^{-1}, which is most likely due to the amide cross-links formed by reaction of the primary amine groups of PAH and the carboxylic acid groups of the DABA segment (Figure 5.2). Assuming that the extinction coefficient for these amides

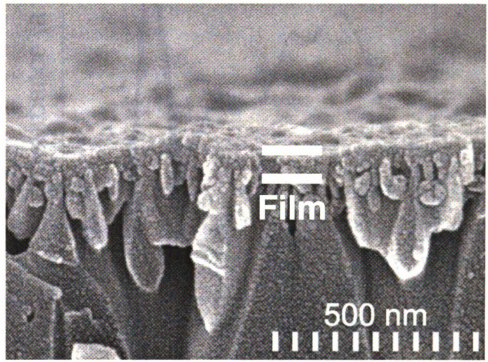

Figure 5.4. Cross-sectional FESEM image of an alumina support coated with an imidized 12.5-bilayer BPDA-DABA/PAH film.

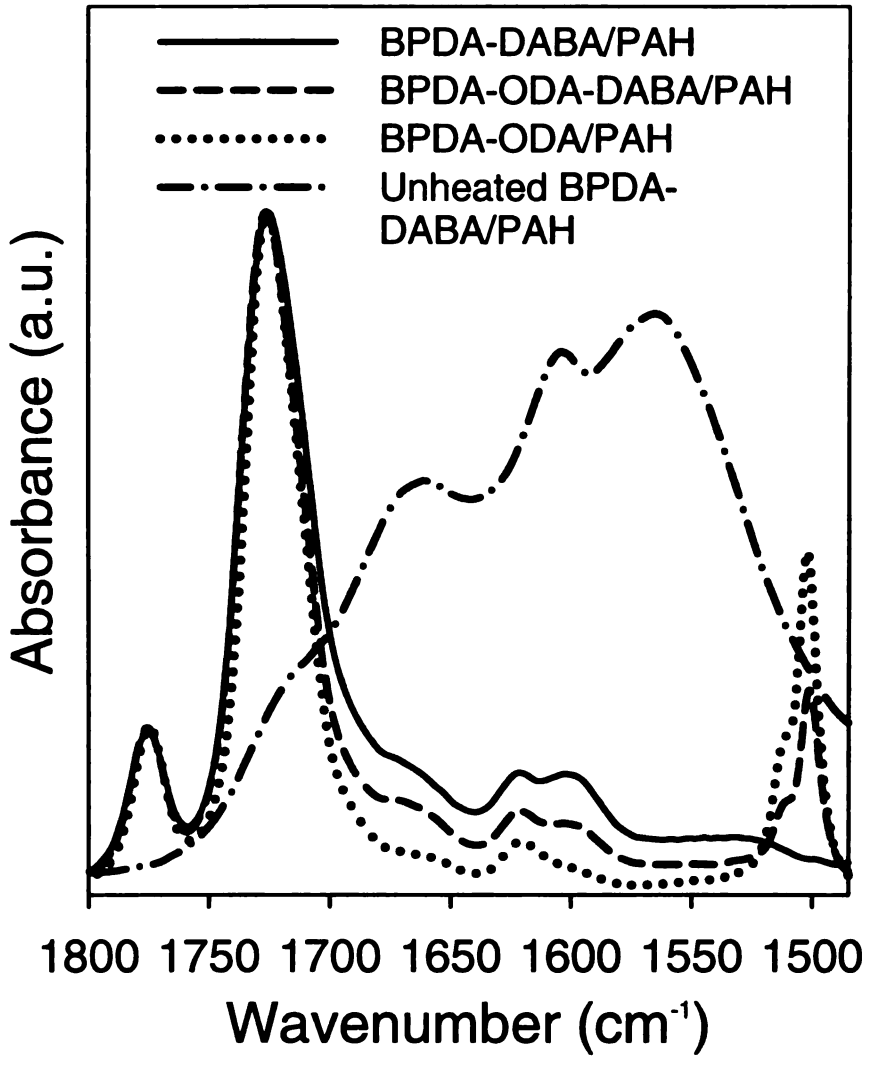

Figure 5.5. Reflectance FTIR spectra of various poly(amic acid)/PAH films deposited on Al-coated Si. The spectra of heated films were normalized to the imide peak of BPDA-DABA at 1725 cm^{-1}, while spectra of heated and unheated BPDA-DABA/PAH films are plotted on a common scale.

is comparable to that of the amides in the unheated poly(amic acid) (1660 cm^{-1}), the spectra suggest that roughly 60% of the DABA groups react to form cross-links. As expected, the absorbance of the 1670 cm^{-1} shoulder decreases by ~50% on going from BPDA-DABA/PAH to BPDA-ODA-DABA/PAH films. However, even BPDA-ODA/PAH films show a small shoulder in this region, which may be due to a small amount of cross-linking with the amic acid or incomplete imidization. The spectrum of imidized BPDA-DABA/PDADMAC is similar to that of BPDA-ODA/PAH in this region (supporting information, Figure 5.1), further suggesting that shoulders at 1670 cm^{-1} in the spectra of BPDA-DABA/PAH and BPDA-ODA-DABA/PAH are due to amide cross-links.

5.3.2 Pervaporation Experiments with non Cross-linkable Membranes. To examine the effect of film imidization on pervaporation selectivity and flux, we initially compared unheated and heated membranes that are unlikely to form amide cross-links. Such systems contain either BPDA-ODA or PDADMAC. Unheated BPDA-ODA/PAH membranes exhibited very low water/alcohol pervaporation selectivities (<4) for any of the alcohol solutions, and fluxes were extremely high, ranging from 50 to 70 $kg \cdot m^{-2} \cdot h^{-1}$ (Table 5.2). FESEM images suggest complete coverage of the support, so we think that the high fluxes result from water-swollen membranes rather than incomplete support coverage. Swelling by water is consistent with the lower water/alcohol selectivities for 10% alcohol solutions relative to 90% alcohol solutions. However, we do not understand why the flux is ~20% higher for the 90% alcohol solutions.

Table 5.2: Permeate Water Concentrations, Selectivity Coefficients (listed in parenthesis), and Fluxes (listed in italics, in $kg \cdot m^{-2} \cdot h^{-1}$) for Pervaporation through several Poly(amic acid)/PAH Membranes at 50 °C.

Membrane material	Pervaporation Solution			
	10% isopropanol	10% ethanol	90% isopropanol	90% ethanol
BPDA-ODA/PAH unheated (10.5 bilayers)	91.5 ± 0.15 (1.2) *51 ± 4*	92.7 ± 2.3 (1.6) *58 ± 4*	27.8 ± 11.1 (3.6) *64 ± 4*	19.6 ± 1.1 (2.2) *67 ± 4*
BPDA-ODA/PAH heated 250 °C (10.5 bilayers)	99.6 ± 0.14 (29) *9.9 ± 2*	98.4 ± 1.9 (16) *12 ± 3*	94.2 ± 2.0 (160) *2.1 ± 0.2*	89.4 ± 2.0 (78) *2.5 ± 0.2*
BPDA-ODA-DABA/PAH unheated (12.5 bilayers)	98.2 ± 0.56 (6.6) *18 ± 1*	92.6 ± 0.76 (1.4) *21 ± 0.6*	96.6 ± 1.3 (290) *3.0 ± 0.1*	57.1 ± 6.9 (12) *7.2 ± 0.3*
BPDA-ODA-DABA /PAH heated 150 °C (12.5 bilayers)	99.92 ± 0.05 (170) *16 ± 1*	98.93 ± 0.24 (11) *16 ± 0.5*	98.29 ± 1.3 (690) *2.2 ± 0.2*	90.1 ± 4.3 (92) *2.3 ± 0.1*
BPDA-ODA-DABA/PAH heated 250 °C (12.5 bilayers)	99.95 ±0.03 (240) *9.7 ± 0.8*	99.64 ± 0.24 (26) *11 ± 1*	98.7 ± 0.58 (690) *1.9 ± 0.1*	93.6 ± 1.4 (130) *2.0 ± 0.3*
BPDA-DABA/PAH heated 250 °C (12.5 bilayers)	99.99 ± 0.003 (1100) *11 ± 1*	99.9 ± 0.08 (100) *12 ± 1*	99.9 ± 0.04 (6100) *2.0 ± 0.2*	97.8 ± 1.1 (500) *1.9 ± 0.3*

Table 5.3: Permeate Water Concentrations, Selectivity Coefficients (listed in parenthesis), and Fluxes (listed in italics, in $kg \cdot m^{-2} \cdot h^{-1}$) for Pervaporation through several Poly(amic acid)/PDADMAC and Poly(amic acid)/LPEI Membranes at 50 °C.

Membrane material	Pervaporation Solution			
	10% isopropanol	10% ethanol	90% isopropanol	90% ethanol
BPDA-ODA-DABA/PDADMAC unheated (10.5 bilayers)	89.6 ± 0.9 (1) *27 ± 3*	90.1 ± 1.0 (1) *32 ± 2*	64.1 ± 7.6 (17) *8.2 ± 3*	43.1 ± 2.1 (6.8) *35 ± 2*
BPDA-ODA-DABA/PDADMAC heated 250 °C (10.5 bilayers)	99.7 ± 0.19 (32) *13 ± 2*	98.1 ± 1.0 (5.8) *16 ± 3*	98.0 ± 1.1 (460) *2.1 ± 0.5*	68.0 ± 3.1 (18) *4.3 ± 1*
BPDA-DABA/PDADMAC heated 250 °C (10.5 bilayers)	99.4 ± 0.48 (12) *16 ± 0.7*	94.1 ± 2.6 (2.2) *19 ± 0.7*	97.0 ± 0.96 (310) *2.7 ± 0.2*	57.1 ± 8.3 (13) *8.5 ± 3*
BPDA-ODA-DABA/LPEI heated 250 °C (7.5 bilayers)	99.9 ± 0.06 (140) *9.3 ± 0.9*	99.8 ± 0.06 (71) *9.8 ± 2*	96.8 ± 2.7 (190) *2.0 ± 0.4*	82.2 ± 12.0 (70) *2.7 ± 0.8*
BPDA-DABA/LPEI heated 250 °C (7.5 bilayers)	99.4 ± 0.2 (22) *14 ± 2*	98.87 ± 0.2 (10) *15 ± 1*	91.2 ± 4.6 (120) *2.5 ± 0.2*	77.6 ± 5.5 (33) *2.8 ± 0.4*

Imidization of BPDA-ODA/PAH membranes yields enhanced selectivities ranging from 16 to 160 (Table 5.2) along with permeate fluxes that are only 3 to 20% of those through the corresponding unheated membranes. Water contact angles (Table 5.1) show that imidization increases hydrophobicity, which should reduce swelling and, hence, increase selectivity and decrease flux. Although heated films are slightly hydrophobic, the polyimides are still sufficiently hydrophilic to allow preferential permeation of water. Pervaporation membranes prepared by casting of pure Kapton™, a similar polyimide, showed water selectivities of 50 for 90% ethanol solutions.[17] Thus, selectivities do not appear to be adversely affected by the presence of PAH.

Similar results occur with BPDA-ODA-DABA/PDADMAC, where unheated membranes show no selectivity in 10% isopropanol and ethanol solutions and modest selectivities in 90% alcohol solutions (Table 5.3). Imidizing the BPDA-ODA-DABA/PDADMAC membranes greatly increases the selectivity, with the most notable result being 98% water in the permeate from a 90% isopropanol feed. We also examined pervaporation through heated BPDA-DABA/PDADMAC, and these systems generally have slightly greater fluxes and slightly lower selectivities than heated BPDA-ODA-DABA/PDADMAC. The presence of more DABA groups in BPDA-DABA than in BPDA-ODA-DABA likely allows an increase in film swelling.

5.3.3 Cross-linkable Membranes. To evaluate the dependence of selectivity on cross-linking density, we compared imidized BPDA-DABA/PAH, BPDA-ODA-

DABA/PAH, and BPDA-ODA/PAH membranes. For all solvent mixtures, the selectivity increases with the amount of DABA in the imidized (250 °C) polymer film (Table 5.2). As an example, the water/alcohol selectivities for 90% isopropanol feed solutions are 160, 690, and 6100 for heated BPDA-ODA/PAH, BPDA-ODA-DABA/PAH, and BPDA-DABA/PAH films, respectively. Remarkably, within experimental error, the flux values are the same for all three of the membranes in nearly every case. We expected the flux to decrease with higher cross-linking densities, but the effect of DABA content on flux appears to be minimal. Remaining non-cross-linked DABA most likely adds a hydrophilic component to the membrane, which increases water transport.

We also used the BPDA-ODA-DABA/PAH system to investigate the effect of the feed solution temperature on transport. Consistent with other pervaporation studies,[53] permeate flux increased with temperature. For 10% isopropanol feeds at 35, 50, and 65 °C, fluxes were 5.0, 9.7, and 17 $kg \cdot m^{-2} \cdot h^{-1}$, respectively. Selectivity, however, did not depend on the feed temperature.

LPEI provides a second polycation that should be capable of forming cross-linked films. We thought that the LPEI would be more hydrophilic than PAH and, hence, provide cross-linked membranes with higher water/alcohol selectivity.[54] Reflectance FTIR spectroscopy (Figure 5.6) confirms that the secondary amine in LPEI allows for cross-linking, although the amide shoulder at 1670 cm^{-1} is about half the intensity of that for PAH-containing films. The lower cross-linking density appears to have a large impact on selectivity. In the case of imidized BPDA-DABA films, the use of LPEI rather than PAH results in 10 to 50-

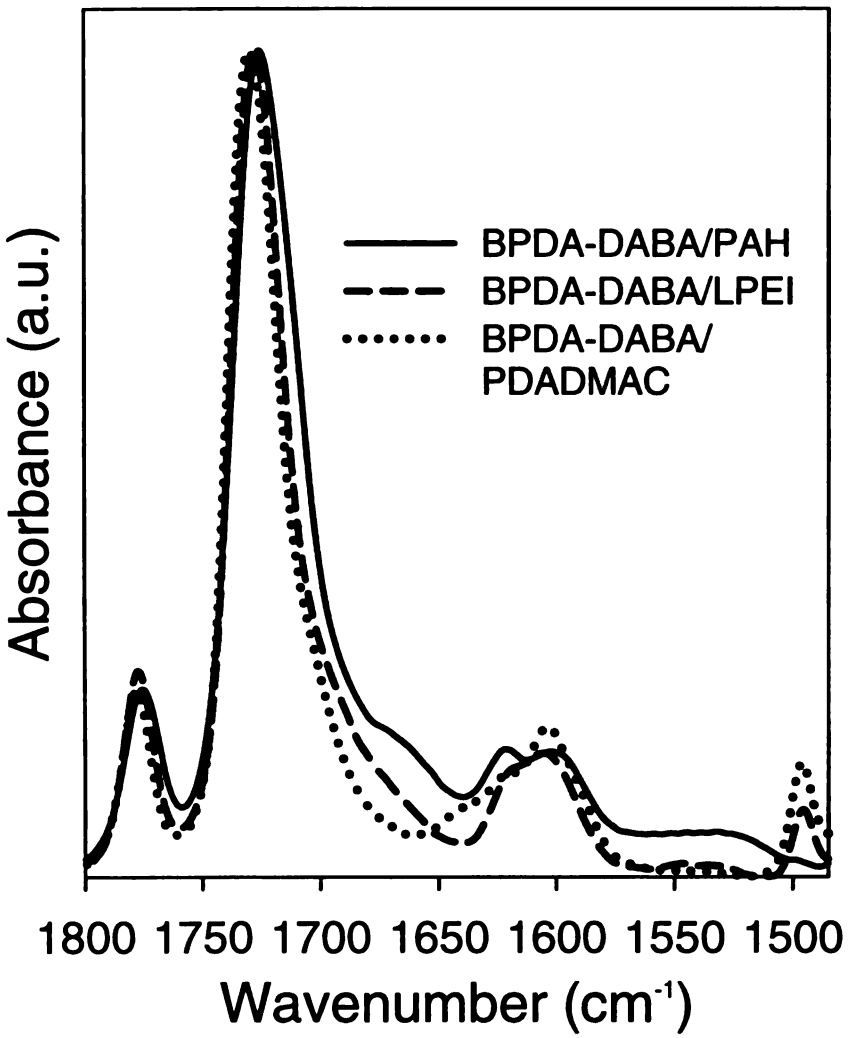

Figure 5.6. Reflectance FTIR spectra of various BPDA-DABA/polycation films deposited on Al-coated Si. The spectra of heated films were normalized to the imide peak of BPDA-DABA/PAH at 1725 cm^{-1}.

fold lower selectivities. The effect is less dramatic for BPDA-ODA-DABA, but selectivities are still 2 to 4-fold lower, except in the case of 10% ethanol. Interestingly, like the PDADMAC but unlike the PAH systems, the BPDA-ODA-DABA/LPEI membranes have higher selectivities than the BPDA-DABA/LPEI membranes. Without as many cross-links, the added hydrophilicity of the DABA may again allow for increased swelling that permits some non-specific transport.

Variation of heating temperature should provide some control over both imidization and cross-linking and, hence, allow manipulation of transport properties. For pure, dip-cast poly(amic acid) membranes, Kang and coworkers showed that partial (60%) imidization gave the highest selectivity in the removal of water from ethanol.[20] They attributed the higher selectivity to a balance between increased hydrophilicity due to remaining amic acid groups and a reduction in swelling due to imidization. In our previous papers we showed that the extent of imidization of multilayer poly(amic acid)/polycation films can be controlled by varying heating temperature.[29] FTIR spectra of films heated at 150 °C for 2 h showed 85% imidization, while full imidization occurred at 250 °C. Thus, to see how membrane performance changes with the extent of imidization, we compared BPDA-ODA-DABA/PAH membranes heated at 150 and 250 °C (Table 5.2). Partial imidization does not provide any advantage in the separation, as it yields selectivities that are as much as 2.4-fold lower than those achieved by heating at 250 °C. Moreover, substantially higher fluxes were observed for the partially imidized membranes only with 10% alcohol feed solutions, and even in that case flux increased by only ~50%. We suspect that a further decrease in

heating temperatures would only result in lower water/alcohol selectivities, as selectivities for unheated membranes are lower than for membranes heated at 150 °C.

5.3.4 Comparison with related membrane systems. Kang and coworkers used pure pyromellitic dianhydride (PMDA)-ODA-DABA membranes that contained various amounts of DABA to dehydrate ethanol solutions.[17] However, they did not use DABA as a site for cross-linking, but only to increase the hydrophilicity of the membrane. Maximum water selectivities and fluxes (320 and 0.06 $kg \cdot m^{-2} \cdot h^{-1}$, respectively for 90% ethanol) occurred when 60% of the polyimide repeat units contained DABA. This selectivity is almost 20-fold higher than that with BPDA-ODA-DABA/PDADMAC films, which contain a similar fraction (50%) of DABA groups, suggesting that PDADMAC does alter film packing to reduce selectivity. In contrast, cross-linked BPDA-DABA/PAH films, in which 100% of the repeat units contain DABA (approximately 60% of these groups participate in cross-linking), show selectivities similar to bulk PMDA-ODA-DABA. Although Kang and coworkers used PMDA rather than BPDA as a monomer, this comparison still suggests that cross-linked polyelectrolyte multilayers are capable of achieving selectivities similar to those in pure polyimide films.

Compared to the majority of pervaporation membranes in the literature, ultrathin BPDA-DABA/PAH composite membranes allow for at least 10-fold larger water fluxes while maintaining comparable selectivities.[49-51] The greater fluxes result from the minimal thickness of the polyelectrolyte multilayers.

Yanagashita showed that polyimide asymmetric membranes can give pervaporation selectivities and fluxes as high as 900 and 1 $kg \cdot m^{-2} \cdot h^{-1}$, respectively, for 95% ethanol feed solutions at 60 °C.[19] These values are comparable to those achieved with BPDA-DABA/PAH films because the asymmetric membranes were prepared by a phase-inversion process that also results in extremely thin separation layers. Compared with the phase-inversion process, APD should allow for greater control over the selective layer thickness. Additionally, less of the relatively expensive polyimide is needed in APD than in the phase-inversion process because in the latter case, the polyimide serves as both the support and the separation layer. However, the high heating temperatures required to drive imidization and cross-linking reactions do greatly restrict the supports that can be used for forming polyimide membranes by APD.

5.4 Conclusions

Alternating electrostatic adsorption of poly(amic acids) and polycations on porous alumina supports followed by post-deposition heating provides ultrathin, polyimide films that selectively remove water from alcohols by pervaporation. By including a pendant carboxylic acid group in the poly(amic acid), amide cross-links can be formed between the poly(amic acid) and PAH or LPEI. In the case of polyimide/PAH films, increasing the cross-linking density results in higher water/alcohol selectivities, and incorporation of a cross-linking group in each repeat unit of the polyimide (BPDA-DABA/PAH) yields a selectivity of 6100 for the removal of water from 90% isopropanol. This selectivity is achieved with films as thin as 50 nm, so fluxes are still 2 $kg \cdot m^{-2} \cdot h^{-1}$ at 50 °C.

References:

(1) Huang, R. Y. M. *Pervaporation Membrane Separation Processes*; Elsevier Science: Amsterdam, 1991; Vol. 1.

(2) Lipnizki, F.; Field, R. W. *Environ. Prog.* **2002**, *21*, 265-272.

(3) Aminabhavi, T. M.; Khinnavar, R. S.; Harogoppad, S. B.; Aithal, U. S. *J. Macromol. Sci. R. M. C.* **1994**, *C34*, 139-204.

(4) Liu, Q.-L.; Xiao, J. *J. Membrane Sci.* **2004**, *230*, 121-129.

(5) Volkov, V. V.; Fadeev, A. G.; Khotimsky, V. S.; Litvinova, E. G.; Selinskaya, Y. A.; McMillan, J. D.; Kelley, S. S. *J. Appl. Polym. Sci.* **2004**, *91*, 2271-2277.

(6) Slater, C. S.; Hickey, P. J.; Juricic, F. P. *Sep. Sci. Technol.* **1990**, *25*, 1063-1077.

(7) Karakane, H.; Tsuyumoto, M.; Maeda, Y.; Honda, Z. *J. Appl. Polym. Sci.* **1991**, *42*, 3229-3239.

(8) Xu, J. B.; Bartley, J. P.; Johnson, R. A. *J. Appl. Polym. Sci.* **2003**, *90*, 747-753.

(9) Kurkuri, M. D.; Aminabhavi, T. M. *J. Appl. Polym. Sci.* **2003**, *89*, 300-305.

(10) Huang, R. Y. M.; Shieh, J.-J. *J. Appl. Polym. Sci.* **1998**, *70*, 317-327.

(11) Rhim, J.-W.; Yeom, C.-K.; Kim, S.-W. *J. Appl. Polym. Sci.* **1998**, *68*, 1717-1723.

(12) Du Prez, F. E.; Goethals, E. J.; Schue, R.; Qariouh, H.; Schue, F. *Polym. Int.* **1998**, *46*, 117-125.

(13) Yu, J.; Lee, C. H.; Hong, W. H. *Chem. Eng. Process.* **2002**, *41*, 693-698.

(14) Chanachai, A.; Jiraratananon, R.; Uttapap, D.; Moon, G. Y.; Anderson, W. A.; Huang, R. Y. M. *J. Membrane Sci.* **2000**, *166*, 271-280.

(15) Chen, X.; Li, W.; Shao, Z.; Zhong, W.; Yu, T. *J. Appl. Polym. Sci.* **1999**, *73*, 975-980.

(16) Yoshikawa, M.; Yukoshi, T.; Sanui, K.; Ogata, N. *J. Polym. Sci., Part A: Polym. Chem.* **1986**, *24*, 1585-1597.

(17) Kang, Y. S.; Jung, B.; Kim, U. Y. *Mol. Cryst. Liq. Crys. A* **1993**, *224*, 137-146.

(18) Rafik, M.; Mas, A.; Guimon, M. F.; Guimon, C.; Elharfi, A.; Schue, F. *Polym. Int.* **2003**, *52*, 1222-1229.

(19) Yanagishita, H.; Maejima, C.; Kitamoto, D.; Nakane, T. *J. Membrane Sci.* **1994**, *86*, 231-240.

(20) Kim, H. J.; Jung, B.; Hong, J.-M.; Kang, Y. S.; Kim, U. Y. *Korea Polym. J.* **1994**, *2*, 148-151.

(21) Kim, J.-H.; Lee, K.-H.; Kim, S. Y. *J. Membrane Sci.* **2000**, *169*, 81-93.

(22) Robeson, L. M. *J. Membrane Sci.* **1991**, *62*, 165-185.

(23) Loeb, S.; Sourirajan, S. *Adv. Chem. Ser.* **1963**, *38*, 117-132.

(24) Kim, S.-G.; Kim, Y.-I.; Yun, H.-G.; Lim, G.-T.; Lee, K.-H. *J. Appl. Polym. Sci.* **2003**, *88*, 2884-2890.

(25) Pinnau, I.; Freeman, B. D. In *Membrane Formation and Modification*; Pinnau, I., Freeman, B. D., Eds.; American Chemical Society: Washington, D.C., 2000, pp 1-22.

(26) Polotskaya, G. A.; Kuznetsov, Y. P.; Goikhman, M. Y.; Podeshvo, I. V.; Maricheva, T. A.; Kudryavtsev, V. V. *J. Appl. Polym. Sci.* **2003**, *89*, 2361-2368.

(27) Liu, X.; Bruening, M. L. *Chem. Mater.* **2004**, *16*, 351-357.

(28) Meier-Haack, J.; Lenk, W.; Lehmann, D.; Lunkwitz, K. *J. Membrane Sci.* **2001**, *184*, 233-243.

(29) Sullivan, D. M.; Bruening, M. L. *J. Am. Chem. Soc.* **2001**, *123*, 11805-11806.

(30) Sullivan, D. M.; Bruening, M. L. *Chem. Mater.* **2003**, *15*, 281-287.

(31) Stroeve, P.; Vasquez, V.; Coelho, M. A. N.; Rabolt, J. F. *Thin Solid Films* **1996**, *284-285*, 708-712.

(32) Kotov, N. A.; Magonov, S.; Tropsha, E. *Chem. Mater.* **1998**, *10*, 886-895.

(33) Decher, G. *Science* **1997**, *277*, 1232-1237.

(34) Bertrand, P.; Jonas, A.; Laschewsky, A.; Legras, R. *Macromol. Rapid Comm.* **2000**, *21*, 319-348.

(35) Shiratori, S. S.; Rubner, M. F. *Macromolecules* **2000**, *33*, 4213-4219.

(36) Dubas, S. T.; Schlenoff, J. B. *Macromolecules* **1999**, *32*, 8153-8160.

(37) Kleinfeld, E. R.; Ferguson, G. S. *Chem. Mater.* **1996**, *8*, 1575-1578.

(38) Harris, J. J.; Stair, J. L.; Bruening, M. L. *Chem. Mater.* **2000**, *12*, 1941-1946.

(39) Krasemann, L.; Toutianoush, A.; Tieke, B. *J. Membrane Sci.* **2001**, *181*, 221-228.

(40) Toutianoush, A.; Tieke, B. *Mat. Sci. Eng. C-Bio. S.* **2002**, *C22*, 459-463.

(41) Anderson, M. R.; Davis, R. M.; Taylor, C. D.; Parker, M.; Clark, S.; Marciu, D.; Miller, M. *Langmuir* **2001**, *17*, 8380-8385.

(42) Baur, J. W.; Besson, P.; O'Connor, S. A.; Rubner, M. F. *Mater. Res. Soc. Symp. Proc.* **1996**, *413*, 583-588.

(43) Moriguchi, I.; Teraoka, Y.; Kagawa, S.; Fendler, J. H. *Chem. Mater.* **1999**, *11*, 1603-1608.

(44) Liu, Y.; Wang, A.; Claus, R. O. *Appl. Phys. Lett.* **1997**, *71*, 2265-2267.

(45) Xu, W.; Paul, D. R.; Koros, W. J. *J. Membrane Sci.* **2003**, *219*, 89-102.

(46) Schleiffelder, M.; Staudt-Bickel, C. *React. Funct. Polym.* **2001**, *49*, 205-213.

(47) Pithan, F.; Staudt-Bickel, C. *Chemphyschem* **2003**, *4*, 967-973.

(48) Martin, C. R. *Science* **1994**, *266*, 1961-1966.

(49) Shieh, J.-J.; Huang, R. Y. M. *J. Membrane Sci.* **1997**, *127*, 185-202.

(50) Wang, X.-P.; Li, N.; Wang, W.-Z. *J. Membrane Sci.* **2001**, *193*, 85-95.

(51) Sun, B.; Zou, J. *Ann. N. Y. Acad. Sci.* **2003**, *984*, 386-400.

(52) Sroog, C. E. *J. Polym. Sci., Macromol. Rev.* **1976**, *11*, 161-208.

(53) Huang, R. Y. M.; Pal, A.; Moon, G. Y. *J. Membrane Sci.* **2000**, *167.*

(54) Clark, S. L.; Hammond, P. T. *Langmuir* **2000**, *16*, 10206-10214.